DISPERSION OF VAPOR FROM LNG SPILLS - SIMULATION IN A METEOROLOGICAL WIND TUNNEL

by

R. N. Meroney*   D. E. Neff**

J. E. Cermak*   M. Megahed**

Prepared Under Contract to
R & D Associates
Marina del Rey, California

Fluid Dynamics and Diffusion Laboratory
Department of Civil Engineering
College of Engineering
Colorado State University
Fort Collins, Colorado 80523

May 1977

* Co-Principal Investigators
** Graduate Research Assistants

CER76-77RNM-JEC-DEN-MM57

DISPERSION OF VAPOR FROM LNG SPILLS -
SIMULATION IN A METEOROLOGICAL WIND TUNNEL

By Meroney, Cermak, Neff and Megahed

ERRATA SHEET

1. Tables 8-15 and 8-16 are incorrect. Ignore, they will be replaced in a subsequent errata.

   Note in explanation: Runs 11 and 12 were initially performed at incorrect flow rates. The tests were repeated and are designated 11R and 12R.

2. Tables 8-9, 8-10, and 8-11 are incorrect. Ignore.

   Note in explanation: Runs 6, 7 and 8 were initially performed at incorrect wind speeds. The tests were repeated and are designated 6R, 7R, and 8R.

3. Table 8-1 to 8-26. All 1/400 scale models utilize a z_{ref} = 33 feet whereas in Figures z_{ref} = 129 feet.
   All 1/106 scale models utilize z_{ref} = 5.3 feet.
   All 1/200 scale models utilize z_{ref} = 25 feet.

4. Figures 23-1b. Eliminate.

5. Figures 25 to 36, Table 8, and Figures 23-1 to -4 and 24-1 to -2. All CO_2 data must be corrected to reflect fact that the number of moles of natural gas released at the cold field conditions exceed number of moles released during isothermal model tests. Hence following formulae must be applied to both figures and tables.

$$x_{p_{corrected}} \cong \frac{x_m}{x_m + (1 - x_m)\dfrac{T_{boiloff}}{T_{ambient}}} = C\, x_m$$

   (Typically C varies from 1.0 to 2.7 as x_m varies from 1.0 to 0.0)

$$K_{p_{corrected}} = \frac{K_m}{\dfrac{T_{ambient}}{T_{boiloff}} x_m + (1 - x_m)} = C'\, K_m$$

   (Q evaluated to ambient or STP conditions)

   (Typically C' varies from 1.0 to 0.3 as x_m varies from 0.0 to 0.3)

EXECUTIVE SUMMARY

Tests were conducted in the Meteorological Wind Tunnel and the Industrial Wind Tunnel Facilities to evaluate the rate of dispersion and extent of downwind hazards associated with the rupture of large liquid natural gas cryogenic storage tanks. These tests were conducted on two different dike storage areas, varying in scale from 1:400 to 1:200. In addition, approximate conditions under which the Capistrano Test 044 (1/106 scale) occurred were simulated to provide a direct validation of wind tunnel to field measurements. Two different model release gases were used to simulate the behavior of the cold methane plume. One was a gas of molecular weight 44 at 70^{o}F and the other was a gas of molecular weight 16 at -260^{o}F. Concentration and temperature measurements, and photographic records were obtained for different wind speeds, wind directions and boiloff rates under both neutral and stable density stratification. On the basis of the experimental measurements reported herein, the following comments may be made:

1. The magnitudes and time variation of Case I Capistrano Test 044 concentrations substantially agree with the behavior of the field measurements at most tested locations. The wind tunnel results follow the mean dilution behavior of the LNG plume, but they do not exhibit the large and intermittent concentration peaks at late times observed in the field. This is attributed to the absence of plume meandering and gustiness in the laboratory.

2. Bimodal plume distributions reported in earlier measurements are once again observed in the ground concentration contours. Variation of the peak concentrations found at a given distance are generally

slightly less than that suggested by equivalent Pasquill Diffusion Category results.

3. Distances to the lower flammability limit (LFL) are slightly greater for the Low Dike model than those observed for the High Dike model under similar meteorological conditions. If the boiloff rates for both models were the same the differences might be even more pronounced.

4. Boiloff rates associated with concrete or insulated concrete floors and walls in the High Dike considerably reduced the hazard zone or distance to LFL.

5. Visualization of the transient boiloff phenomena suggest that continuous releases should represent an upper bound to the transient phenomenon. Unfortunately possible systematic errors between the gas chromatograph and the aspirated hot-wire anemometer probe may preclude any quantitative statement in certain cases.

6. Continuous releases made from 1/200 scale models of the High Dike utilizing CO_2 result in concentrations which agree well with earlier Freon-Air release simulations. These measurements generally exceed values taken behind the 1/400 models under equivalent situations by a factor of two. This suggests a significant influence of the tunnel side walls persists in the 1/200 scale models.

7. The dimensionless concentration coefficient $\chi_{max}\overline{U}_{ref}H^2/Q$ is a function of non-dimensional downwind distance x/H. Results for both High and Low Dike, neutral and stable flows, and insulated versus

conducting floor surfaces for the continuous releases studied generally decay similar to Pasquill Diffusion Category C-D.

8. No consistent influence of the insulated versus the conducting floor condition could be identified during continuous releases of He-N_2 model gas. The effects are thus judged to be small.

9. Visualization results suggest that heat transfer to an uncooled dike model are excessive in the laboratory. No visible plume occurs when He-N_2 releases are made with plastic or room temperature steel models.

10. Visualization of the influence of a ramp slope of 1/50 on a continuous boiloff rate from a model dike indicates slope of this magnitude may cause significant plume asymmetries, large case to case variabilities, and upwind movement of the cloud.

11. Upwind model tanks tend to introduce additional turbulence which lessen the influence of slope and disperse gases more rapidly.

12. Plume liftoff experiments with line, area, and point sources suggest that dimensionless distance to plume liftoff x/ℓ_b is a function of a Froude number based on characteristic plume width, i.e., $Fr = \frac{\rho_a \overline{U}^3 w}{g \Delta\rho Q}$ and a buoyancy length scale, $\ell_b = \frac{g\Delta\rho Q}{\rho_a \overline{U}^3}$.

ACKNOWLEDGMENTS

The support of R & D Associates in carrying out this study is gratefully acknowledged. Construction of the models was accomplished by personnel of the Engineering Research Center Machine Shop. Mr. James A. Garrison supervised photographic records of flow visualization. Mr. James Maxton supervisor operation of gas chromatograph concentration measuring equipment.

TABLE OF CONTENTS

LIST OF FIGURES

LIST OF FIGURES (continued)

LIST OF TABLES

LIST OF SYMBOLS

Dimensions are given in terms of mass (M), length (L), time (t), moles (n), and temperature (t)

Symbol	Definition	
CH_4	Methane	
CO_2	Carbon Dioxide	
D	Tank diameter	[L]
d	Dike diameter	[L]
E	Voltage	
g	Gravitational acceleration	$[Lt^{-2}]$
H	Tank height	[L]
h	Dike height	[L]
h_c	Convective heat transfer coefficient	
He	Helium	
L	Stability length parameter	[L]
ℓ_b	Buoyancy length scale	[L]
L.S.	Length scale	
M	Molecular weight	
m	Mass boiloff rate	$[Mt^{-1}]$
N_2	Nitrogen	
n or c	Moles	$[mo^{1}]$
n	Exponent of velocity distribution power law	
Q	Volumetric rate of gas flow	$[L^3t^{-1}]$
q	Quantity of heat	$[L^2Mt^{-2}]$

Symbol		
S.G.	Specific gravity	
T	Temperature	[T]
ΔT	Temperature difference across some reference layer	[T]
t	Time	[t]
U, u	Wind speed	$[Lt^{-1}]$
w	Plume width at release location	[L]
x	Mole fraction of gas	
x	General downwind coordinate	[L]
y	General lateral coordinate	[L]
z	General vertical coordinate	[L]
z_o	Surface roughness parameter	[L]
δ	Boundary layer thickness	[L]
θ	Time of plume trajectory	[t]
ν	Kinematic viscosity	$[L^2t^{-1}]$
ρ	Density	$[ML^{-3}]$
$\Delta\rho$	Density difference between methane gas and air	$[ML^{-3}]$
σ_y	Standard deviation of plume distribution in the y-direction	[L]
σ_z	Standard deviation of plume distribution in the z-direction	[L]
χ	Volume dilution ratio	

1.0 INTRODUCTION

The objective of this study was to evaluate the rate of dispersion and extent of downwind hazards associated with the rupture of large liquid natural gas (LNG) cryogenic storage tanks. In particular the use of diked storage areas to ameliorate the extent of potential damage was examined. It is estimated that in the 1980 time period 0.04 trillion cubic meters per year of natural gas will be supplied in the form of LNG. Thus safety at LNG facilities is of utmost importance to the gas industry and the public. The hazards associated with LNG release are fire and thermal radiation from such fires. If ignition does not occur immediately during an accidental LNG release, the boiling LNG produces vapors which are mixed with ambient air and transported downwind. This cloud is potentially flammable until the atmosphere dilutes the gas mixture below the lower flammable limit (LFL) (a local concentration for methane below 5 percent by volume).

However the ultimate purpose of this study is to provide basic information on the structure of vapor plumes resulting from LNG spills on land for a realistic range of meteorological variables, source variables and site features. Small scale models of the tank-dike complex were placed in a meteorological wind tunnel capable of simulating the appropriate meteorological conditions. Mean concentrations of LNG vapor were determined by sampling concentrations of tracer gas released from the LNG spill with CO_2 or a cooled He-N_2 gas mixture to simulate the LNG vapor. Overall plume goemetry and behavior were obtained by photographing smoke or water vapor condensed by the chilled gas.

1.1 REVIEW OF PREVIOUS SIMULATION EFFORT

Dispersion of the LNG vapor and the resulting concentrations are affected by the following primary factors:

A. Meteorological variables--wind speed, wind direction, thermal stratification, relative humidity, and temperature of the land surfaces relative to temperature of the air.

B. Source characteristics--geometry of tank-dike complex, and source strength (boil-off rate).

C. Site features--topographical features and thermal properties of soil.

During Phase I research (see Neff, et al., 1977) on the influence of gas and site features on dispersion during an LNG spill, it was found that ground level concentrations may remain at levels above the Lower Flammability Limit (LFL) for distances in excess of 1,500 meters. These tests included high and low tank-dike combinations, neutral and stably stratified flow fields, and various continuous boiloff rates. On the basis of experimental measurements reported in Neff, et al. (1977), the following conclusions were drawn:

1) The dimensionless concentration coefficient $\chi \bar{u} H^2/Q$ is a function of non-dimensional downwind distance x/H. This function suggests an initial decay rate in the region $x/H < 10$ that is less than the decay rate in the region of $x/H > 10$, and perhaps data should be evaluated in terms of a different length scale related to buoyancy parameters.

2) The dimensionless concentration coefficient curves asymptotically approach the slope of those given by the appropriate Pasquill diffusion category for both neutral and stable flow.

3) Visualization of similar tests for the range of model scales used (1:130 to 1:666) indicate a similar plume geometry. Concentration results of the different model scales agree to within the experimental accuracy of approximately $\pm$ 20%. Similarly identical tests also show good agreement.

4) The effect of the increased aerodynamic turbulence of the High Dike over that of the Low Dike does not appear to influence the far downwind dispersion of methane gas for a continuous release. (Note however that one expects the boiloff rate of the Low Dike to be greater than that of the High Dike)

5) Modeling of an adiabatic plume in a low humidity atmosphere by the use of a Freon 12-N_2 simulation gas at 70^oF tends to give lower concentrations at the same sampling positions than that of modeling unrestricted plume behavior with the use of a He-N_2 simulation gas at -260^oF. This difference was noted to be as high as 1:6.

A number of questions were left unresolved by the Part I study, these include the effects caused by:

a) Initial heat transfer to the plume at the tank dike complex,

b) Heat transfer to the cold plume from the underlying surface,

c) Influence of local terrain on plume shape and trajectory,

d) Variable boiloff rates versus continuous releases at a constant rate, and

e) The influence of model scale compared to full scale spill behavior.

1.2 MEASUREMENT PROGRAM

Part II measurements will examine the sensitivity of distance to LFL for continuous and transient releases to features such as:

a) Initial heat transfer to the plume at the tank/dike complex,

b) Heat transfer to the cold plume from the underlying surface, and

c) Influence of local terrain on plume shape and trajectory.

The following sections discuss the details of each measurement phase.

1.2.1 Heat Transfer Influence on LNG Plume Behavior

The influence of heat transfer on LNG plume dispersion can be divided into three phases. First, the temperature (and hence S.G.) of the plume at exit from the dike is dependent on the thermal diffusivity of the tank-dike materials, the volume of the tank-dike structure, the actual boiloff rate, and the details of dike geometry. A second plume phase involves the heat transfer from the ground surface beyond the dike to lower the plume density. A series of tests were performed to bound the potential heat transfer to a LNG plume. Since earlier measurements indicate that background stratification is a predictable characteristic in plume dispersion only a few stable stratification conditions are considered. Thirdly, once the plume is heated to a buoyant condition there is still some questions as to whether lift off will occur. A separate series of tests were performed to permit determination of an appropriate lift off parameter to characterize plume lift off.

1.2.1.1 Tank/Dike Transient Heat Transfer Study

Several time scales are involved in this process--i.e., the time scale for heat conduction ($t \sim \rho \frac{C_p L}{k}$), the time scale for heat transfer to the LNG gases ($t \sim \frac{\rho C_p V}{A h_c}$), and the time scale of the buoyant plume ($t \sim \frac{L}{U}$). Matching these time scales simultaneously would require analysis of the interior structure of an actual tank complex, specification of special materials for model constriction, and model construction.

An evaluation of this problem suggests no tank model materials exist which will satisfactorily model heat transfer time scales adequately. Cases were considered to evaluate sensitivity of the transient plume dispersal to tank/dike changes; however there is no guarantee these will result in quantitatively similar results to a field case. Rather it is expected a bounding influence of different conditions can be determined. The influence of dike material on heat transfer was studied by visualization of He-N_2 model gases. The appropriate runs are cases 35-42 in the test matrix.

1.2.1.2 Controlled Surface Heat Flux Study

The trajectory of an LNG plume will be dependent upon the rate of entrainment of water vapor andthe rate of heat transfer to the plume from the ground surface or the unmixed ambient air. Large addition of heat can result in a buoyant LNG gas plume early in its release history. Some analysts have suggested this rate is sufficient to cause vertical department of the flammable plume from the area.

Laboratory and field measurements made to date do not seem to support a rising plume scenario. Nevertheless, it would be informative to determine under what circumstances plume rise may occur. Runs 45-54 were performed to examine the influence of heat transer from soil surface to LNG plume.

1.2.1.3 Plume Lift Off Experiment

Whether or not a buoyant plume or puff can lift itself off the ground in the presence of turbulent diffusion and wind shear depends on how the buoyancy-induced velocities compare with the turbulent velocity fluctuations. A criteria suggested by Briggs (1973) for lift off is

$$LP = \frac{gH(\Delta\rho/\rho)}{U*^2}$$

Analytical considerations suggest a value of 2 → 2.5 for a critical value. Unfortunately no measurements are available to confirm this number. Briggs himself suggests a factor of ± 4 accuracy in the number he recommends. Order of magnitude calculations for typical LNG release conditions suggest that even with large heat transfer to the plume the conditions may be marginal for plume lift off for many meteorologically typical situations. (A plume where S.G. ≃ 0.975, a depth of 2 meters, and in a wind field at 4m/sec would not necessarily rise!)

A program was included to evaluate the physics of this lift off process. Buoyant gases under point, line, or area release configurations at ground level were examined for lift off visually at various wind speeds. Plume buoyancy was regulated by changing Helium volumetric source strength, and visualization was affected by marking with $TiC\ell_4$ smoke trace.

1.2.2 Time Dependent Plume Behavior

Peak to mean concentration information and transient concentration conditions represent an important facet in the evaluation of plume flammability limits. Past plume measurements suggest peak/mean ratios may vary between 2-10 depending upon the circumstances and location within the plume. Because of the scale distortion of time, phenomena occur much faster in the laboratory than in the atmospheric prototype. Time scale in the laboratory varies as $t_m = t_p \frac{U_p}{L_p} \frac{Lm}{Um}$, and the velocity scale is determined by Froude number scaling, thus $U_m = U_p \sqrt{\frac{Lm}{Lp}}$

Thus for $\frac{Lm}{Lp} \simeq \frac{1}{400}$

$$\frac{tm}{tp} = \sqrt{\frac{Lm}{Lp}} = \sqrt{\frac{1}{400}} \quad \alpha \quad \frac{1}{20}$$

Since fluctuations of 0.1 sec are significant in the atmosphere, a response to 0.01 sec phenomena is at least required in the laboratory.

The use of different molecular weight gases suggest the use of thermal conductivity type probes (TSI-1440) capable of response to 100 khz. These probes are jointly responsive to temperature, plume concentration, and humidity to the first order as

$$E^2 \alpha \frac{\Delta T}{\sqrt{M}}$$

where M is molecular weight and ΔT is temperature difference between a sample and the sensor wire. Currently Colorado State University staff are evaluating the characteristics of a conventional single film TSI-1440 as well as a two-film design specified by Colorado State University. The two-film design has been utilized in an isothermal release situation to examine probe characteristics and phenomena variations to bound the behavior.

To validate the instrumentation an 80 foot field spill performed at Capistrano as part of the AGA Phase II program has been simulated. Capistrano test 044 from American Gas Association (1974) was simulated at a 1 to 106 scale. Runs 9,10 and 23,24 include continuous and variable boiloff releases for this case.

A systematic evaluation of the characteristics of boiloff near typical High and Low Dike designs at two model scales encompasses runs 1 to 8, 11 to 22, and 30 to 33 in the text matrix. These measurements include two wind speeds, two boiloff ratios, two model scales, and two stratification conditions in different combinations.

TEST MATRIX FOR QUANTITATIVE INSTRUMENTATION EXPERIMENTS

MEASUREMENT TECHNIQUE	RUN NO.	DIKE** HIGH	DIKE** LOW	SIMULATED WIND SPEED (mph) 7*	12Δ	16*	STRATIFICATION NEUTRAL	GIFFORD CAT.G	-115°C/100m	SIMULATED BOILOFF RATE CONTINUOUS	VARIABLE	lbm/sec (OR DESCRIPTION IF VARIABLE)	MODEL CONSTRUCTION STEEL PRECOOLED	STEEL	PLASTIC	SURFACE DESCRIPTION ALUMINUM (CONDUCTING)	INSULATED
	CO_2 TESTS CONCENTRATION																
GAS CHROMOTOGRAPHY	1	✓		✓			✓			✓		2400		✓		✓	
	2	✓		✓			✓			✓		1400		✓		✓	
	3	✓				✓	✓			✓		2400		✓		✓	
	4	✓				✓	✓			✓		1400		✓		✓	
	5		✓	✓			✓			✓		2400		✓		✓	
	6	✓		✓				✓		✓		2400		✓		✓	
	7	✓		✓				✓		✓		1400		✓		✓	
	8		✓					✓		✓		2400		✓		✓	
	9	CAPISTRANO 044			✓		✓		✓	✓		202		✓		✓	
	10	CAPISTRANO 044			✓		✓		✓	✓		141		✓		✓	
	11	✓ 1/200		✓			✓			✓		1400		✓		✓	
	12	✓ 1/200				✓	✓			✓		1400		✓		✓	
TSI ASPIRATED PROBE	13	✓		✓			✓				✓	SOIL		✓		✓	
	14	✓		✓			✓				✓	CONCRETE		✓		✓	
	15	✓		✓			✓				✓	INSUL.CONCRETE		✓		✓	
	16	✓				✓	✓				✓	SOIL		✓		✓	
	17	✓				✓	✓				✓	CONCRETE		✓		✓	
	18	✓				✓	✓				✓	INSUL.CONCRETE		✓		✓	
	19		✓	✓			✓				✓	SOIL		✓		✓	
	20	✓		✓				✓			✓	SOIL		✓		✓	
	21	✓		✓				✓			✓	CONCRETE		✓		✓	
	22		✓	✓				✓			✓	SOIL		✓		✓	
	23	CAPISTRANO 044			✓		✓		✓		✓	CASE I		✓		✓	
	24	CAPISTRANO 044			✓		✓				✓	CASE II		✓		✓	
	CO_2 VISUALIZATION																
FLOW VISUALIZATION	25	✓		✓			✓				✓	SOIL		✓		✓	
	26	✓				✓	✓				✓	SOIL		✓		✓	
	27		✓	✓			✓				✓	SOIL		✓		✓	
	28		✓			✓	✓				✓	SOIL		✓		✓	
	HeN_2 VISUALIZATION																
	29	✓		✓			✓				✓	SOIL	✓			✓	
	30	✓				✓	✓				✓	SOIL	✓			✓	
	31	✓		✓			✓				✓	SOIL			✓	✓	
	32	✓				✓	✓				✓	SOIL			✓	✓	
	33		✓	✓			✓				✓	SOIL	✓			✓	
	34		✓			✓	✓				✓	SOIL	✓			✓	
	35		✓	✓			✓				✓	SOIL		✓		✓	
	36		✓			✓	✓				✓	SOIL		✓		✓	
	HeN_2 CONCENTRATION																
GAS CHROMOTOGRAPHY	37	✓		✓			✓			✓		2400	✓			✓	
	38	✓				✓	✓			✓		2400	✓			✓	
	39		✓	✓			✓			✓		2400	✓			✓	
	40		✓			✓	✓			✓		2400	✓			✓	
	41	✓		✓			✓			✓		2400	✓				✓
	42	✓				✓	✓			✓		2400					✓
	43		✓	✓			✓			✓		2400	✓				✓
	44		✓			✓	✓			✓		2400	✓				✓
	45	✓		✓				✓		✓		2400	✓			✓	
	46		✓	✓				✓		✓		2400	✓			✓	

*DEFINED AT 10 METER HEIGHT

ΔDEFINED AT HEIGHT OF 5 FT

**1/400 SCALE UNLESS OTHERWISE STATED

1.2.3 Ramp Effects

Since the LNG plume is buoyancy dominated, surface slope can act to either accelerate or decelerate a dense plume lying on that surface. Earlier tests performed by Hall, et al. (1975), at Warren Springs Labs, U.K., demonstrated that for some Froude number/slope combinations this may be an effect of first order. Since the proposed Salton Sea site for a field program has slopes up to 1/50, a series of flow visualization tests were performed. To isolate the influence of slope, a series of simple area source releases were studies as well as releases from the 1/400 High Dike model both alone and in the presence of dummy upward tank structures.

This report is supplemented by a motion picture (in color) which shows the plume behavior for different dike configurations and ramp and dummy tank arrangements. Black and white plot sequences for the ramp and dummy tank arrangements as well as the plume lift off results have been provided R & DA.

Details of the model and test configurations are presented in Section 2.0. In addition experimental equipment are described. Section 3.0 discusses the results obtained and their significance.

1.3 MODELING CRITERIA

The increasing need to study environmental problems in areas of complex boundary conditions has motivated serious efforts to simulate atmospheric boundary layers in the laboratory. Successful simulation permits both applied and fundamental studies of flows with complex boundary conditions on a scope which would be prohibitive in the field because large expenditures of time and money would be required.

Modeling criteria has been discussed in detail in the report by Neff, et al. (1977), "Wind Tunnel Study of the Negatively Buoyant Plume Due to an LNG Spill", Section 2.0. Additional consideration during phase II has been given to the constraints imposed by simulation of heat transfer characteristics of the plume dynamics.

2.0 DATA ACQUISITION AND ANALYSIS

Measurements in wakes require considerable care, both in their acquisition and in their interpretation. In this section the methods used to make measurements and the techniques used in converting directly measured quantities to meaningful physical quanties are discussed. Attention is drawn to the limitations in the techniques in an attempt to prevent misinterpretation or misunderstanding of the results to be presented in the next section. Some of the methods used are conventional and need little elaboration.

2.1 WIND TUNNEL FACILITIES

The majority of the experiments were performed in the Meteorological Wind Tunnel (MWT) shown in Figure 1. This wind tunnel, expecially designed to study atmospheric flow phenomena, incorporates special features such as an adjustable ceiling, a rotating turntable, temperature controlled boundary walls, and a long test section to permit adequate reproduction of micrometeorological behavior. Mean wind speeds of 0.2 to 130 ft/sec (0.14 to 90 mi/hr) in the MWT can be obtained. Boundary-layer thickness up to four feet can be developed "naturally" over the downstream 20 feet of the MWT test section. Thermal stratification in the MWT is provided by the heating and cooling systems in the section passage and test section floor. The flexible test section roof on the MWT is adjustable in height to permit the longitudinal pressure gradient to be set at zero. A set of vortex generators were installed two feet downwind of the entrance to give the simulated boundary layer an initial impulse of growth. From six to 40 ft a set of 12 roll-bond aluminum panels were placed on the tunnel floor. These panels were connected to the facility refrigeration system and cooled to approximately 32°F. From 40 ft to the end of the test section a permanently installed set of cooling panels were used to also lower the aluminum floor temperature to a level of 32°F. The free stream temperature was raised to a level near 115°F as prescribed by the Bulk Richardson number. The facility is described in detail by Plate and Cermak (1963).

Visualization experiments associated with the influences of ground slope, the wake influence of additional upwind LNG storage tanks, and the character of buoyant plume lift off were performed in the Industrial Aerodynamics Wind Tunnel (IWT) shown in Figure 2. This wind tunnel features an adjustable ceiling, a rotating turntable, and large uninterrupted expanses of glass side walls which facilitate photography.

2.2 MODEL CONFIGURATIONS

Capistrano Test 044 Model

Test 044 from the Capistrano Series supported by the American Gas Association (1974) involved spills into an 80 ft diameter by 1.5 ft high dike. This test was modeled utilizing a 1/106 scale circular plenum with a porous punched plate upper surface. The plenum diameter was 9.0 inches, and the plenum was fed by a tube inserted beneath the model through the oval tunnel floor.

Representative High and Low Dike Models

Two different LNG tank and dike facilities were modeled, one entitled the Representative High Dike, the other the Representative Low Dike. The drawings indicating full-scale dimensions were supplied by R & D Associates and are presented as Figure 5. For both the High and Low Dikes two different model scales were made--1:400 and 1:200. The 1:200 scale models were constructed from lucite and styrofoam. At the

1:400 scale, two High Dike models were made, one of plastic and one of steel. These two steel models were made in the form of liquid nitrogen reservoirs so that a release gas of helium and nitrogen at -260°F would not be preheated during flow within the model. Figure 6 shows a schematic of the construction of these models.

Terrain and Dummy Tank Models

A false floor with a rising slope of 1 to 50 was constructed to insert into the IWT. This floor shown in Figure 7 was inserted 30 feet from the tunnel entrance and extended 24 ft downwind. The 1/400 Representive High Dike Model and the 1/106 Capistrano Area Series were placed on the sloping floor ~8.5 feet from its inception.

Dummy tanks were constructed from styrofoam at the 1/400 scale High Dike dimensions. These were placed 2 to 3 dike diameters upwind of the model High Dike to evaluate wake influence on the continuous LNG spill conditions.

Line, Area and Point Source Models

Figure 8 reviews the dimensions and locations of representative line, area and point sources installed in the IWT dummy plume lift off visualization.

Reference velocity measurements were made at a one foot height. Typical velocity profiles have a power law index $n \simeq .15$.

2.3 FLOW VISUALIZATION TECHNIQUES

Smoke was used to define plume behavior over the LNG Facility. The smoke was produced by passing the simulation gas mixture through a container of titanium tetrachloride located outside the wind tunnel and transported through the tunnel wall by means of a tygon tube terminating at the dike inlet within the model. The plume was illuminated with arclamp beams. A visible record was obtained by means of pictures taken with a Speed Graphic camera utilizing Polaroid film for immediate examination. Additional still pictures were obtained with a Hasselblad camera. Stills were taken with camera speeds of approximately one second. A series of color motion pictures were also taken with a Bolex motion picture camera mounted on a movable dolly which was traversed the length of the tunnel parallel to the plume trajectory at the average wind speed. A film log of the scenes recorded on 16mm film is included as Table 3.

2.4 WIND PROFILES AND TEMPERATURE MEASUREMENTS

A Datametrics Series 800-L Linear Flow Anemometer was utilized to measure the upstream velocity profiles in both the neutrally and stably stratified flow fields. This instrument is accurate to within two percent of its reading. Measurements of temperature were made with a miniature thermistor (Fennal glass coated bead) system constructed by Yellowsprings Corp. (YSI Model 42 SC).

All the concentration and visualization experiments were carried out over the range of conditions shown in Table 2. For the neutral flow situation a velocity profile similar to that shown in Figure 9 was obtained. This profile may be approximated by the relation $\frac{U(z)}{U_{ref}} = (\frac{z}{z_{ref}})^{0.12}$ where z_{ref} and U_{ref} for the prototype conditions are presented with the profile in Figure 9. For the stable flow situation a velocity and temperature profile similar to that shown in Figure 10 was obtained. This velocity profile may be approximated by the relation $\frac{U(z)}{U_{ref}} = (\frac{z}{z_{ref}})^{0.4}$. The Bulk Richardson number for stable flow was 0.67.

2.5 MEASUREMENT TECHNIQUE FOR CONTINUOUS BOILOFF SIMULATION

Two different simulation gases were premixed and stored in large high pressure tanks. One was pure carbon dioxide, CO_2, which was released at room temperature. The other was a mixture of 50% helium and 50% nitrogen which was precooled in a liquid-nitrogen filled heat exchanger and released at -260°F. These two gas mixtures had molecular weights of 44 and 16 respectively. Depending upon the test being undertaken, one of these gas mixtures was allowed to flow from the model, simulating the exit flow rate and buoyancy effects due to the density difference between LNG vapor and the ambient atmosphere. This gas was metered by Fischer-Porter precision flow rators which were adjusted for pressure, temperature, and molecular weight effects as necessary. Figure 11 contains an outline of the two different gas release systems.

For all of the tests involving continuous release concentration data the release gas flow rates were held at different constant values selected from the time history of the full scale boiloff rate curves. Magnitudes simulated are indicated in the Summary of Concentration Tests, Table 4.

2.5.1 Gas Concentration Measurements

After the flow in the tunnel was stabilized, the appropriate model gas was released from the model dikes at the required rate. Samples of air were withdrawn from the sample points isokinetically and analyzed. The flow rate of the model gas mixture was controlled by a pressure regulator at the supply cylinder outlet and monitored by a Fischer and Porter precision flow meter. The sampling and detection systems are shown in Figure 11.

Samples were analyzed by use of a Model 8500 Carle Gas Chromatograph with a thermal conductivity cell sensor.

The procedure for analyzing the samples was as follows:

1) 2 cc volumes of the source gas, tunnel background air, and sample gases from within the plume were introduced into the thermal conductivity cell of the Model 8500 Carle Gas Chromatograph individually.
2) The output from the heated thermister was integrated for each of these gases and the readings in volt-seconds were recorded.
3) The correction for background level was performed on the sample gases. $(\text{volt-sec sample})_{\text{corrected}} = (\text{volt-sec sample}) - (\text{volt-sec background})$
4) The percentage of source gas remaining at each sample point is expressed as percent methane.

$$(\%\ \text{methane}) = \frac{(\text{volt-sec sample})_{\text{corrected}} \chi (100)}{(\text{volt-sec source})}$$

5) The dimensionless concentration parameter $(\chi \overline{u}_{ref} L^2/Q_m$ was calculated for each sampling point knowing that

   $\chi = (\%\ \text{methane}) \div 100$

   $\overline{u}_{ref}$ = mean speed of wind at reference height

   L = reference length (either tank height H or reference height z_{ref})

   subscript m = under model conditions
6) Since the dimensionless concentration parameters are equivalent between model and prototype, one may calculate percent methane at points in the field under any condition with an equivalent Froude number, density ratio, and dimensionless source ratio and similar approach velocity and Richardson number profiles.

For example, say that a boiloff of 944.6 lbm/sec of methane under a mean wind speed of 22 ft/sec over a tank height of 129 ft is of interest. Then for a point where

$$\left(\frac{\chi \bar{u}_{ref} H^2}{Q}\right)_m = 1.0; \; Q_p = \frac{944.6}{.1047} = 9021 \text{ ft}^3/\text{sec, and where}$$

ρ_{CH_4} gas @ -260°F = .1047lbm/ft^3.

$$\%\text{methane} = 100 \; \chi_p = \frac{\chi \bar{u} \, H^2}{Q}\Big|_m \times \frac{Q}{\bar{u} \, H^2}\Big|_p \times 100$$

$$= 1.0 \times \frac{9021}{22(129)^2} \times 100 = 2.5.$$

2.5.2 Errors in Concentration Measurement

The reference state for the thermal conductivity detector is established by a constant carrier gas flow. At this baseline level the output from the detector was set at zero. When a sample passes through the detector the output from the detector rises to a level proportional to the amount of tracer gas flowing through the detector. Since the chromatograph used features a temperature control there is very low drift. The integrator circuit is designed for linear response over the range considered. A total system error can be evaluated by considering the standard deviation found for a set of measurements where a precalibrated gas mixture is monitored. For an appropriate calibration gas (helium or carbon dioxide) the average standard deviation from the integrator was five percent.

Since the source gas was premixed to the appropriate molecular weight and repetitive measurements were made of its source strength the confidence in source strength concentration is similar. The flow rate of the source gas was monitored by Fischer-Porter Flowmeters which are expected to be accurate to ± two percent including calibration and scale fraction error. The wind tunnel velocity was constant to ± 20 percent at such low settings. Hence the cumulative confidence in the measured values of $\chi\overline{u}H^2/Q$ will be a standard deviation of about ± 20 percent, whereas the worst cumulative scenario suggests an error of no more than ± 30 percent.

The lower limit of measurement is imposed by the instrument sensitivity and the background concentrations of tracer gas in the air within the wind tunnel. Background concentrations were measured and subtracted from all measurements quoted herein; however, a lower limit of ~5-10 ppm of the source gas is unavoidable as a result of background CO_2 of He levels plus previous model gas releases. An upper limit with the instrument used does not exist; however, long chromatograph columns are necessary to avoid overwhelming the detector when concentrations are very high.

2.6 MEASUREMENT TECHNIQUE FOR VARIABLE BOILOFF SIMULATION

To obtain an accurate prediction of the extent of hazard associated with the vaporization of liquefied natural gas spill the model should simulate the variable boiloff rate of the gaseous methane characteristic to that of a given spill configuration. For the model simulations performed in the present study R & D Associates provided the desired characteristic boiloff rate curves for the models tested. These boiloff curves for the prototype situation along with the actual model gas release rates measured by a Datametrics Series 1000 Mass Flow Transducer are presented in Figures 12-17. These gas flow rate curves with time were obtained by the use of a programmed cam to close a micrometer needle valve controlling the flow of simulation gas at a predetermined rate.

Figure 18 shows a schematic of this valve arrangement and the location of the mass flow transducer used to measure the resultant flow rate vs. time.

2.6.1 Gas Concentration Measurements

As a result of this time dependent release of simulation gas (CO_2 for all tests performed), concentration measurements at test points downwind of the spill site must be taken on a real time basis. It was necessary to have a high frequency response to concentration so that peaks of methane concentrations above 5% (the lower flammability limit of methane in air, LFL) would be detected. To satisfy these requirements an aspirating dual film probe was designed for use with this study.

The basic principles governing the behavior of such a probe have been previously discussed by Blackshear and Fingerson (1962), Brown and Rebollo (1972), and Kuretsky (1967). A diagram of the design of this probe is presented in Figure 19.

A vacuum source sufficient to choke the flow through the small orifice just downwind of the sensing elements was applied. One film was operated in a constant temperature mode at a temperature above that of the ambient air temperature. This was accomplished by a feedback amplifier which maintained a constant resistance through adjustment of the heating current. A change in output voltage from this sensor circuit corresponds to a change in heat transfer between the hot-wire and the sampling environment.

The heat transfer rate from a hot cylindrical film to a gas flowing over it depends upon the film diameter, the temperature difference between the film and the gas, the thermal conductivity and viscosity of the gas, and the gas velocity. For a film in an aspirated probe with a sonic throat, the gas velocity can be expressed as a function of the ratio of the probe cross-sectional area at the film position to the area at the throat, and the specific heat ratio and velocity of sound in the gas. The latter two parameters, as well as the thermal conductivity and viscosity of the gas mentioned earlier, are determined by the gas composition and temperature. Hence, for a fixed probe geometry and film temperature, the heat transfer rate, or the related voltage drop across the film, is a function only of the gas composition and temperature.

Figure 21 shows the measured variation of the voltage drop with percentage of CO_2 in a CO_2-air mixture, for a typical mixture temperature and four different values of the film temperature. For an overheat ratio of 1.23, the voltage drop varies essentially linearly with the CO_2 concentration, so this particular overheat ratio was used in the wind tunnel measurements.

The voltage drop of the hot film also depends upon the ambient gas temperature. In the tests involving a stable (thermally stratified) atmospheric boundary layer, the gas temperature varied over several degrees, and this produced an additional voltage variation which was essentially linear with temperature (Figure 20). To compensate for this variation, the second film in the probe was operated as a resistance thermometer by passing a very small constant current through it. The resulting voltage drop varied linearly with the gas temperature, as shown in Figure 20 and was independent of gas composition. This voltage was electronically amplified by the proper factor and subtracted from the voltage of the first film to give a signal which varied linearly with CO_2 concentration and was independent of temperature (within a few percent) over the temperature range of the wind tunnel tests. Figure 22 presents a flow chart of the instrumentation used to process the signals and record the results. Eleven different cases were considered with a variable boiloff. These were summarized in Table 4. For each test the different locations where instantaneous concentration vs. time plots were obtained are shown in Figure 4. For each test position up to five replications were performed.

2.6.2 Errors in Concentration Measurement

Without temperature compensation and the flared fitting attached to the front of the probe to reduce pressure fluctuations (Figure 19) the noise and baseline drift detected were so severe concentration measurements of 5% CO_2 in air were barely detectable in a wind tunnel environment. But with the addition of these two improvements the noise level was reduced to 0.1% CO_2 in air and the maximum baseline drift was also about this value. Since the effective sampling area of the probe is now greater than the area of the probe inlet and the sensor is located 4 in. from the probe inlet the fine structure of concentration variation may be partially erased. The limiting factor for the upper frequency response of the actual concentration signal is that of the travel time from the sensor to the sonic choke. At high frequencies the correlation between concentration fluctuation and velocity fluctuations (velocity fluctuations are a result of the changes of sonic velocity with concentration) at the sensor begin to decline. With the probe used an upper frequency response of 1000 Hz would be a fair estimate.

It is difficult to estimate the maximum possible error in these measurements due to the involved relation between temperature and concentration responses of the sensor. Considering the errors involved in thermal compensation and the accuracy of the concentration standard used, one might estimate a maximum error of about 3.5% of the reading for above 4% CO_2 and $\pm$0.15% for readings less than 4% CO_2.

3.0 TEST PROGRAM RESULTS

The test program consisted of (1) a qualitative study of the flow field around the different tank and dike facilities by visual observation of the plume released from a model area; and (2) a quantitative study of gas concentrations produced by the release of a tracer from the model area. The test conditions are summarized in Table 4 and the test matrix in Section 1.2. Both of these qualitative and quantitative studies were performed with two different model simulation gases. One was Carbon Dioxide at 70°F to model the characteristics of an adiabatic plume in a low humidity atmosphere. The other was a Helium-Nitrogen gas mixture at -260°F to model plume behavior without placing the above restrictions on heat transfer rate and atmospheric conditions. For a more complete description of simulation gas characteristics refer to Sections 2.5 and 2.6.

Downwind distances refer to lengths converted from model to prototype as measured from the center of the respective model. Unless otherwise noted, the term wind velocity refers to the velocity in the approach stream at a reference height of 10 meters for the High and Low Dike Tests and 5 feet for the Capistrano 044 tests. A velocity at any reference height is available by referring to the appropriate velocity profile (Figures 9-10).

3.1 CONTINUOUS BOILOFF RELEASE CASES

Turbulent diffusion of a simulated LNG plume for three different LNG tank and dike complexes, two model gas mixtures, two atmospheric stratifications, two scale ratios, and a number of wind speed and boil-off rate combinations were studied in Runs 1-12 and 45-54. Mean concentration measurements were obtained for as many as 23 different sample points distributed over a ground level zone up to 900 feet wide and from 160 to 6500 feet long and in the vertical over a height of 0 to 200 feet. A representative layout of the grids used is shown in Figure 3. One is referred to Table 8 and the locator table provided for the specific location of each sampling point for the tests performed. All concentration data has been placed into the forms of

$K = \frac{\chi \bar{u}_{ref} H^2}{Q}$ and $\chi \times 100$ in Table 8. χ represents a normalized concentration or dilution observed at a sample point, Q is a volumetric boiloff rate, $\bar{u}_{ref}$ is the mean wind speed measured at z_{ref}. An explanation of how these values are obtained and how to use them is given in Section 2.5.1. The ranges of the various scaling parameters and test conditions are summarized in Tables 1 and 2 for prototype and model, respectively. For the specific test conditions for each test performed one is referred to in Table 4.

3.1.1. Behavior of CO_2 Model Gas Simulation

Continuous releases made from 1/200 scale models of the representative high dike utilizing CO_2 result in concentrations which agree well with earlier Freon-12-N_2 simulations performed by Neff, et al. (1976). Dilutions measured during Run 11 of the present report at a boiloff rate $\dot{m}$ = 250 lbm/sec fall between Runs 19 and 30 of the earlier report where $\dot{m}$ = 420 lbm/sec and $\dot{m}$ = 160 lbm/sec, respectively. Similarly, results from Run 11R of this report at $\dot{m}$ = 1400 lbm/sec fall between measurements of Runs 9 and 19 where $\dot{m}$ = 2400 lbm/sec and $\dot{m}$ = 420 lbm/sec respectively. These measurements generally exceed values taken behind the 1/400 models under equivalent situations up to a factor of two.

Since in the earlier study by Neff, et al. (1976) Run 1 therin at 1/200 scale and Run 101 at 1/500 scale displayed a similar trend the more recent results suggest a continued significant influence of the tunnel side walls persists for 1/200 scale models.

In order to obtain a comparable characteristic curve among sites of different tests, the test conditions were grouped on the basis of model, release gas flow rates, stability, and simulation gas. Figures 23-1 to 23-4 present CO_2 model gas results in terms of $\chi\ \overline{u}_{ref}\ H^2/Q$ vs. χ/H. The data do follow trends expected for dispersion in the atmosphere. Values fall between or somewhat below Pasquill Diffusion Category C and D.

In Neff, et al. (1976) stable background stratification tended to result in concentration decay rates which approached Pasquill Diffusion Category F. In the present results, there is no significant difference noticeable between the neutral and stable dispersion cases. Since one might expect that a buoyant plume will generate its own entrainment rate this seems reasonable. Perhaps the earlier differentiation noticed for 1/200 scale models is again a result of plume blockage.

3.1.2. Behavior of $He\text{-}N_2$ Model Gas Simulation

Runs 45 to 54 concerned tests made to discern the effects of surface heat transfer characteristics and stratification on $He\text{-}N_2$ model gas releases from 1/400 scale models of the representative high and low dike cases. Figures 23-5 and 23-6 present the $He\text{-}N_2$ model gas results in terms of $\chi\ \overline{u}_{ref}\ H^2/Q$ vs. χ/H as before. The data follow similar trends to the CO_2 release situations. No significant differentiation appears between high and low dike or neutral versus stable stratification.

No consistent influence of the insulated versus the conducting floor conditions could be identified. The effects are thus judged to be small.

3.2 VARIABLE BOILOFF RELEASE RESULTS

A comparison of model data (Case I) with Capistrano Field data is presented in Figures 25 and 26. Curves of mean concentration decay, with height for selected downwind sites of the Capistrano Cases, Representative High Dike, and Representative Low Dike are presented in Figures 27, 28 and 29, respectively. Selected curves of mean concentration decay with distance for the Capistrano Cases and the Representative High Dike are presented in Figures 30 and 31, respectively. Ground contour plots of peak concentration, obtained by visual interpolation, for all tests except those with a dike surface of insulated concrete are presented in Figures 32, 33 and 34. Observed lower flammability limit (LFL = 5 percent) contours as a function of time after the spill are presented for a Representative High Dike and a Representative Low Dike in Figure 35. Figure 36 presents ground contours of the hazard zone (zone in which a peak value of five percent was observed) for the High and Low Dikes under the different conditions tested. Table 6 presents the maximum distance to the lower flammability limit for all the tests performed. Tables 7-1 to 7-11 summarize the maximum peak concentration value observed in each test and the maximum peak at different times observed in each test.

3.2.1. Comparison of Capistrano 044 Field Data with Model Test Data

The model Capistrano Case I test yield consistently higher concentrations than that of Case II test, which is to be expected since it describes a higher boiloff rate. In a comparison of the mean behavior of these model tests to those of the Capistrano 044 Fîeld test, the Case II model results always yield lower concentrations than those observed in the field. When a comparison is made between model Case I and the field, the time and magnitude of highest concentrations observed at most of the test locations is in good agreement. Figures 25 and 26 display the dilution time history of the model Case I and the field situation superimposed upon each other for the test positions (320', 0', 0') and (640', 0', 0') respectively. The three differences observed between the results are (1) the timing of the plume's arrival at the measurement location is not exactly the same, (2) the concentrations in the plumes leading edge for the model are lower than that observed in the field, and (3) the model does not predict the large and intermittent concentrations peaks at late times that were observed in the field. The first two differences may be explained by considering that diffusion of air across the perforated release plate into the cavity below occurs between model tests. This would result in low concentrations of model gas within the plenum being released at the start of each test. These lower concentrations would be entrained by the wind and swept downwind faster than the main plume's bulk, thus giving the appearance of a faster travelling plume with low concentrations at the leading edge. These arguments are reinforced by noting that in the model the first major peak (the plume actual leading edge) occurs at the same time as that observed in the field. The third major difference, that of high peaks observed at late times for the field case, may be do to gustiness and changes in wind direction and speed that are present in the atmosphere but not present in the wind tunnel.

The above inconsistencies between model and prototype may not be of major importance for hazard evaluation since in the plume leading edge where the highest concentration occurs the model and prototype agree quite well. Similar agreement for model and prototype was observed for test locations (320', 0', 10'), (320', -80', 0'), (640', -100', 0') but for location (160', 0', 0') the agreement was poor. The field data observed a maximum peak of 47 percent while the model data observed a maximum peak of 17 percent. This inconsistency may be the result of bad field data, improper modeling of the ground and release geometry, or the large effective sampling area on the instantaneous concentration sampling probe. If the plume thickness was significantly less than the height of the effective sampling area of the probe the high concentrations at the ground level may be under estimated.

3.2.2. Comparison of High and Low Dikes

The existence of a bimodal plume distribution as cited by Neff, et al. (1976) for the High and Low Dikes is once again observed in the ground contour plots of concentration for the Representative Low and High Dikes (Figures 33 and 34). The characteristic-signature of this bimodal distribution disappears with a low wind speed for the High Dike, whereas it is still a very strong characteristic with Low Dike at a low wind speed. For the Low Dike, this bimodal distribution may be both a function of the aerodynamic flow pattern around the tank and the geometric layout of the square dike being placed at a 45° angle to the wind direction. As a result of uneven spreading of the plume from the Low Dike, the distances to the LFL (Table 6) are slightly greater than those observed for the High Dike under similar meteorological conditions and similar boiloff rates (Figures 13 and 16). By inspection of observed hazard zone contours (Figure 36) this effect may be of greater importance than shown in Table 6 as the distance to LFL is still increasing at the most lateral sample position tested for neutral flow. If the wind direction at the Low Dike was at 0°, this effect of bimodal spreading possibility would not be as pronounced, thus yielding a hazard zone distance similar to that of the High Dike. The effects of the plume release at a more elevated plane and the increased aerodynamic turbulence of the High Dike do not appear to reduce its hazard zone over that of the Low Dike. But it should be clarified that for the boiloff rates considered, the volume of spilt LNG is much greater for the High Dike than for the Low Dike. The modeling of boiloff rates for utilization of concrete and insulated concrete floors and walls in the High Dike were very effective in reducing the hazard zone--see Table 6.

3.3 VISUALIZATION RESULTS

Visual examination of gaseous plume outlines tagged with a smoke tracer or moisture provide qualitative guidance concerning the significance of different parameters. Plume behavior has been recorded photographically on black and white stills and 16 mm color film where appropriate. Print copies and film records have been forwarded separately to R & D Associates. Only those black and white views which display a typical behavior pattern are included herein since report reproduction methods limit the quality of half-tone copies.

3.3.1 Tank/Dike Heat Transfer Results

Film records of Runs 30 to 42 listed in Table 3 document the visual behavior of transient boiloff releases of cooled He-N_2 from High and Low Dike LNG tanks. Releases from the precooled steel tank models produced dense plumes which rolled over the dike lips and moved downward with a shallow, wide cross-section. There was no evidence of plume liftoff. The appearance of the transient boiloff plume some moments after passing a given downwind station looked very similar to the structure and size of continuous release plumes of equivalent boiloff rate examined by Neff, et al. (1976).

When a room-temperature steel model or a room-temperature plastic model was utilized under the same release conditions as above, no visible plume was obtained. Apparently the precooled He-N_2 warms significantly inside the model/dike walls; since plume visualization depends upon moisture condensation, no visible plume appeared. This behavior confirms the earlier estimates that heat transfer time scales during laboratory release will be significantly less than the equivalent release and dispersion time scale. This effect is an apparently unavoidable result of different governing physics and scaling laws for dispersion versus conduction within the model.

3.3.2 Ground Slope Effects

Table 11 summarizes the flow visualization tests. The picture numbers refer to the flow visualization photographs submitted separately to R & D Associates. Pictures 1 through 24 illustrate the effects of ground plume geometry. Pictures 1A through 24A present the same conditions on a flat (zero slope) surface. All pictures presenting a side-on view were taken first. The test runs were then repeated for the overhead sequence. A comparison of the side-on and overhead pictures taken under the same conditions indicates a lack of repeatability of the basic shape of the plume (e.g., Pictures 3 and 4). Two caveats are in order, however. First the lighting conditions (and shadows) make the overhead pictures difficult to interpret; secondly, permanent light-colored blotches, unrelated to the presence of LNG vapor, appear in both sets of photographs.

The sloped section of the wind tunnel floor begins about 7 feet upwind of the model and ends about 15 feet downwind. Thus, one would expect that for a range of wind speeds enough vapor would accumulate downstream (upslope) to overcome the wind pressures. The vapor should then begin to travel upwind. Since this phenomenon is an unstable one, it is not inconceivable that the transients associated with the start-up process could influence the final steady state condition. Also, random perturbations could conceivable cause the vapor motion to switch from an upwind to a downwind character.

In addition to the lack of repeatability, a marked asymmetry in the vapor cloud was occasionally observed (e.g., Picture 8A, overhead). This type of asymmetry is almost certainly caused by a non-planar perturbation in the wind field, either associated with the vapor injection (a Coanda attachment perhaps) or irregularities in the ramp construction. In either case, such asymmetries could probably be removed in highly controlled experiments. Symmetric vapor clouds are illustrated in Pictures 9A through 12A. A comparison of these pictures, which were taken under flat terrain conditions, with Pictures 9 through 12 (2 percent slope) indicates the effect of ground slope, which for the higher boiloff rates resulted in upwind travel of the vapor.

The location of the upwind boundary of a dense plume on a rising slope is a result of the balance between gravity forces and the drag forces imposed on the cloud eddy by the approach wind. Since for a continuous release the total cloud excess weight continues to increase it is not surprising that for significant boiloff rates upstream flow eventually results. Thus the cloud behavior becomes a complicated function of Froude number, Reynolds, and time. A short finite release even at a large boiloff rate may not be expected to continue upwind spread as its cross-sectional (or frontal area) increases since this increases the drag by the approach wind.

Figure 37 displays the typical behavior of a dense plume emitted from the 1/400 Representative High Dike Model at two prototype windspeeds. In the upper photograph although plume reflection from the side walls has occurred upwind motion is minimal. At the lower wind speed, however, the dense plume develops its own reverse circulation and reverse wake near the surface! Notice the circular wave produced by the dense spill at the base of the tank. Figure 38 displays the equivalent conditions as the previous figure but for a zero ground slope.

3.3.3 Upwind Tank Influence

Pictures 25 through 36 from Table 11 show the effect of two upstream obstacles on the shape of the vapor cloud. A comparison of, for example, Pictures 21 through 24 with Pictures 25 through 28 seem to suggest that the presence of obstacles tends to lessen the effects of ground slope. In addition, they seem to discourage the formation of asymmetrical vapor clouds. The presence of one upstream obstacle does not appear to have as significant an influence on the vapor cloud as does the presence of two obstacles.

The diluting influence of added wake turbulence is not unexpected. Earlier investigators have suggested effective increases in plume standard deviation weighted by obstacle size and upwind obstacle. One expects increases proportional to

$$\sigma_{obstacle} \simeq \sigma_{wo\ obstacles} \times (1 + CAf(\Delta x))$$

where A = cross sectional area of obstacle

$f(\Delta x)$ = decreasing function of separation distance

C = constant of order one.

3.3.4 Buoyant Plume Liftoff Behavior

Whether or not a buoyant plume or puff can lift itself off the ground in the presence of a shear flow depends upon the buoyancy induced forces compared with the velocity induced pressures on the buoyant gas cloud. More than fifty-eight combinations of source configurations, and velocity, and plume flow rate were considered to evaluate the behavior of a buoyant gas versus a neutrally buoyant gas. Table 10 records the estimated distance to plume lift off for these cases. Thirty-four cases of interest were recorded on black and white film. Typical lift off behavior is displayed in Figure 39.

Since plume kinematics may be expected to be governed by buoyancy and inertial forces these results have been sealed by the relevant buoying length scale, ℓ_b. Hence,

$$\frac{x}{\ell_b} = \frac{x}{\frac{g\Delta\rho Q}{\rho_a \bar{U}^3}}$$

versus

$$Fr = \frac{\rho_a \bar{U}^3 W}{g\Delta\rho Q}$$

has been plotted in Figure 40. The data clearly show that for conditions to the right of the solid line a buoyant plume may be expected to remain near the ground surface; whereas for low windspeeds or high buoyant flow rate situations lift off may occur for conditions to the left of the line.

REFERENCES

American Gas Association (1974), "LNG Safety Program, Interim Report on Phase II Work," Report on American Gas Association Project IS-3-1, Battelle Columbus Laboratories.

Blackshear, P. L., Jr. and Fingerson, L. (1962), "Rapid Response Heat Flux Probe for High Temperature Gases,: ARS Journal, November, 1962, pp. 1709-1715.

Brown, G. L. and Rebollo, M. R. (1972), "A Small, Fast Response Probe to Measure Composition of a Binery Gas Mixture," AIAA Journal, Vol. 10, No. 5, pp. 649-652.

Cermak, J. E. (1975), "Applications of Fluid Mechanics to Wind Engineering, A Freeman Scholar Lecture," J. of Fluids Engineering, Vol. 97, Ser. 1, No. 1, pp. 9-38.

Hall, D. J., Barrett, C. F., and Ralph, M. O. (1975), "Experiments on a Model of an Escape of Heavy Gas," Warren Spring Laboratory Report CR882 (AP), Dept. of Trade and Industry, United Kingdom.

Kuretsky, W. H., (1967) "On the Use of an Aspirating Hot-Film Anemometer for the Instantaneous Measurement of Temperature," Thesis, Master of Mechanical Engineering, University of Minnesota, Minneapolis.

Neff, D. E., Meroney, R. N., and Cermak, J. E. (1976), "Wind Tunnel Study of Negatively Buoyant Plume Due to an LNG Spill," Report Prepared for R & D Associates, California, Fluid Dynamics and Diffusion Laboratory Report CER76-77DEN-RNM-JEC22, Colorado State University, Fort Collins, 241 p.

Plate, E. J. and Cermak, J. E. (1963), "Micro-Meteorological Wind-Tunnel Facility: Description and Characteristics," Fluid Dynamics and Diffusion Laboratory Report No. CER63-EJP-JEC9, Colorado State University, Fort Collins.

F I G U R E S

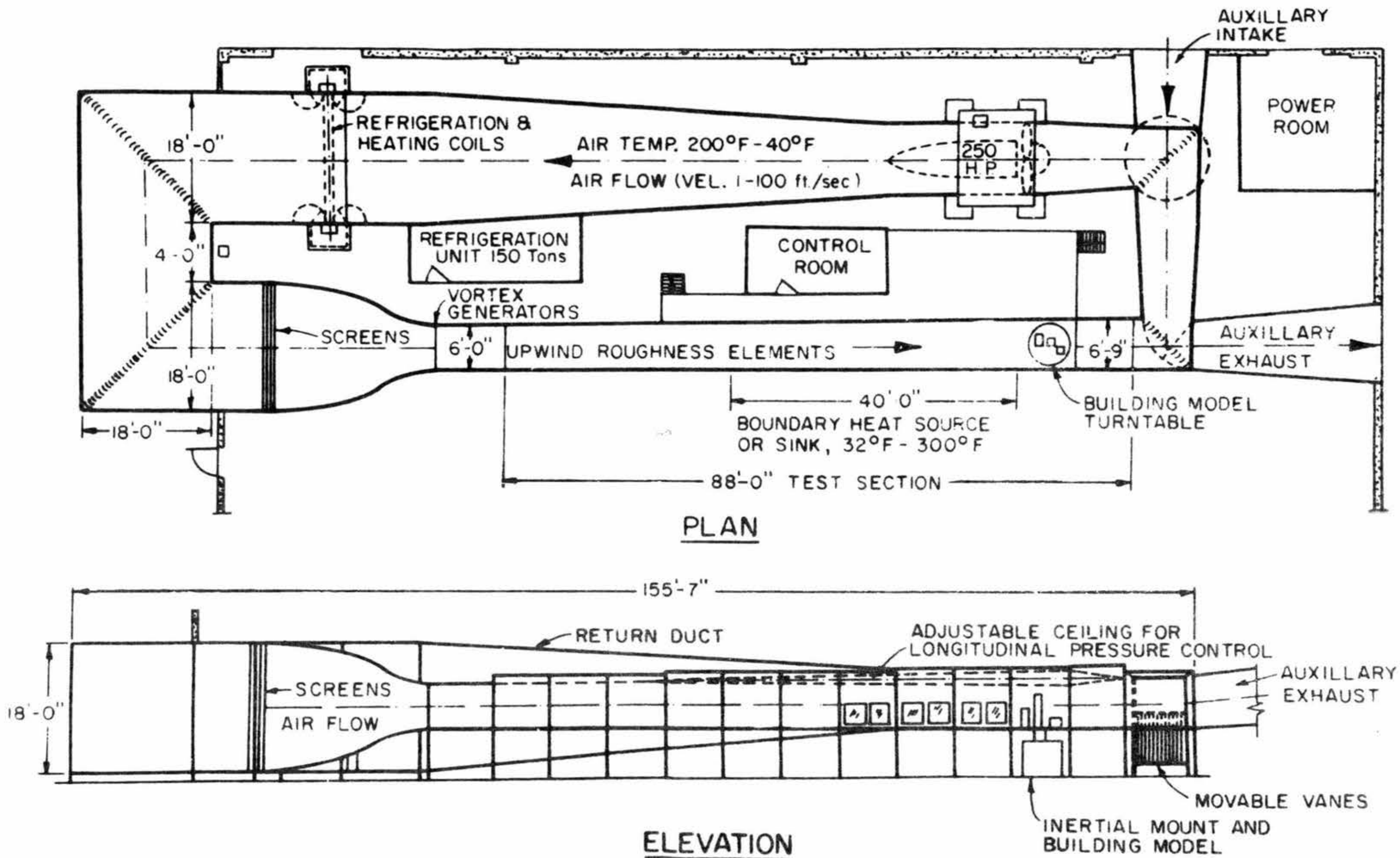

Figure 1. The Meteorological Wind Tunnel

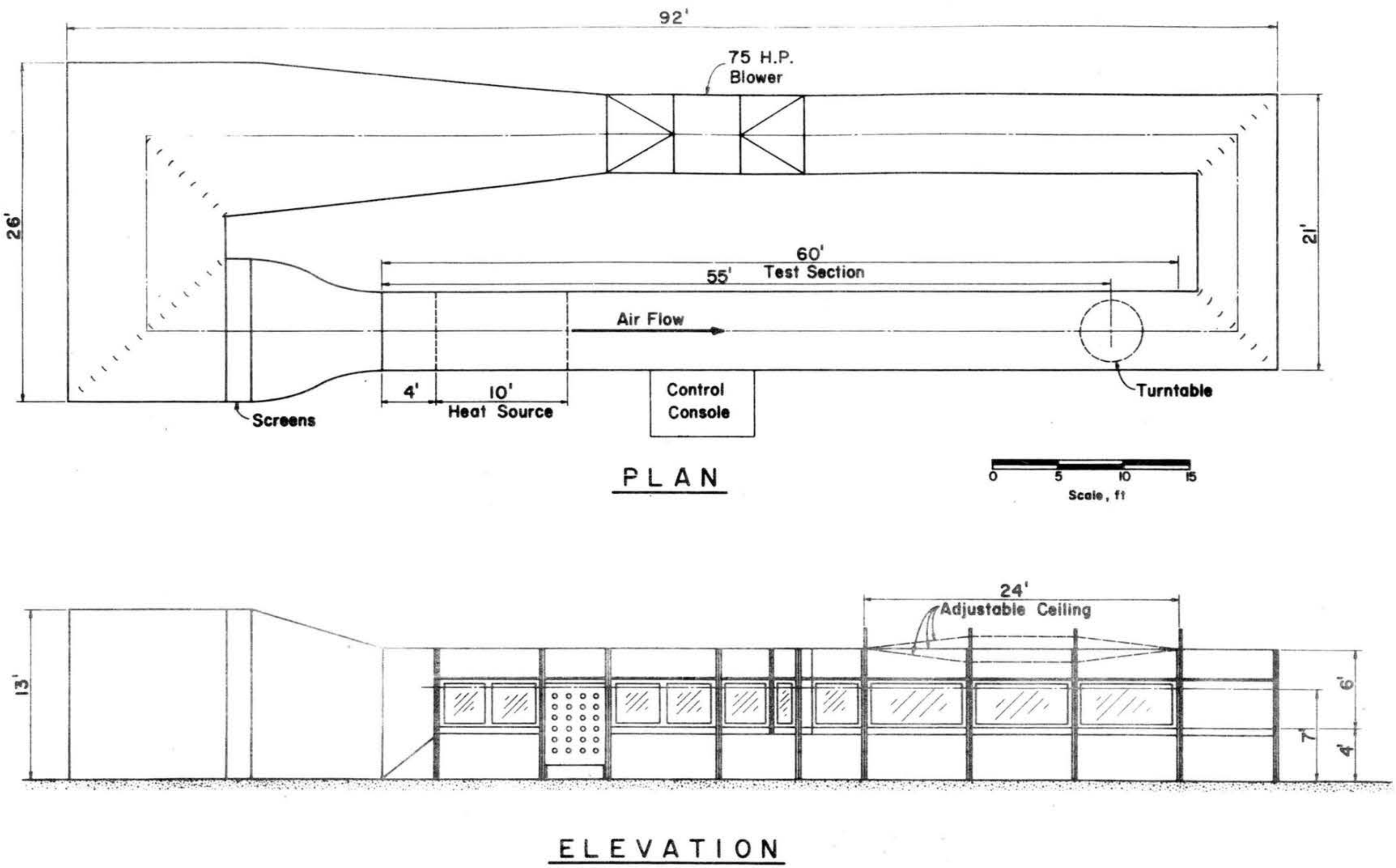

Figure 2. The Industrial Wind Tunnel

Capistrano Test Position Locations

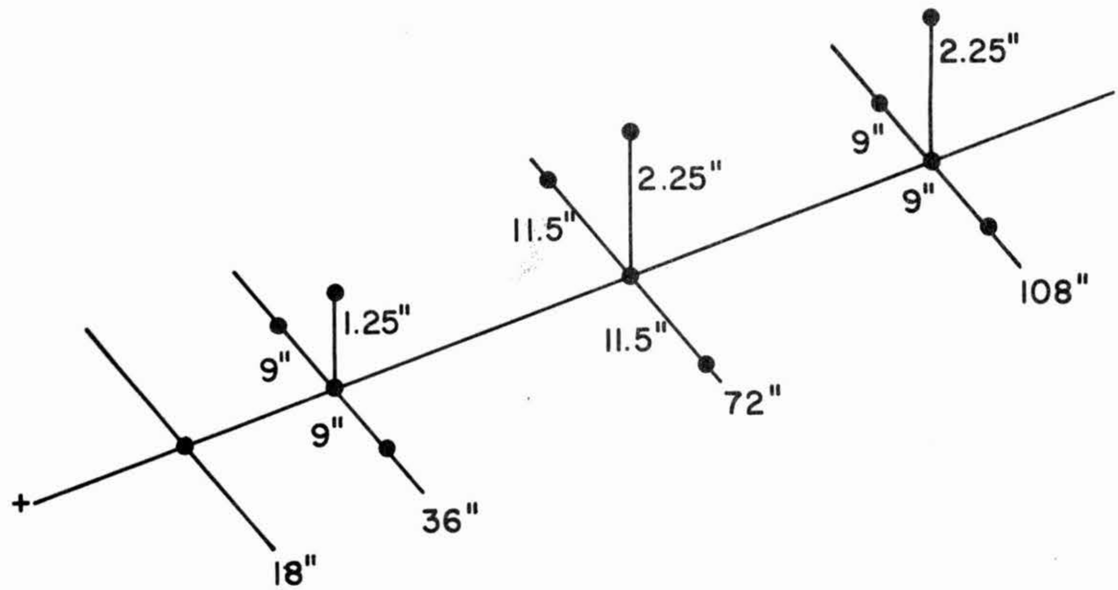

1: 400 Scale Test Position Locations

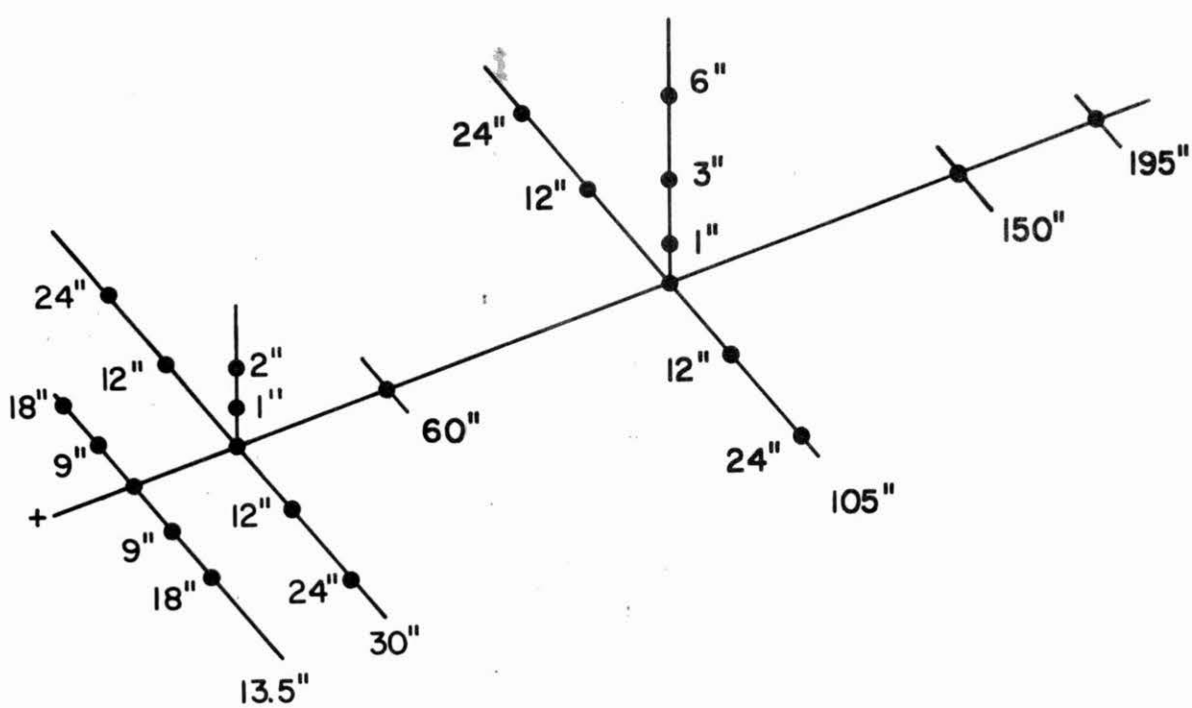

Figure 3. Coordinates for Mean Concentration Measuring Locations

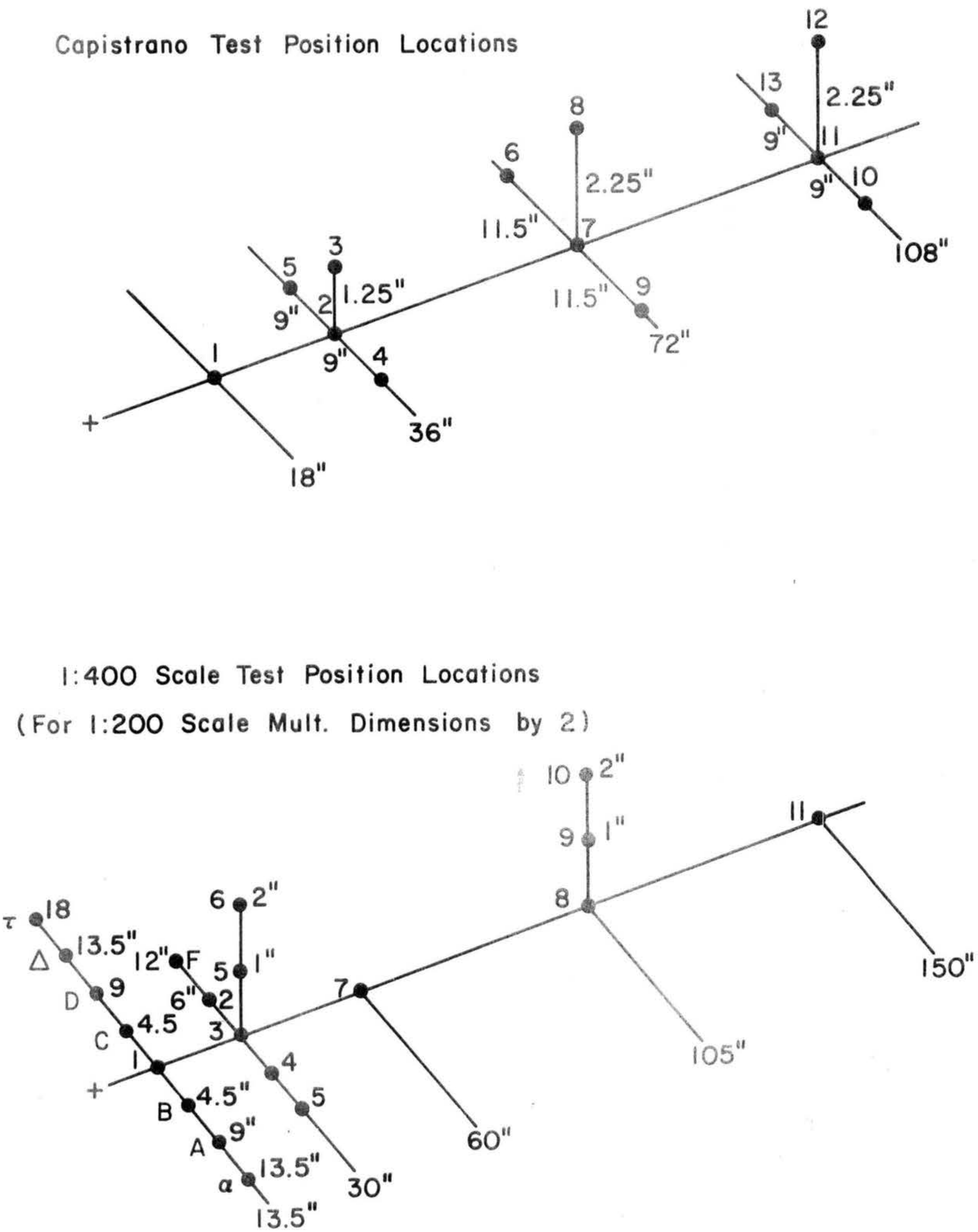

Figure 4. Coordinates for Instantaneous Concentration Measuring Locations

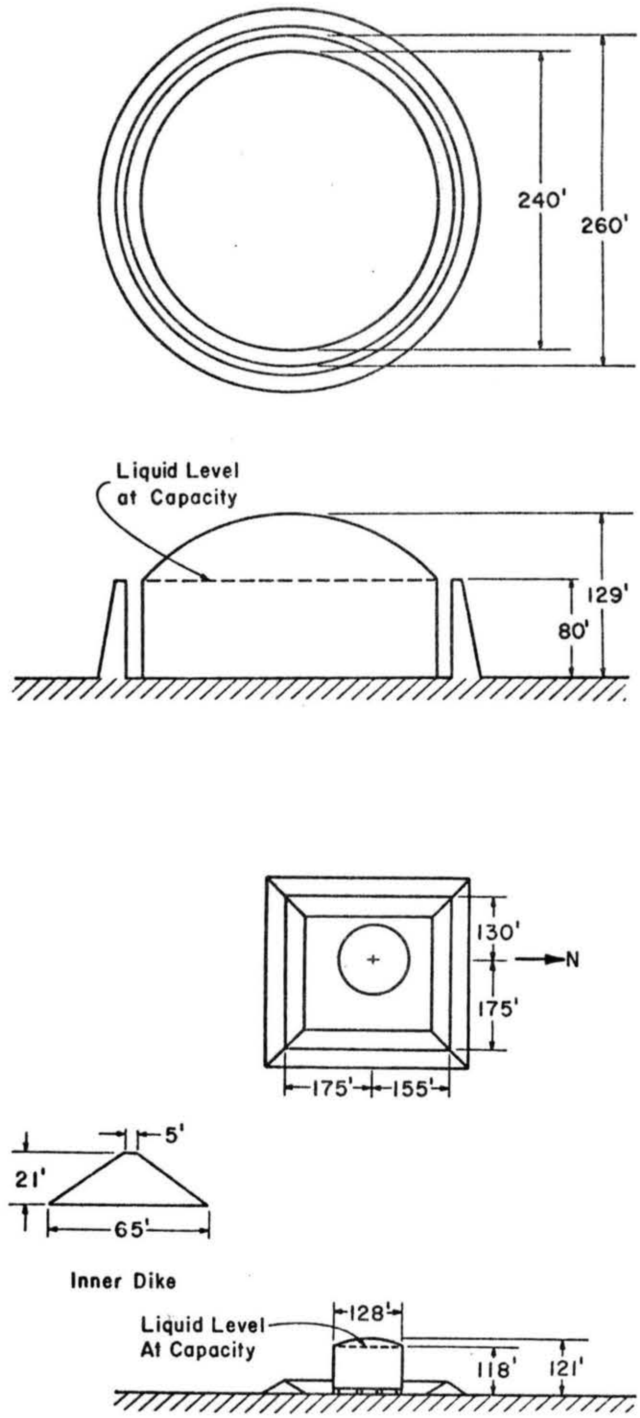

Figure 5. Representative High Dike and Representative Low Dike

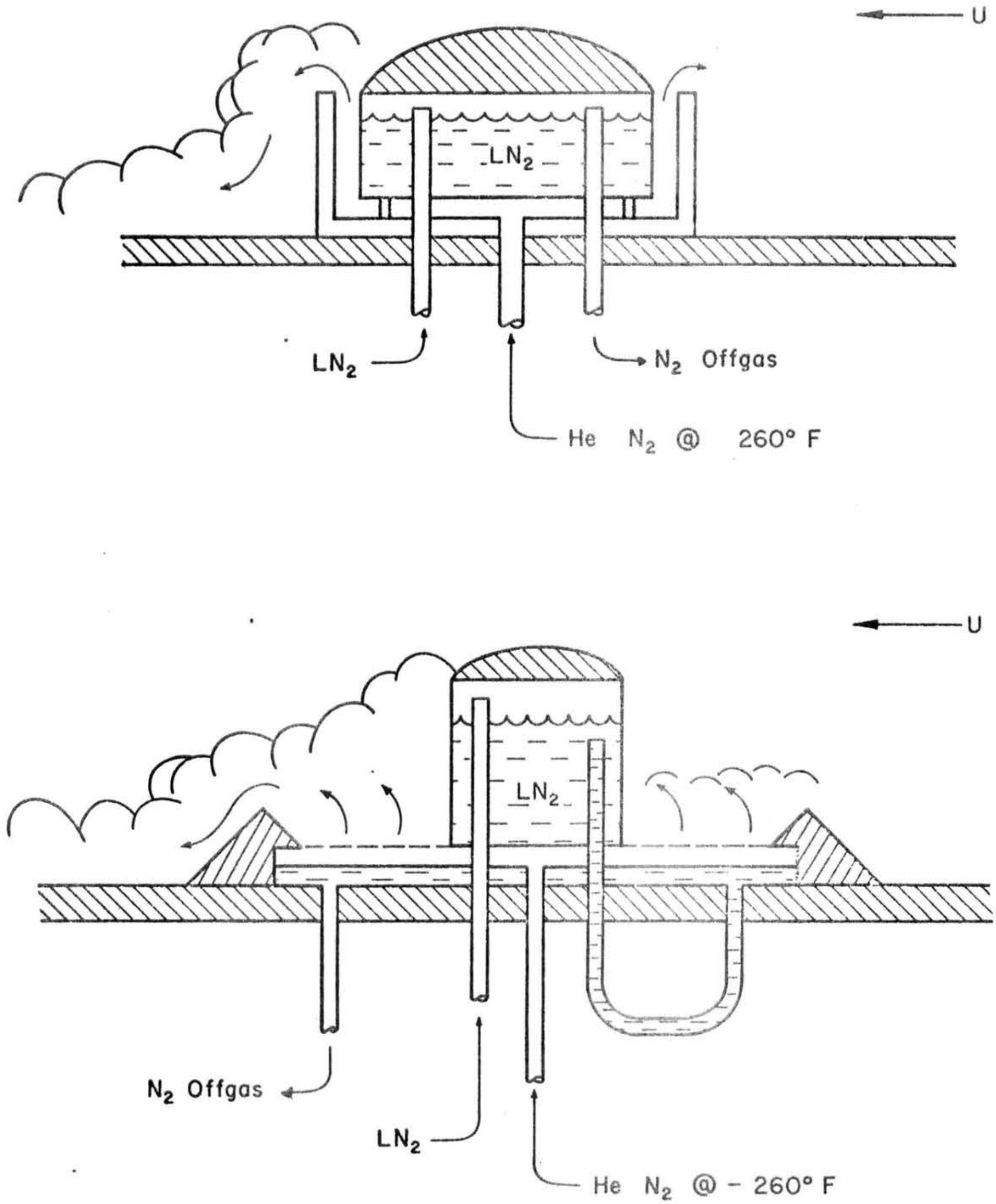

Figure 6. High and Low Dike Models for Simulation with Helium-Nitrogen Gas Mixture

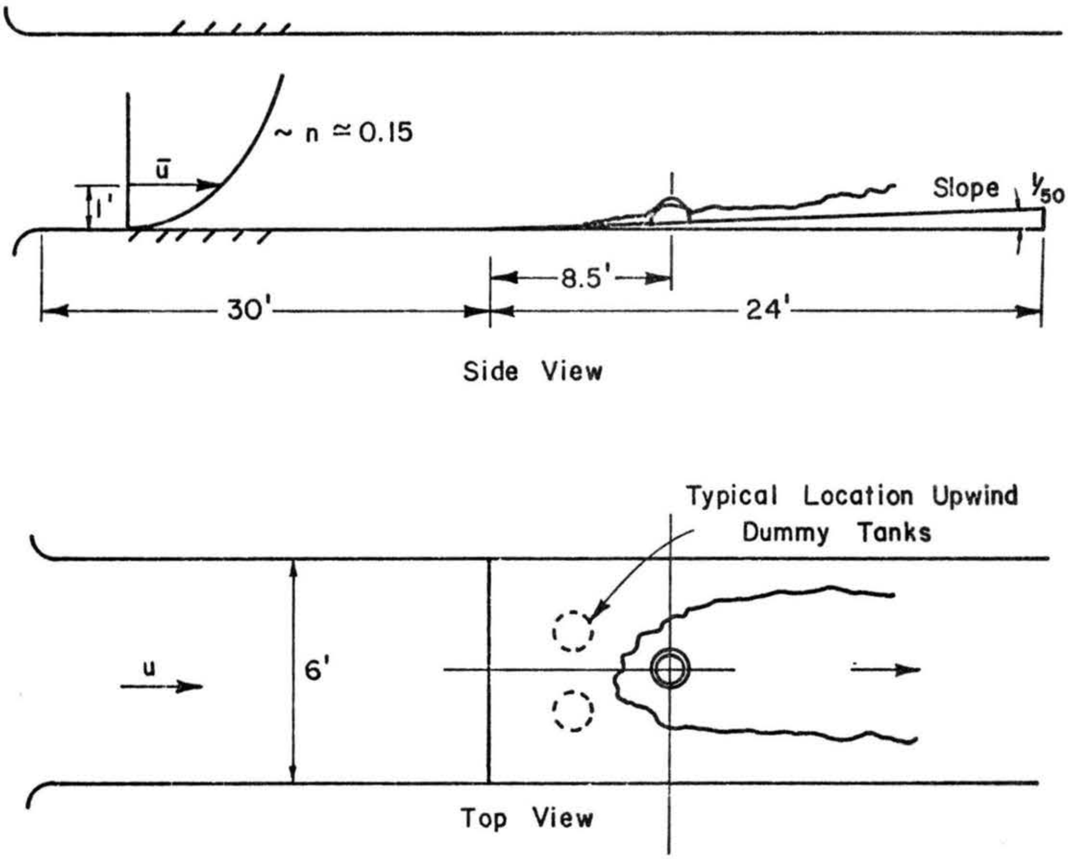

Figure 7. Sketch of Ramp Construction

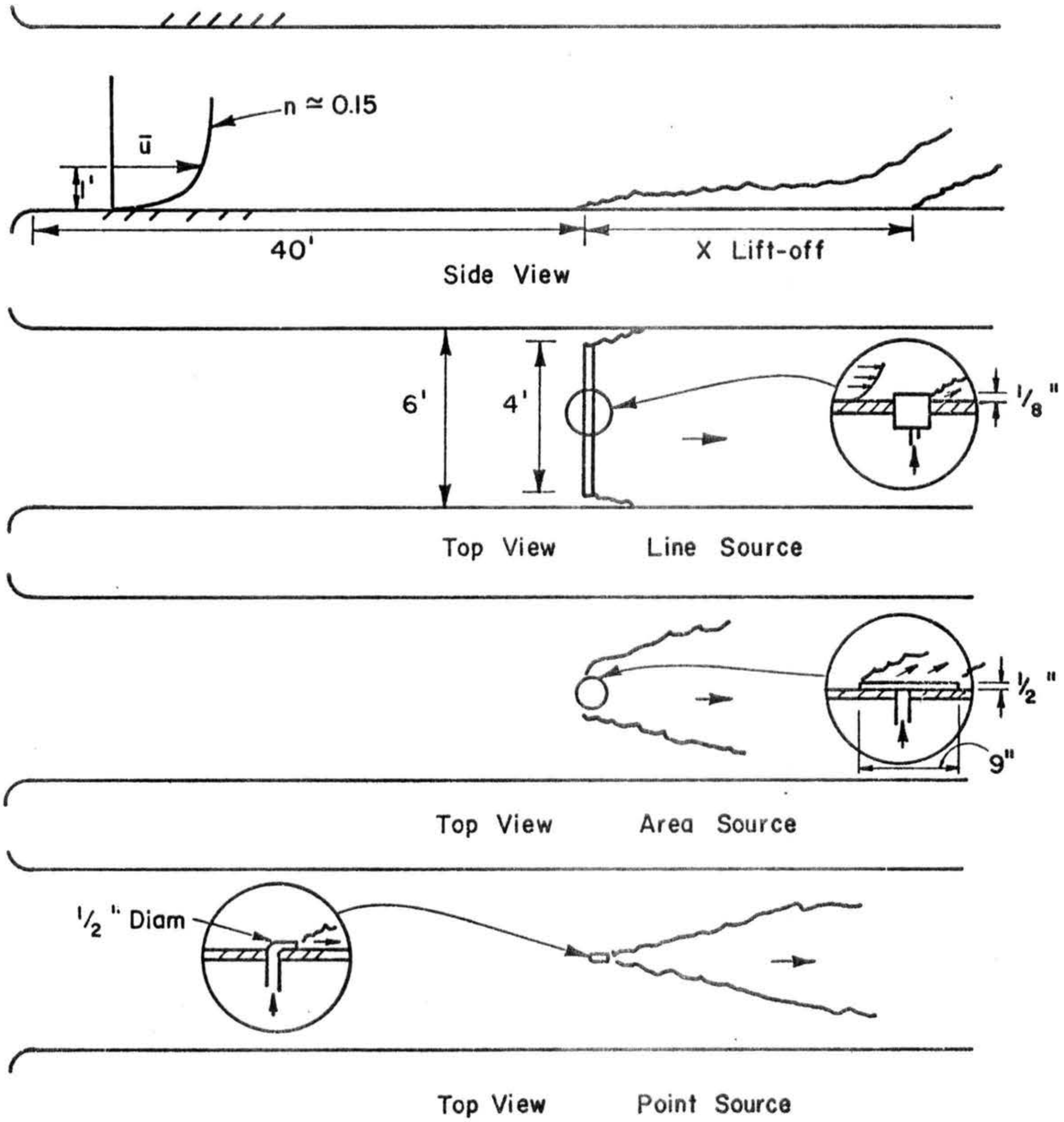

Figure 8. Sketch of Line, Area, and Point Source Configurations

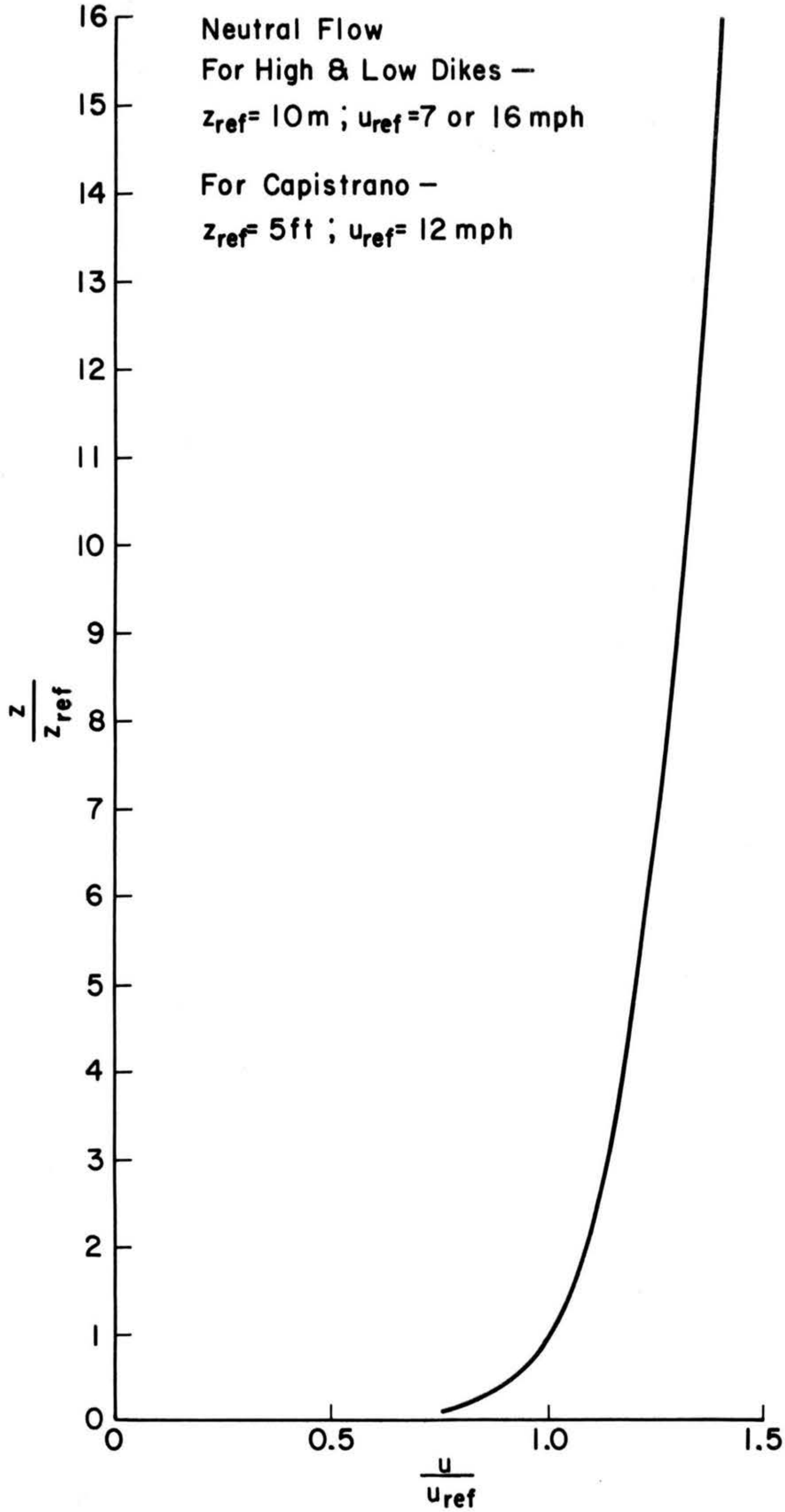

Figure 9. Typical Velocity Profile for Neutral Flow

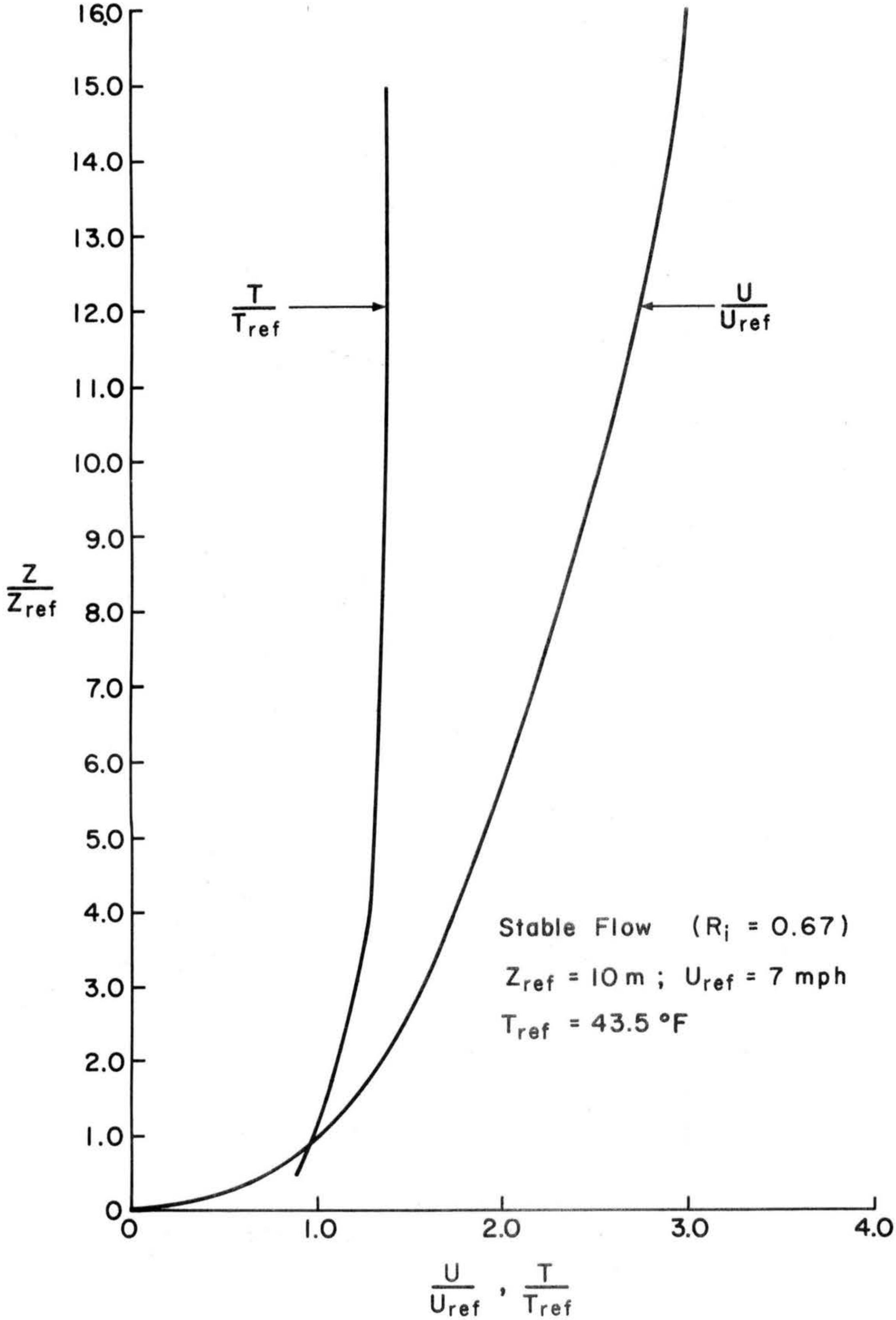

Figure 10. Typical Velocity and Temperature Profile for Stable Flow

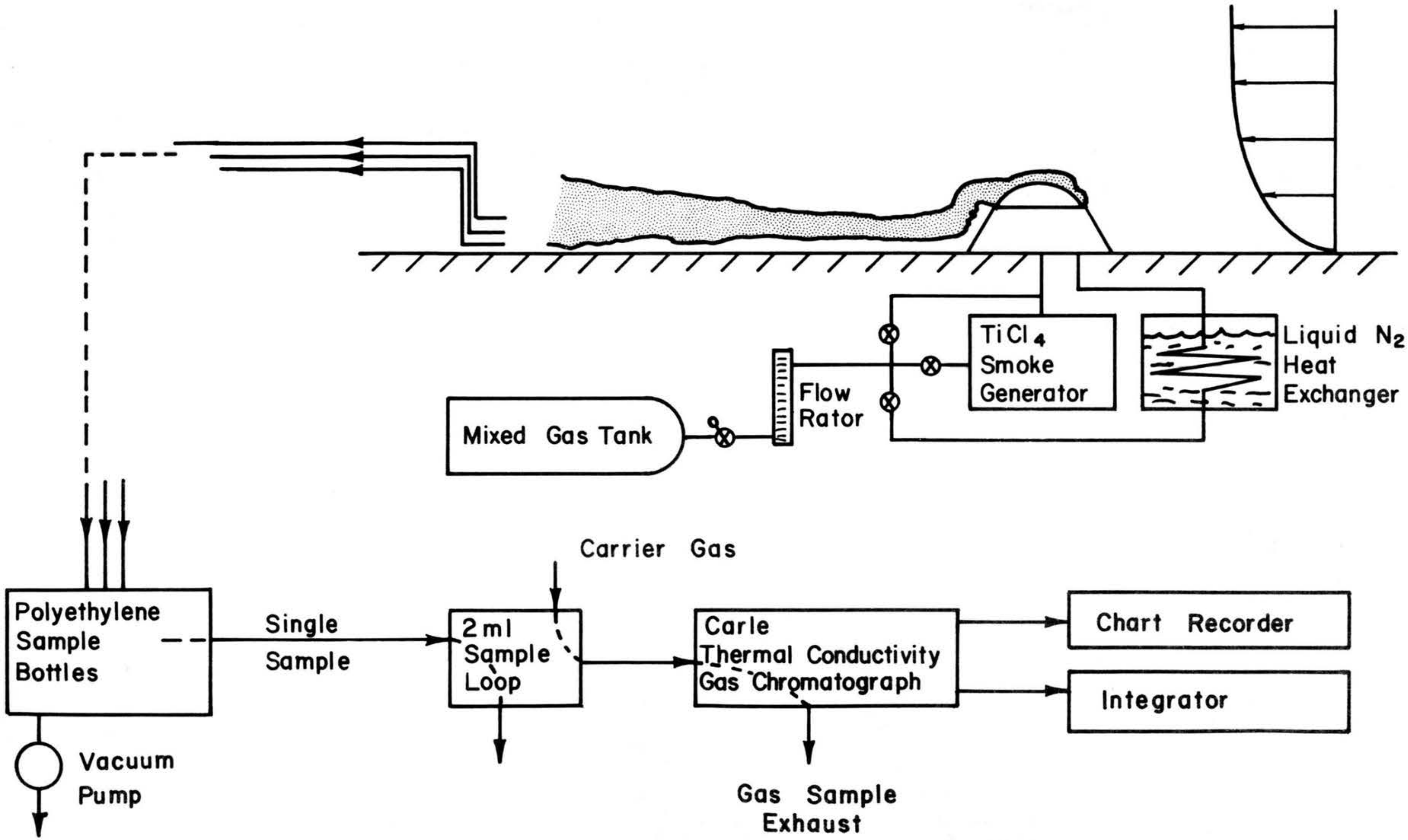

Figure 11. Flow Chart of Mean Concentration Sampling System

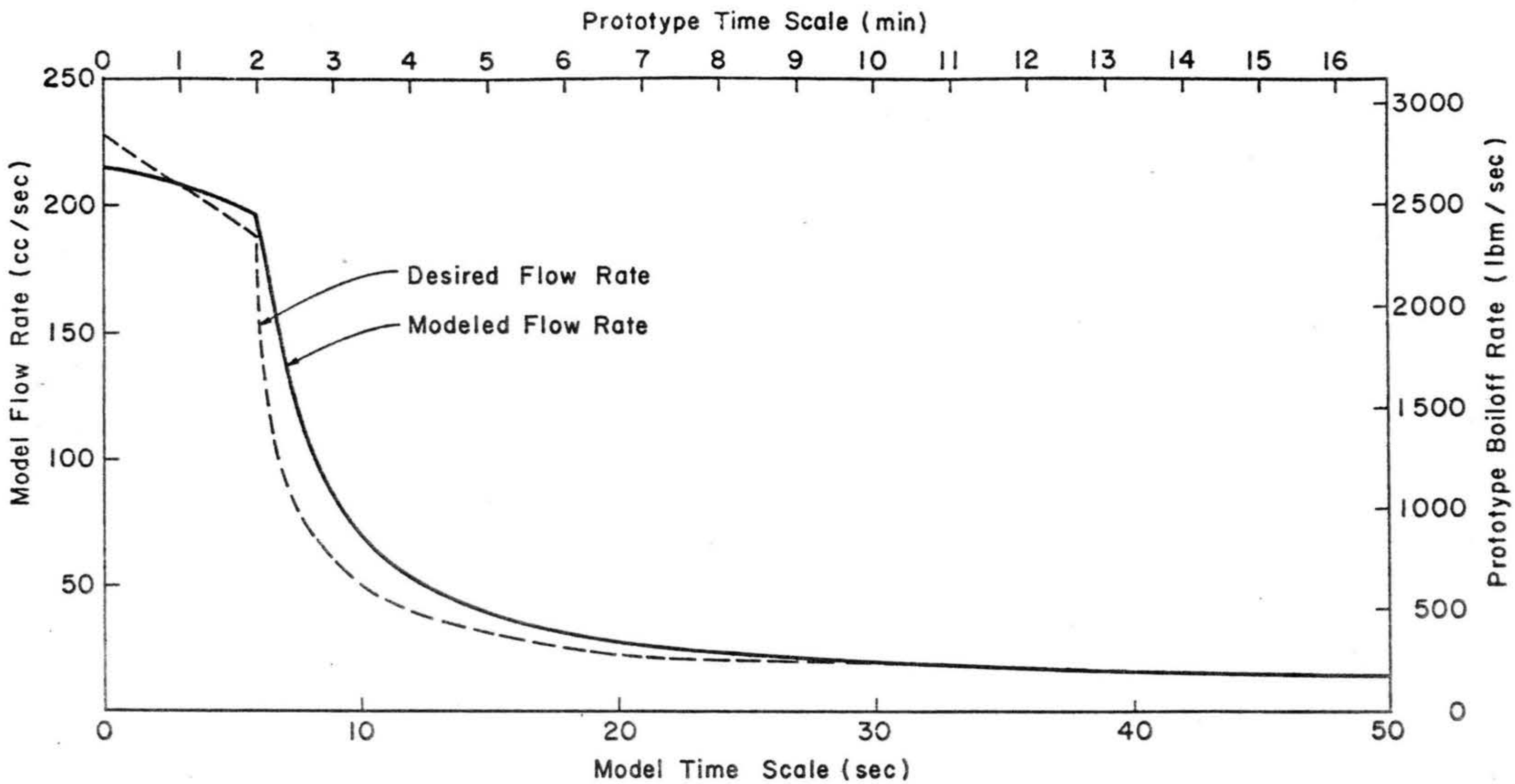

Figure 12. High Dike Gas Release Rates for Model and Prototype for a Spill on Soil

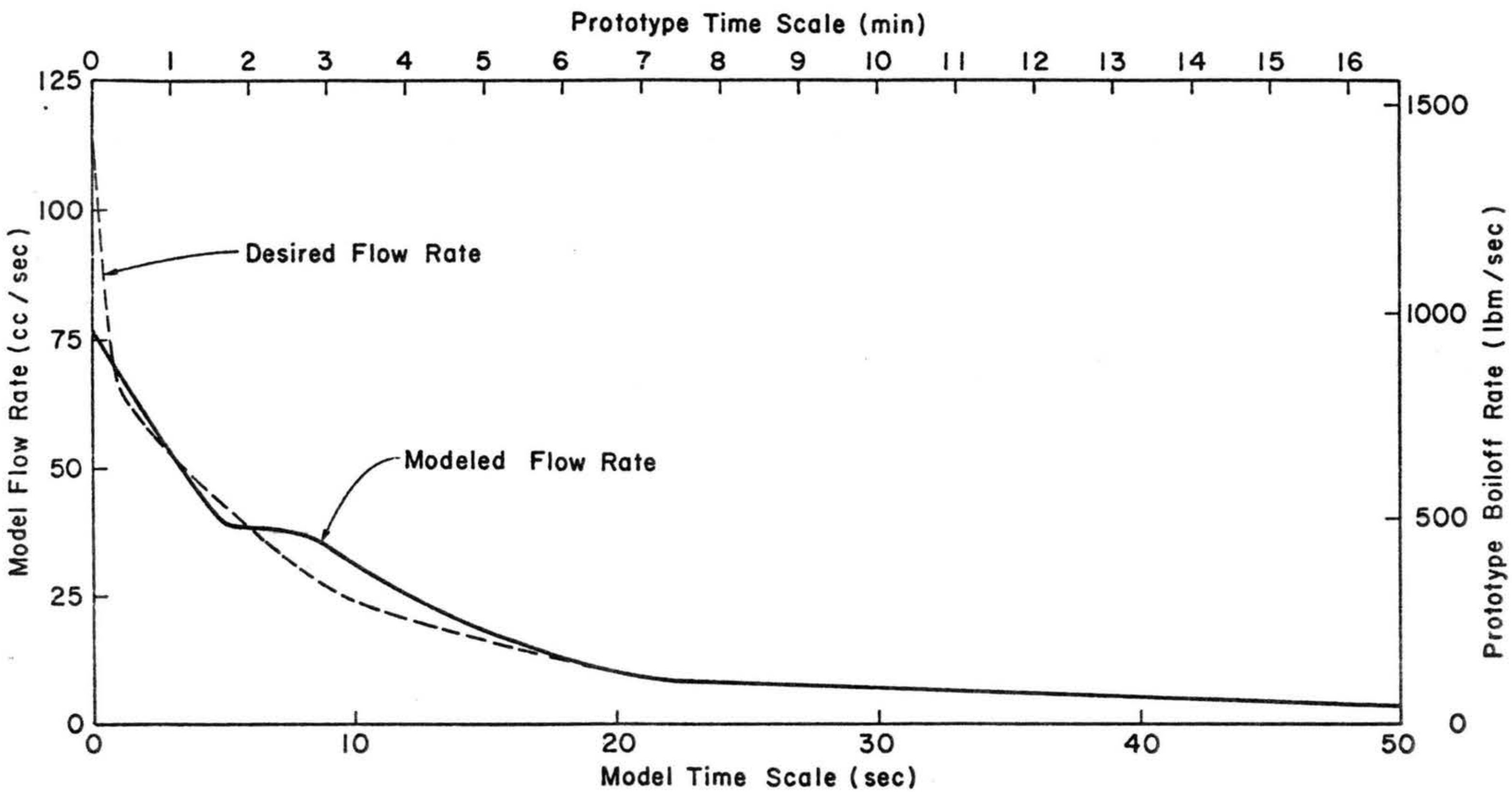

Figure 13. High Dike Gas Release Rates for Model and Prototype for a Spill on Concrete

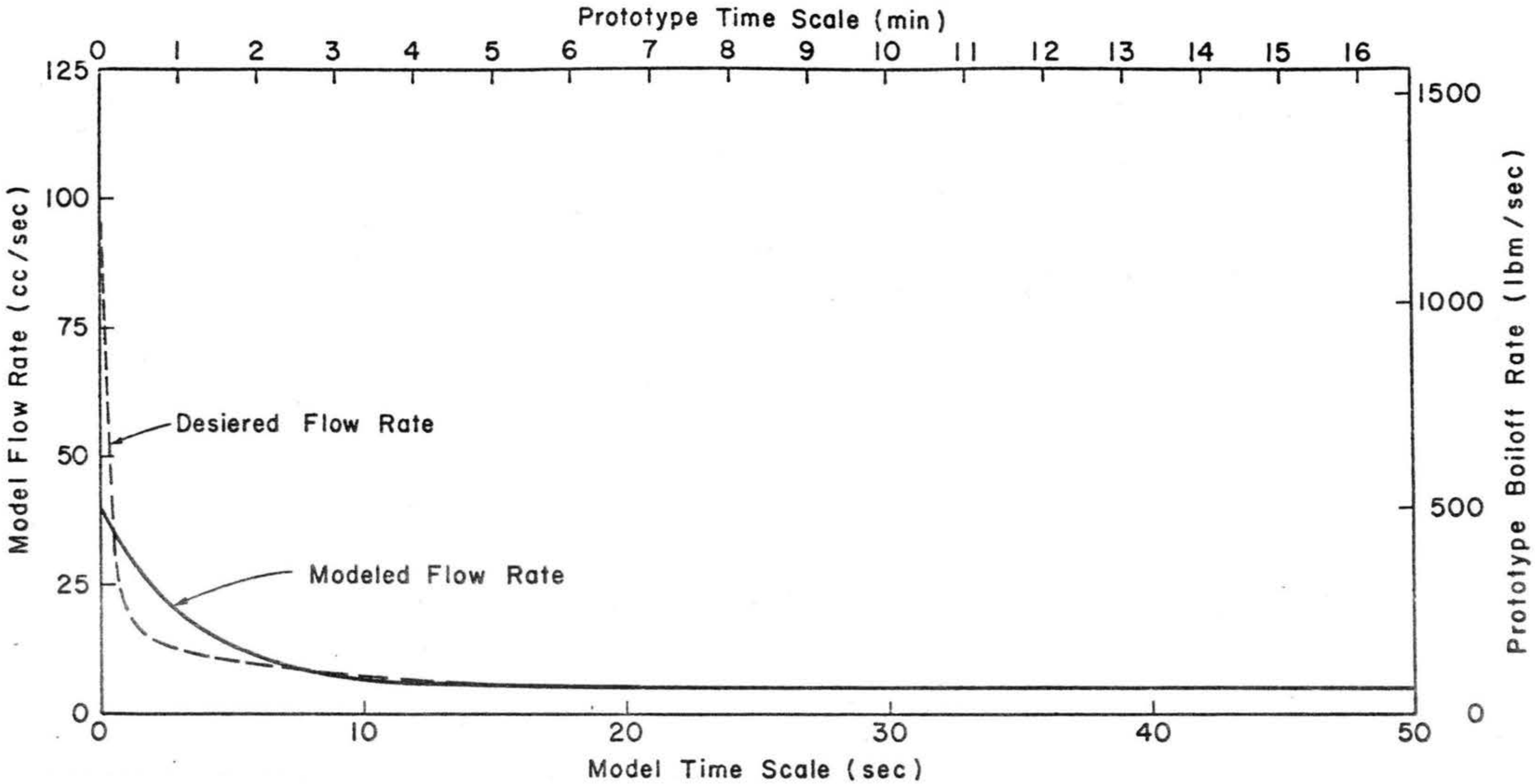

Figure 14. High Dike Gas Release Rates for Model and Prototype for a Spill on Insulated Concrete

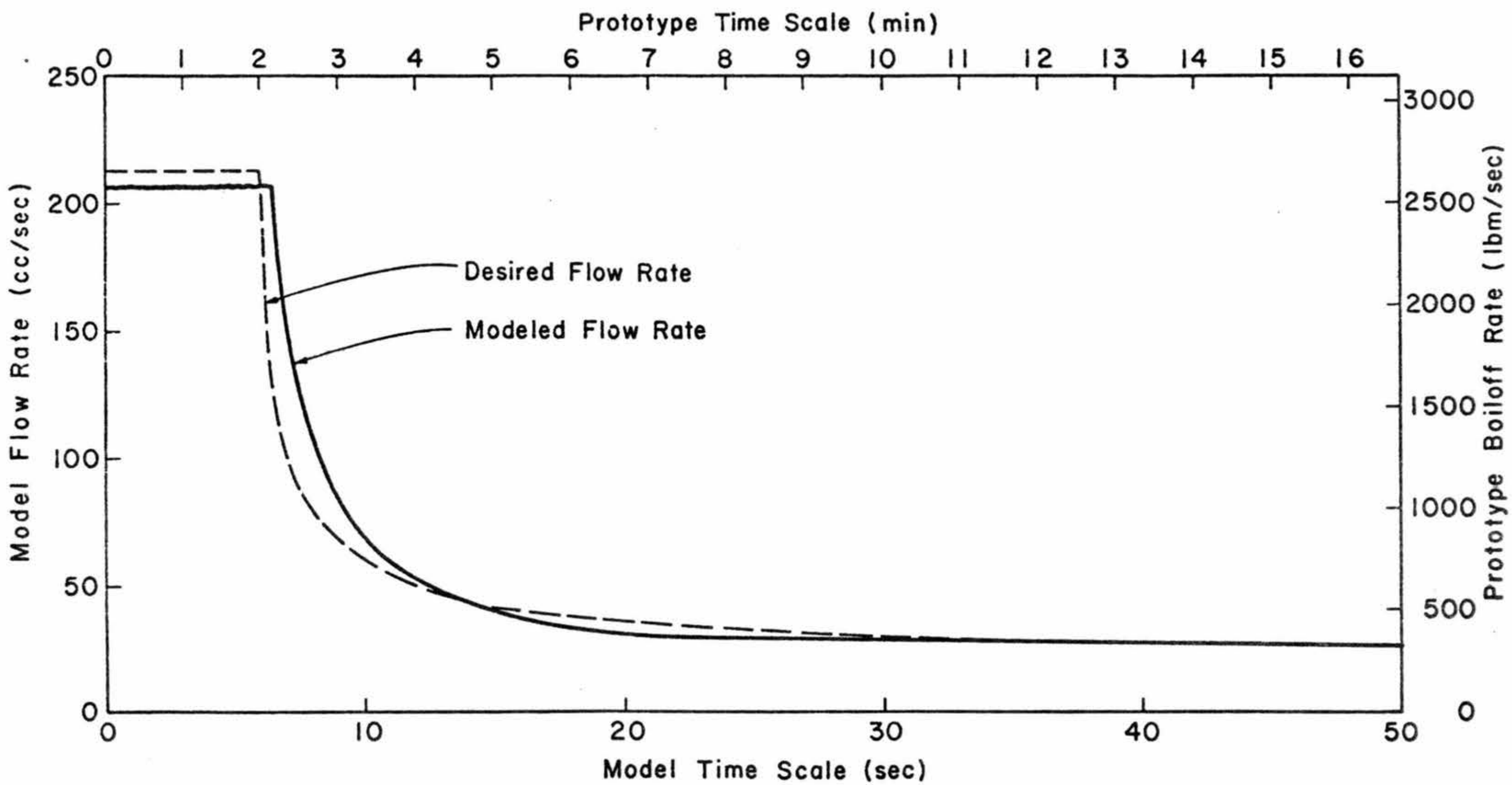

Figure 15. Low Dike Release Rates for Model and Prototype for a Spill on Soil

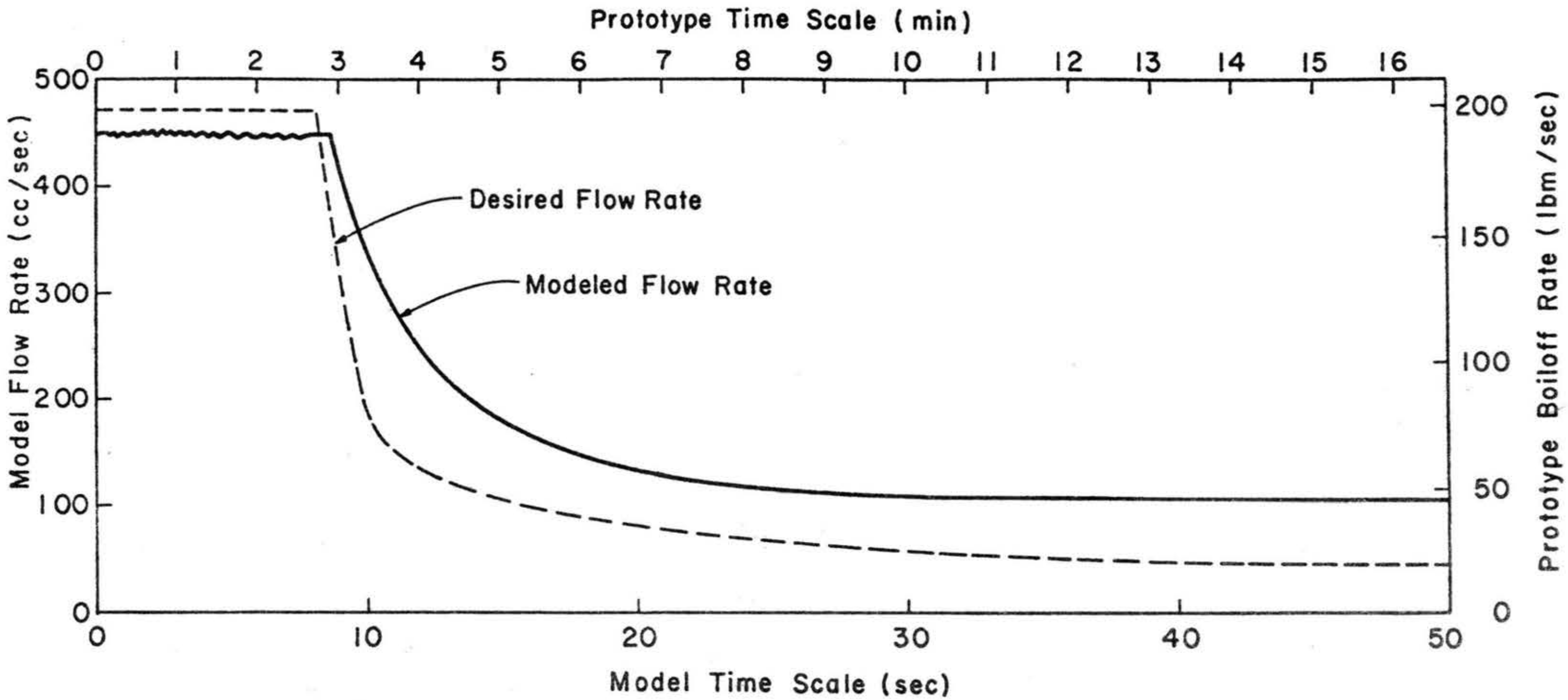

Figure 16. Capistrano 044 Gas Release Rates for Model and Prototype for Case I

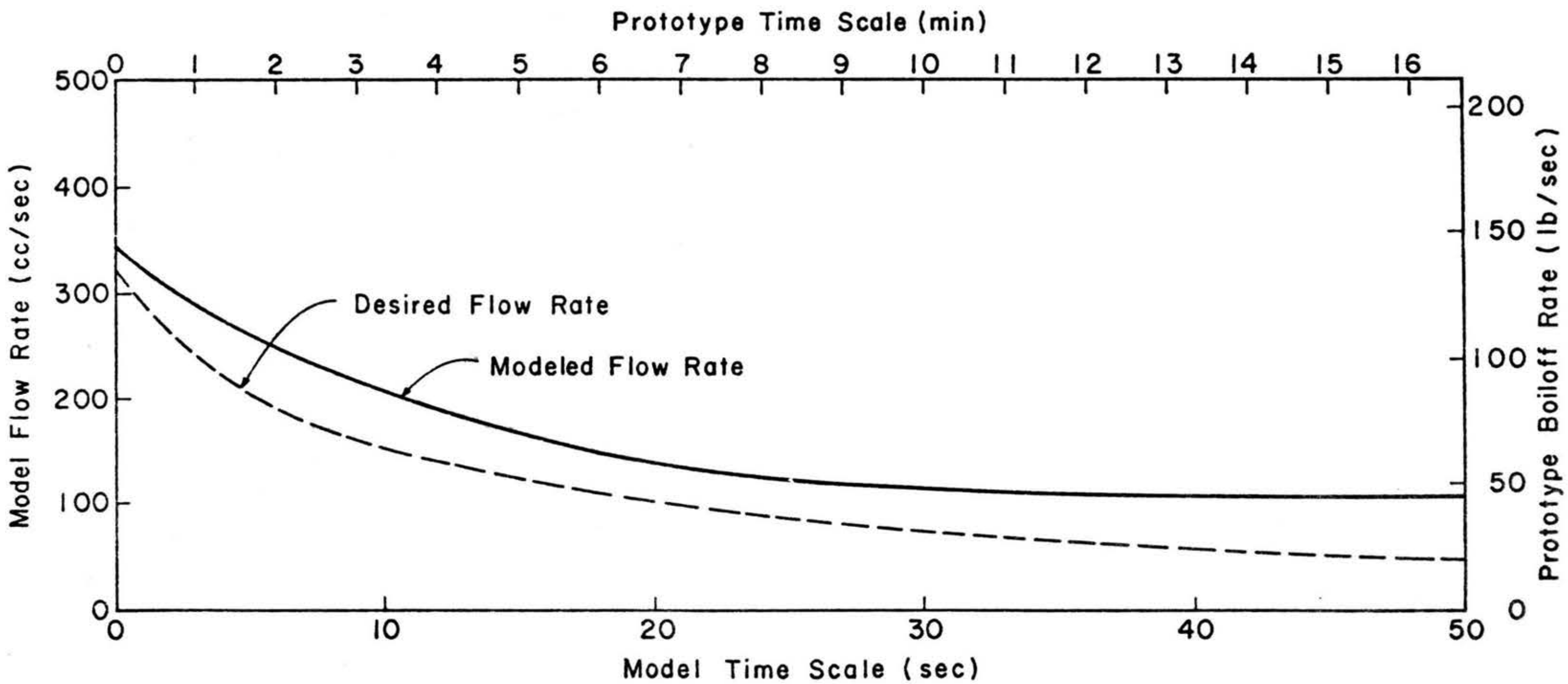

Figure 17. Capistrano 044 Gas Release Rates for Model and Prototype for Case II

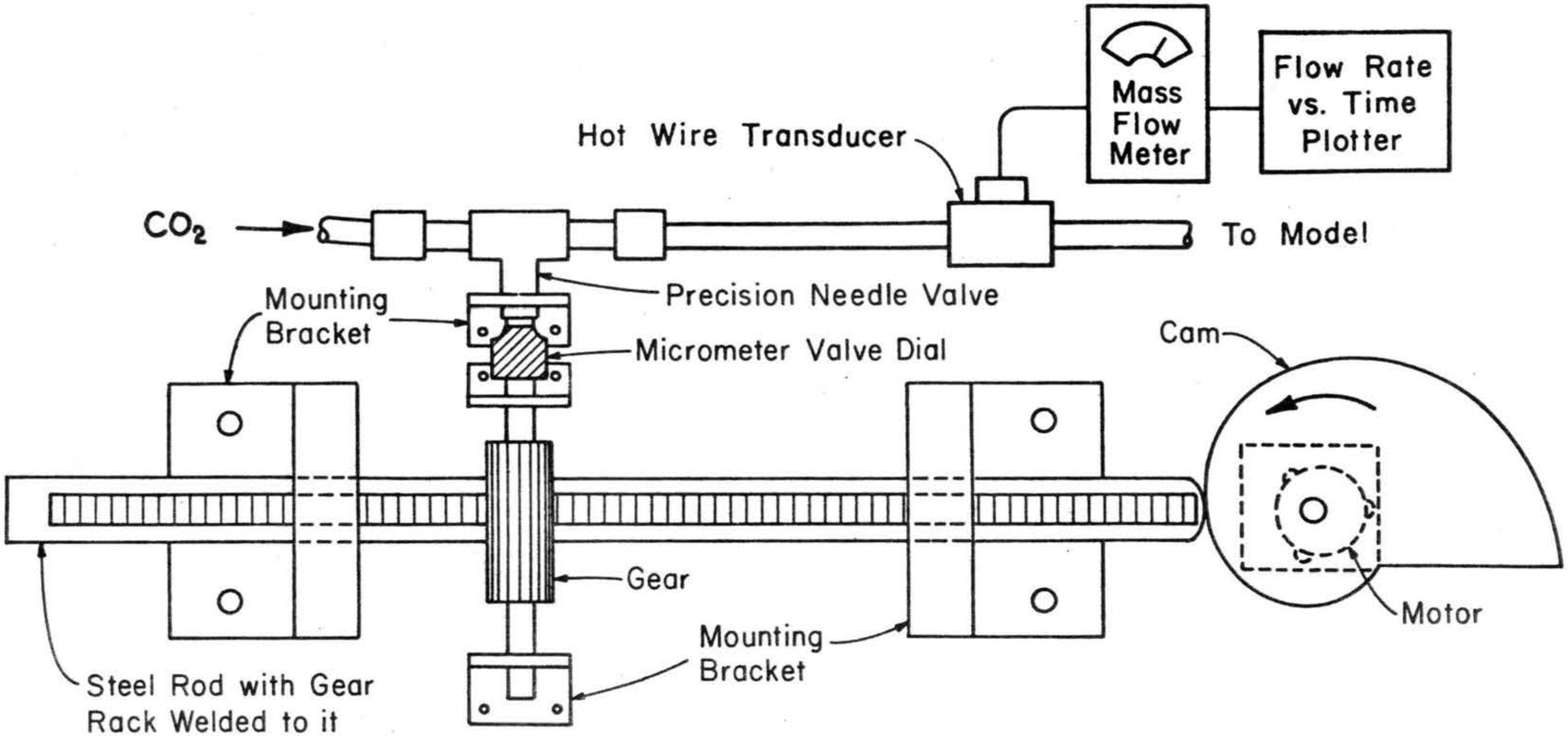

Figure 18. Variable Flow Rate Control Valve

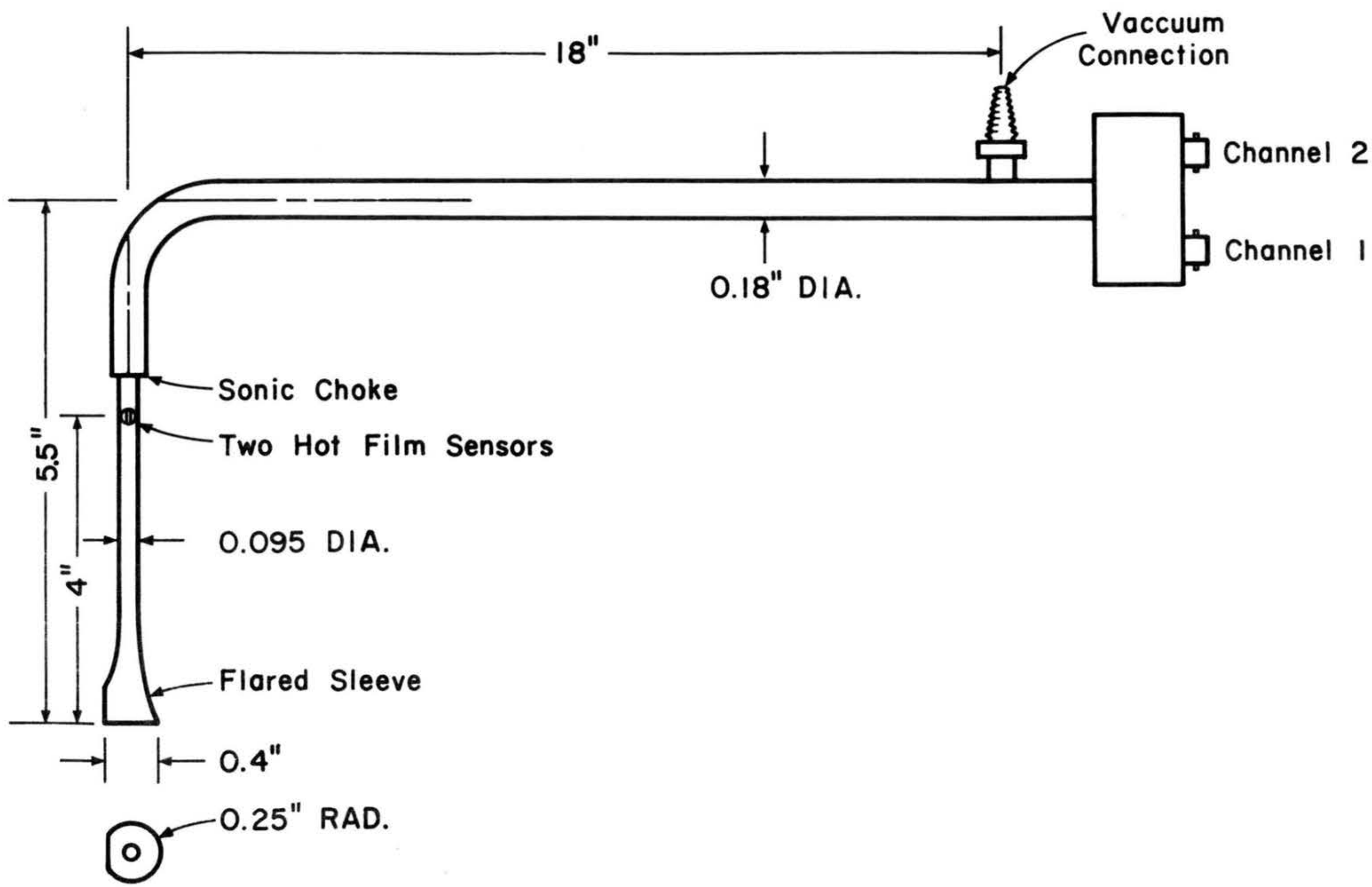

Figure 19. Aspirating Probe Design

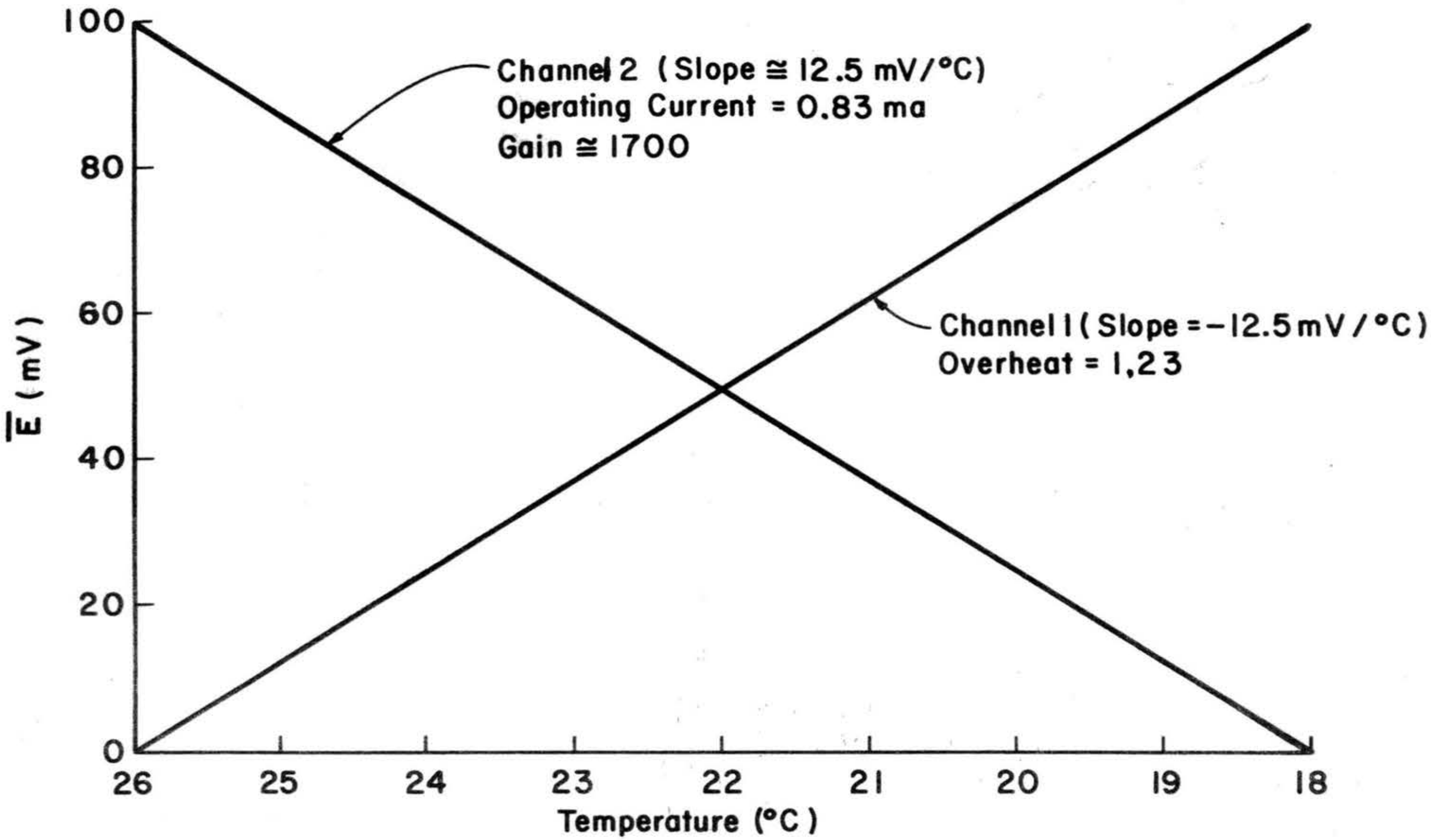

Figure 20. Typical Response of Hot Film Aspirating Probe Versus Temperature

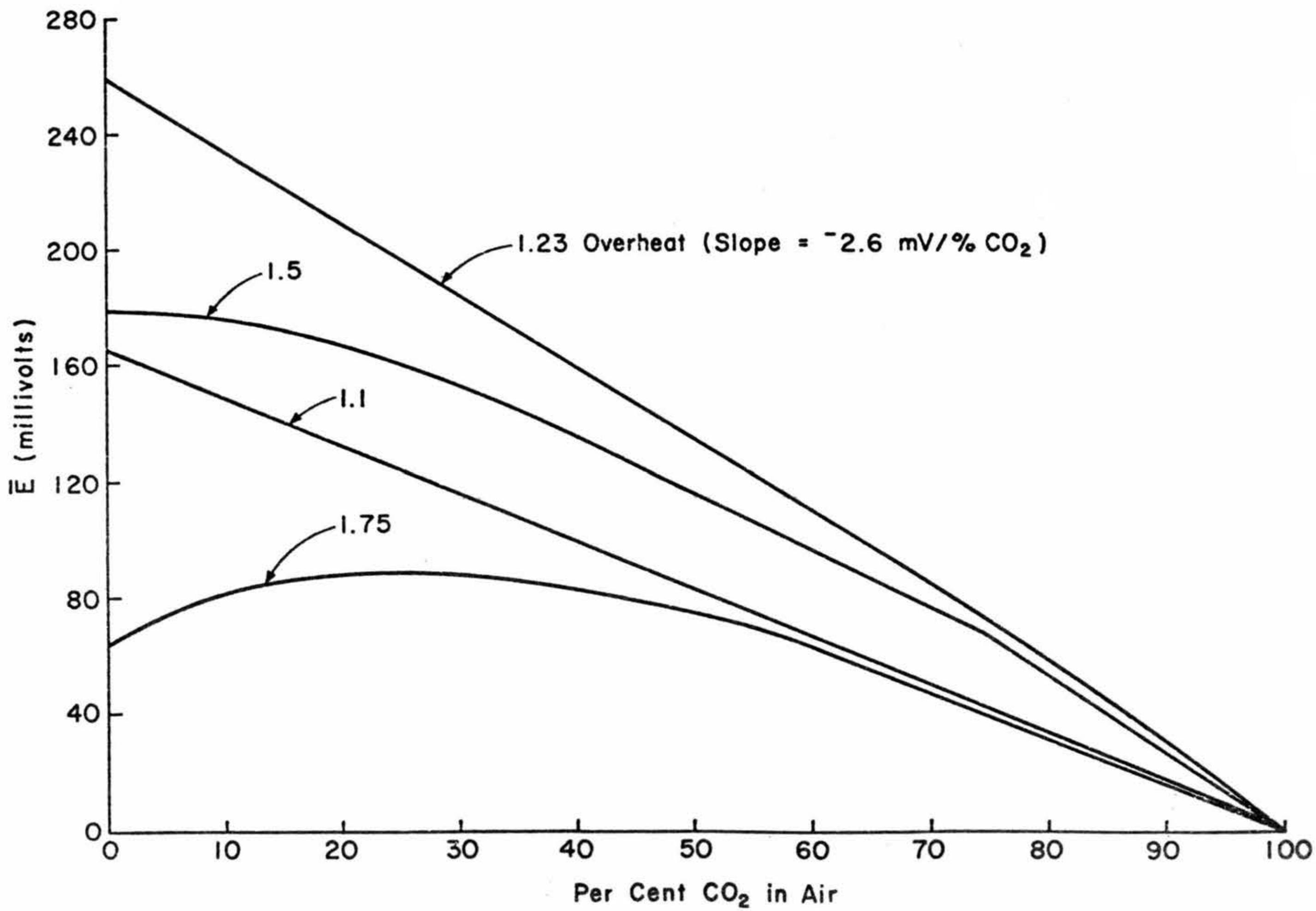

Figure 21. Typical Response of Hot Film Aspirating Probe Versus % CO_2 in Air for Different Overheat Ratios

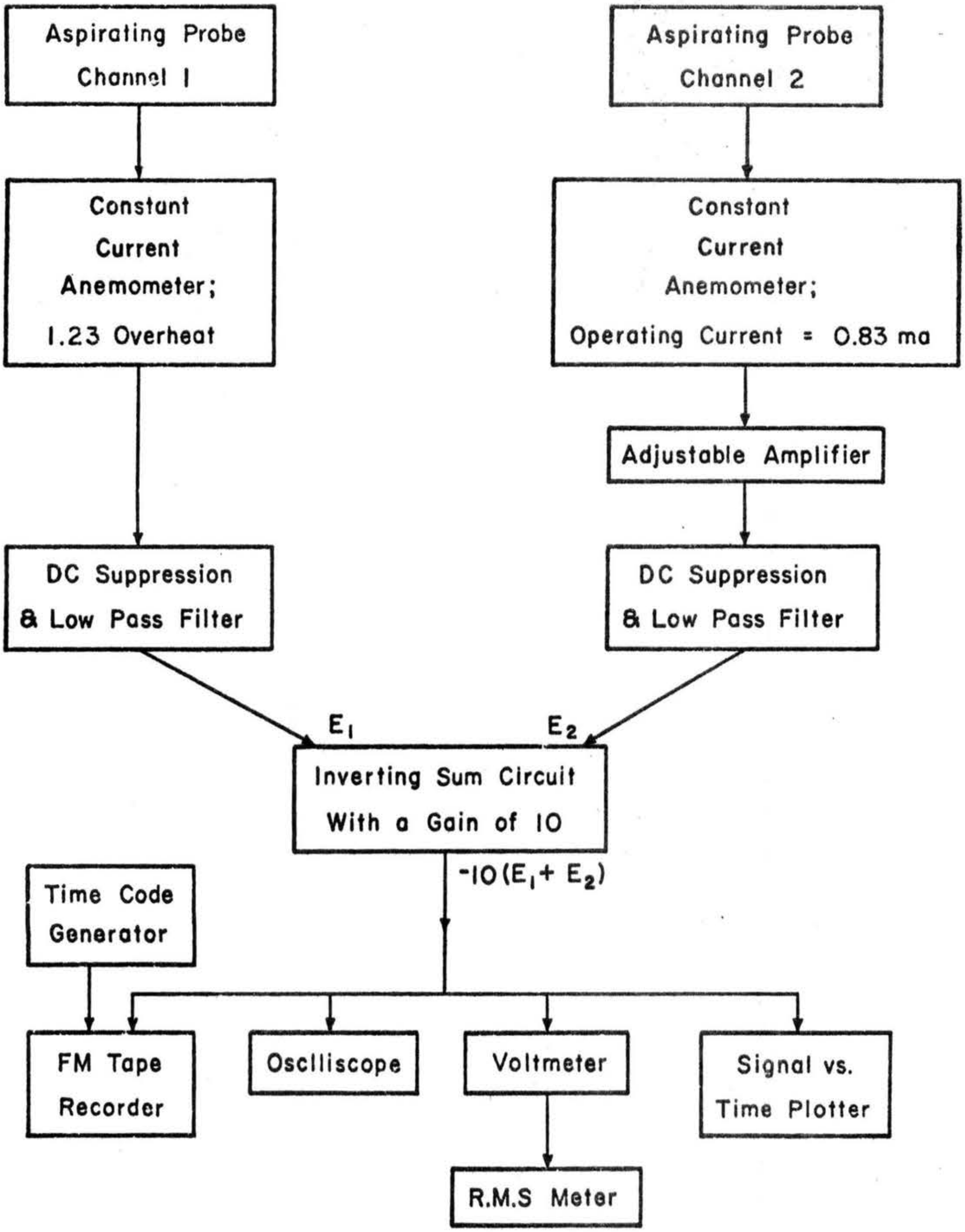

Figure 22. Flow Chart of Aspirating Probe Instrumentation

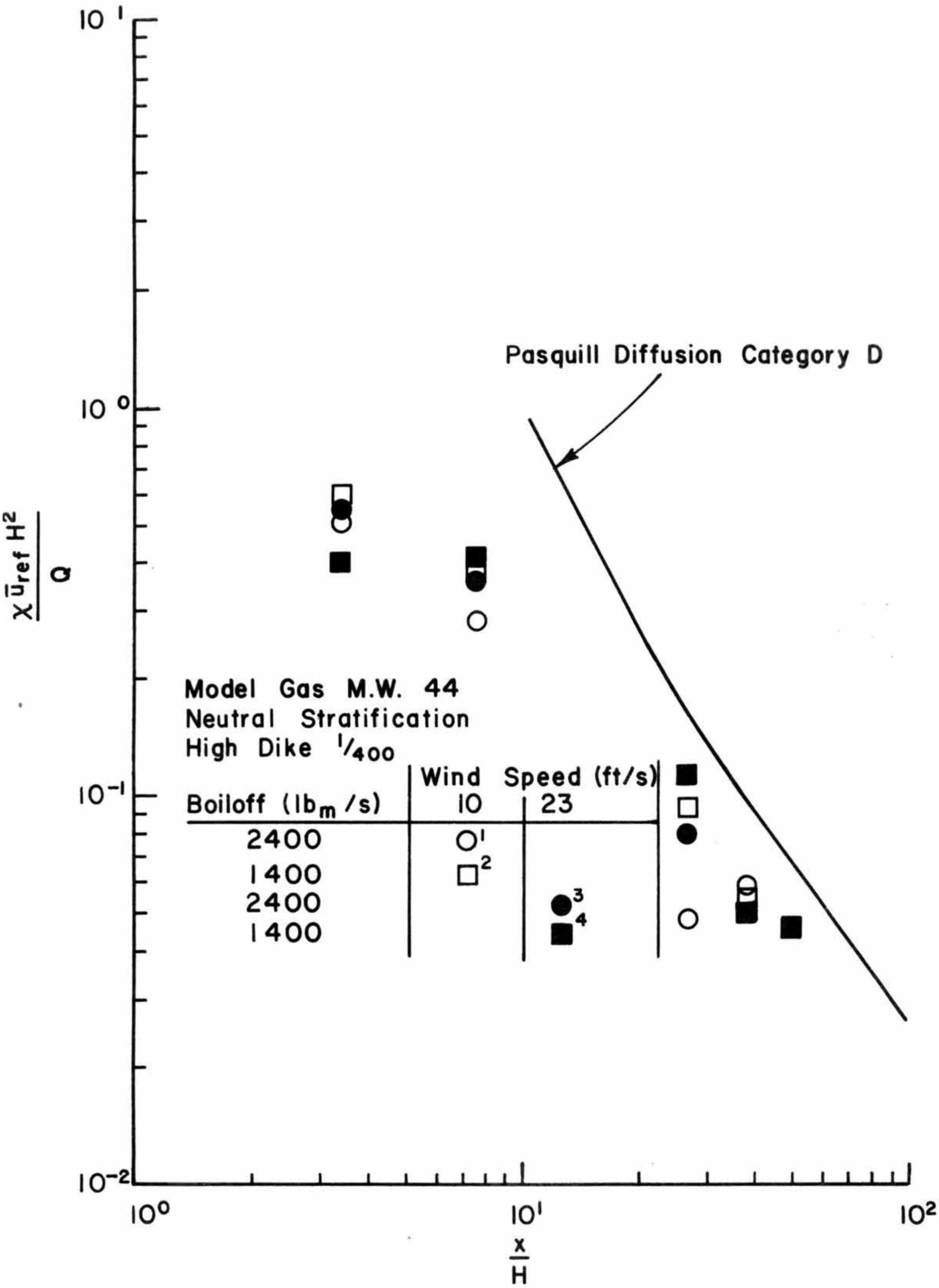

Figure 23-1a. Dimensionless Concentration Coefficient Versus Non-Dimensional Downwind Distance

23-1 to -4 Please refer to errata on verso of title page.

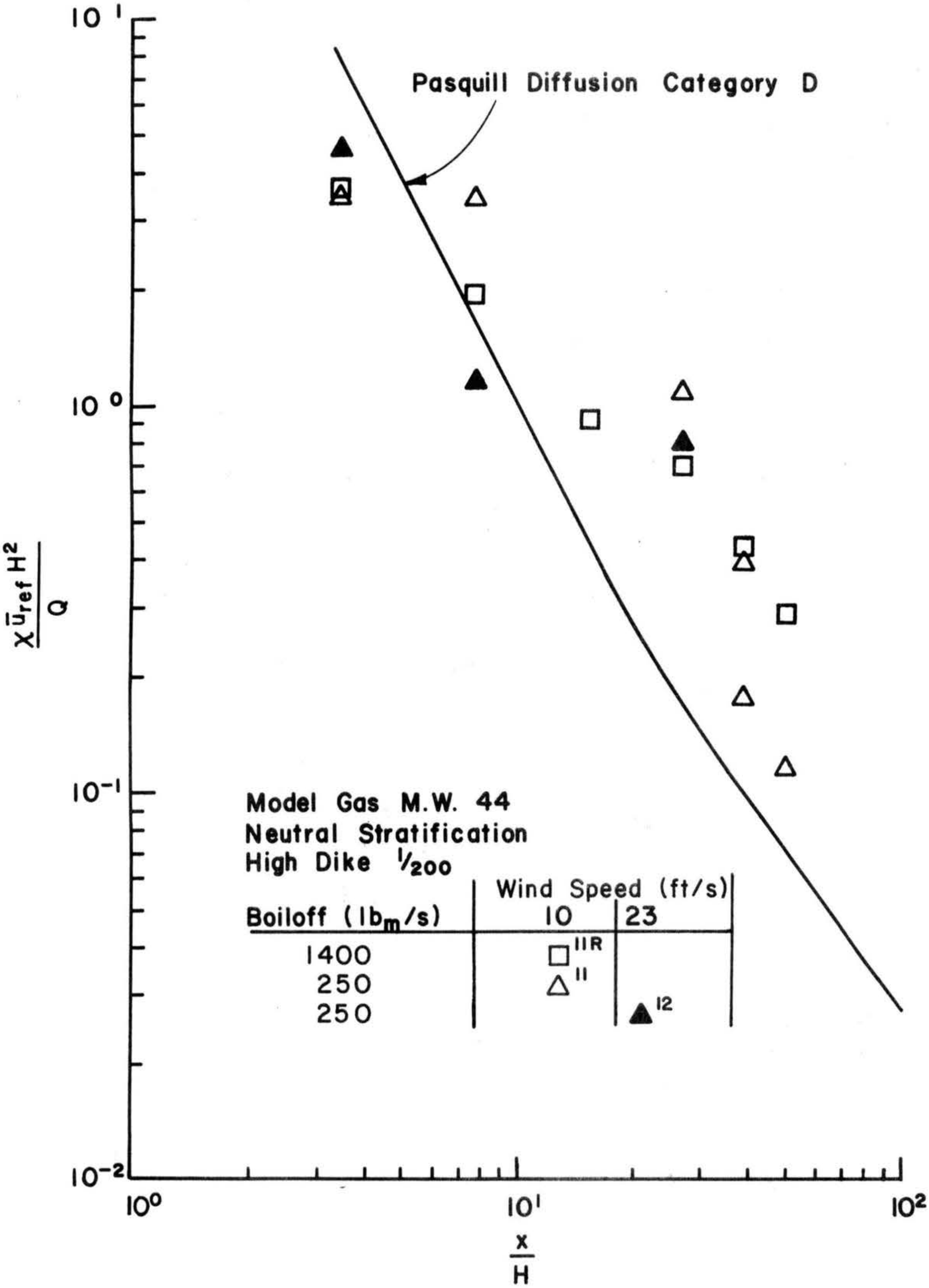

Figure 23-1b. Dimensionless Concentration Coefficient Versus Non-Dimensional Downwind Distance

Please refer to errata on verso of title page.

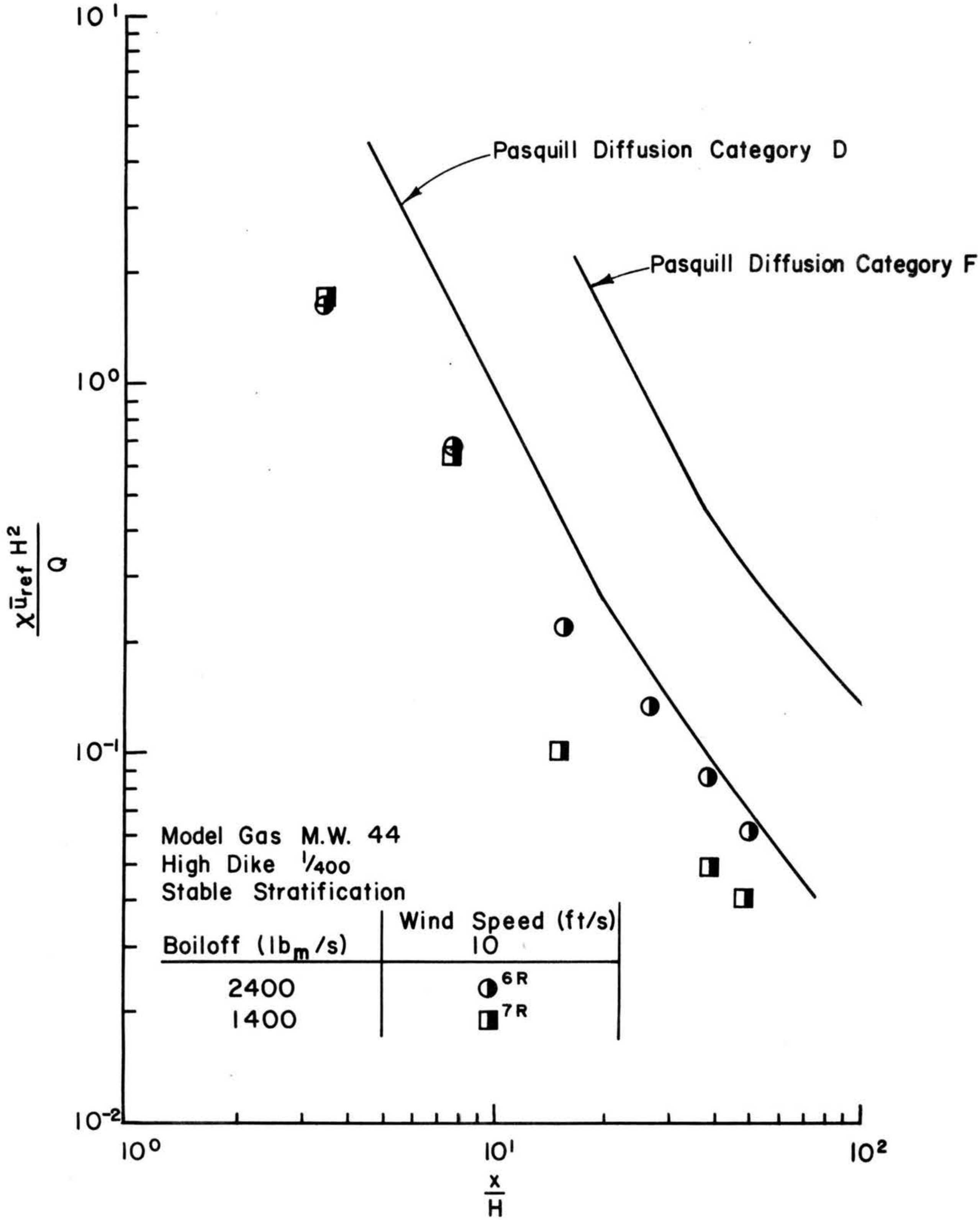

Figure 23-2. Dimensionless Concentration Coefficient Versus Non-Dimensional Downwind Distance

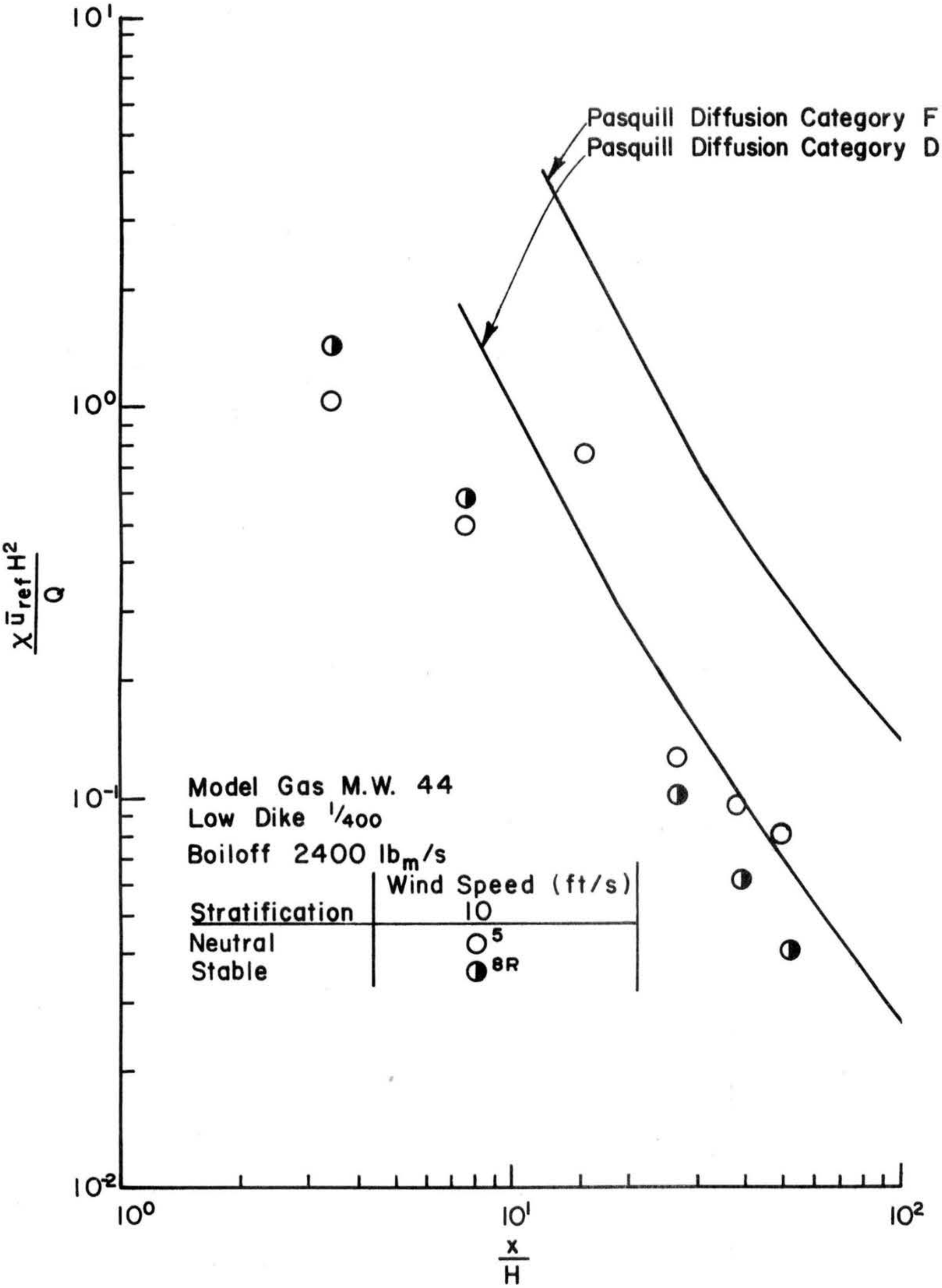

Figure 23-3. Dimensionless Concentration Coefficient Versus Non-Dimensional Downwind Distance

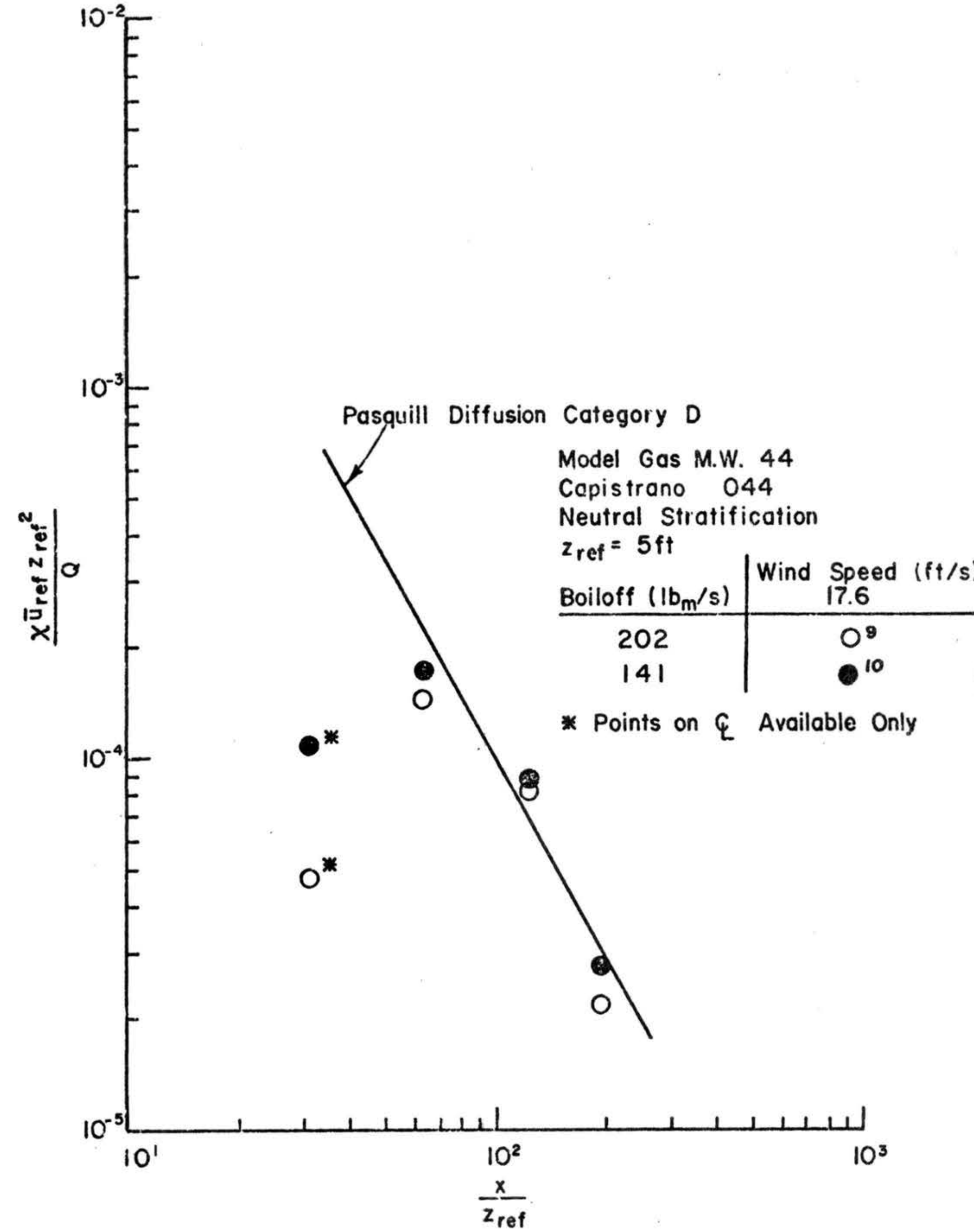

Figure 23-4. Dimensionless Concentration Coefficient Versus Non-Dimensional Downwind Distance

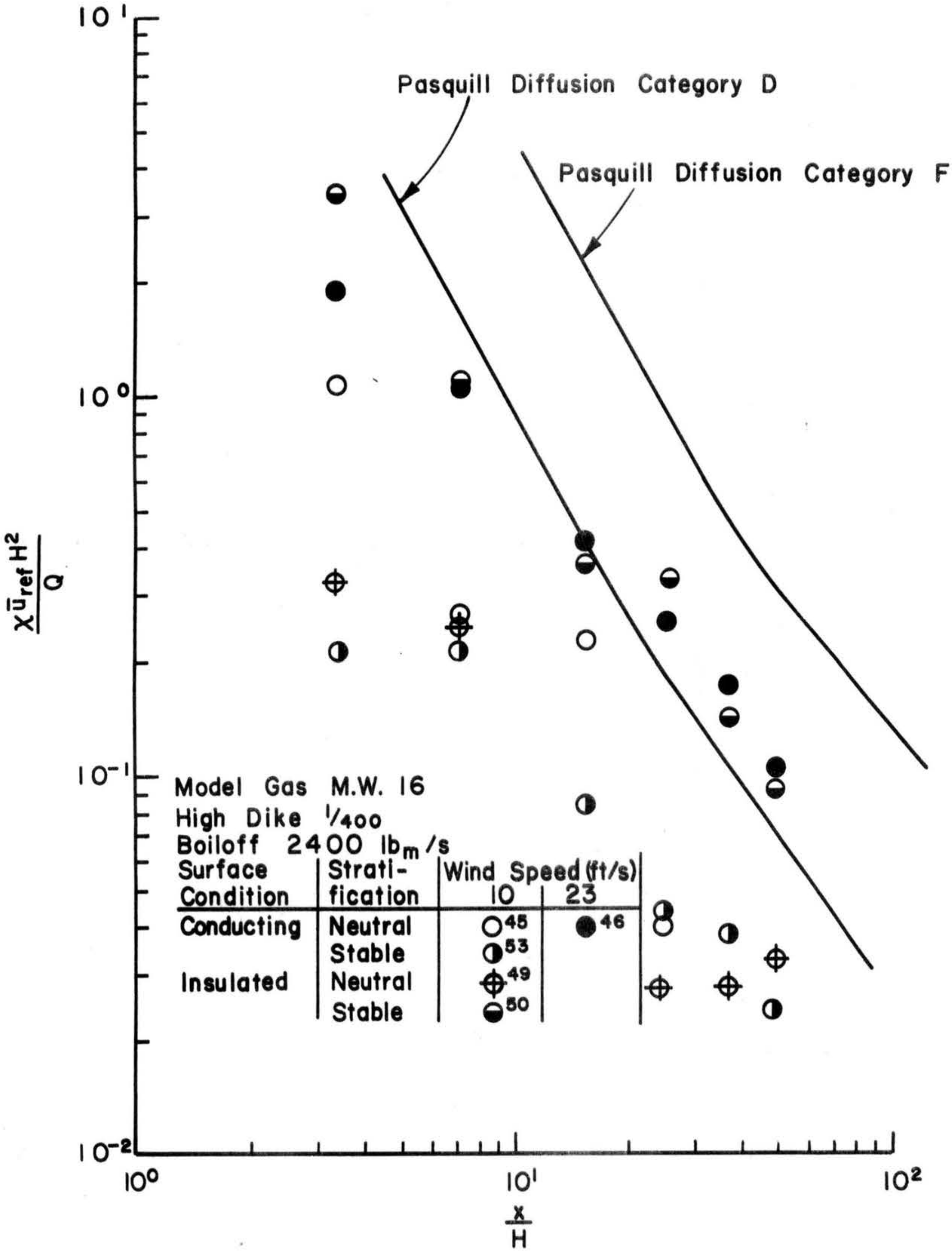

Figure 23-5. Dimensionless Concentration Coefficient Versus Non-Dimensional Downwind Distance

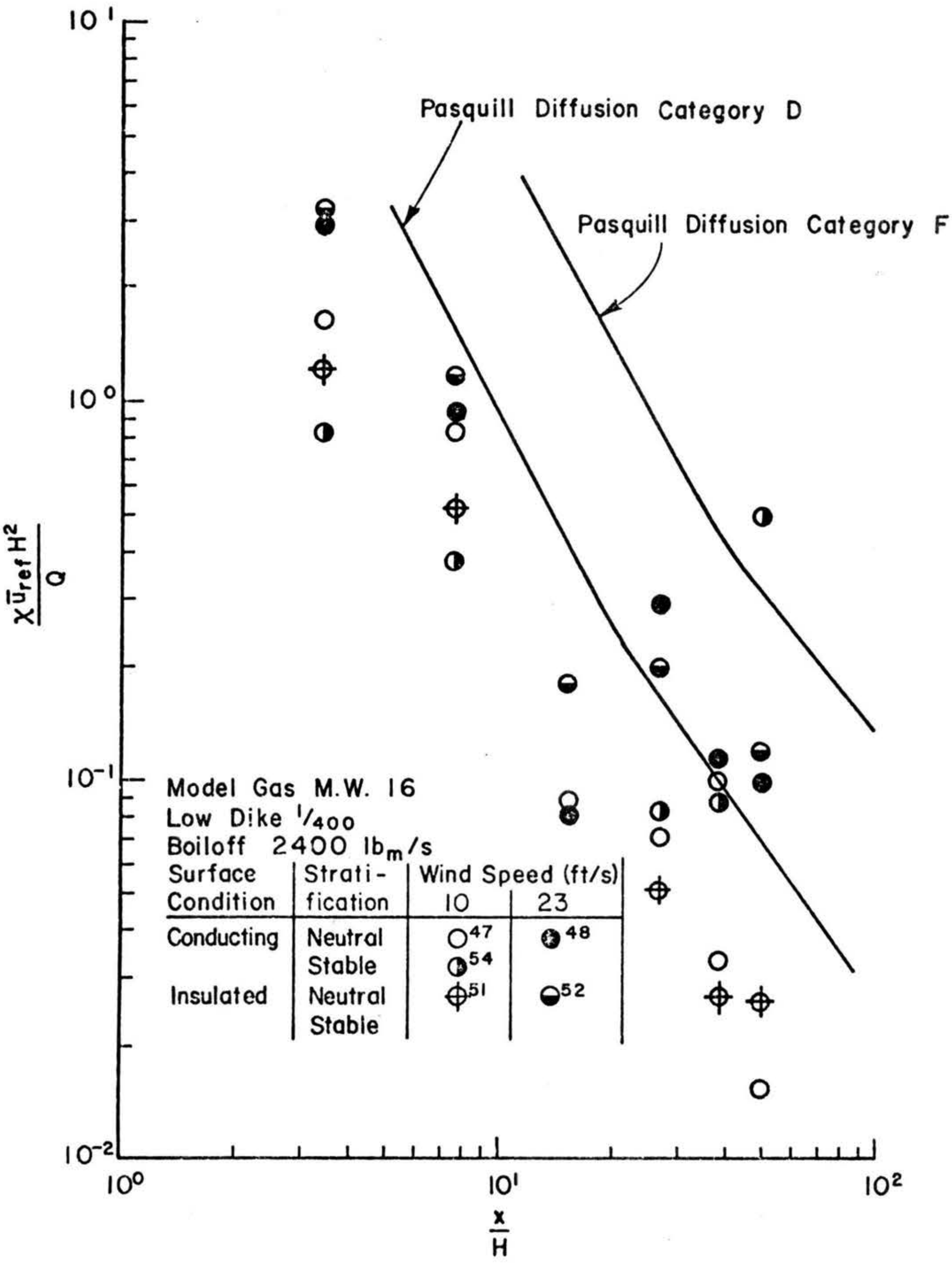

Figure 23-6. Dimensionless Concentration Coefficient Versus Non-Dimensional Downwind Distance

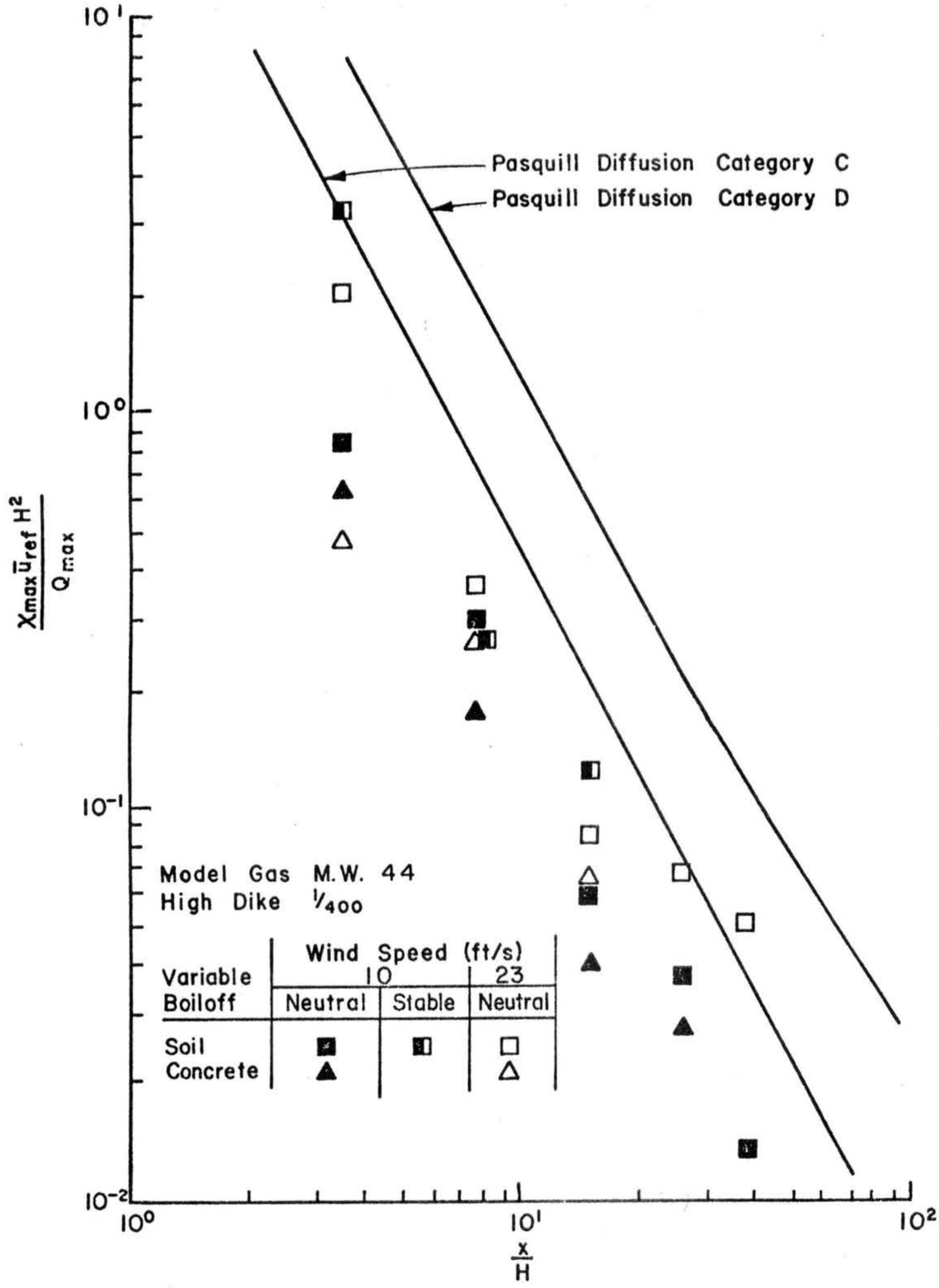

Figure 24-1. Dimensionless Concentration Coefficient Versus Non-Dimensional Downwind Distance Variable Boiloff Results

Please refer to errata on verso of title page.

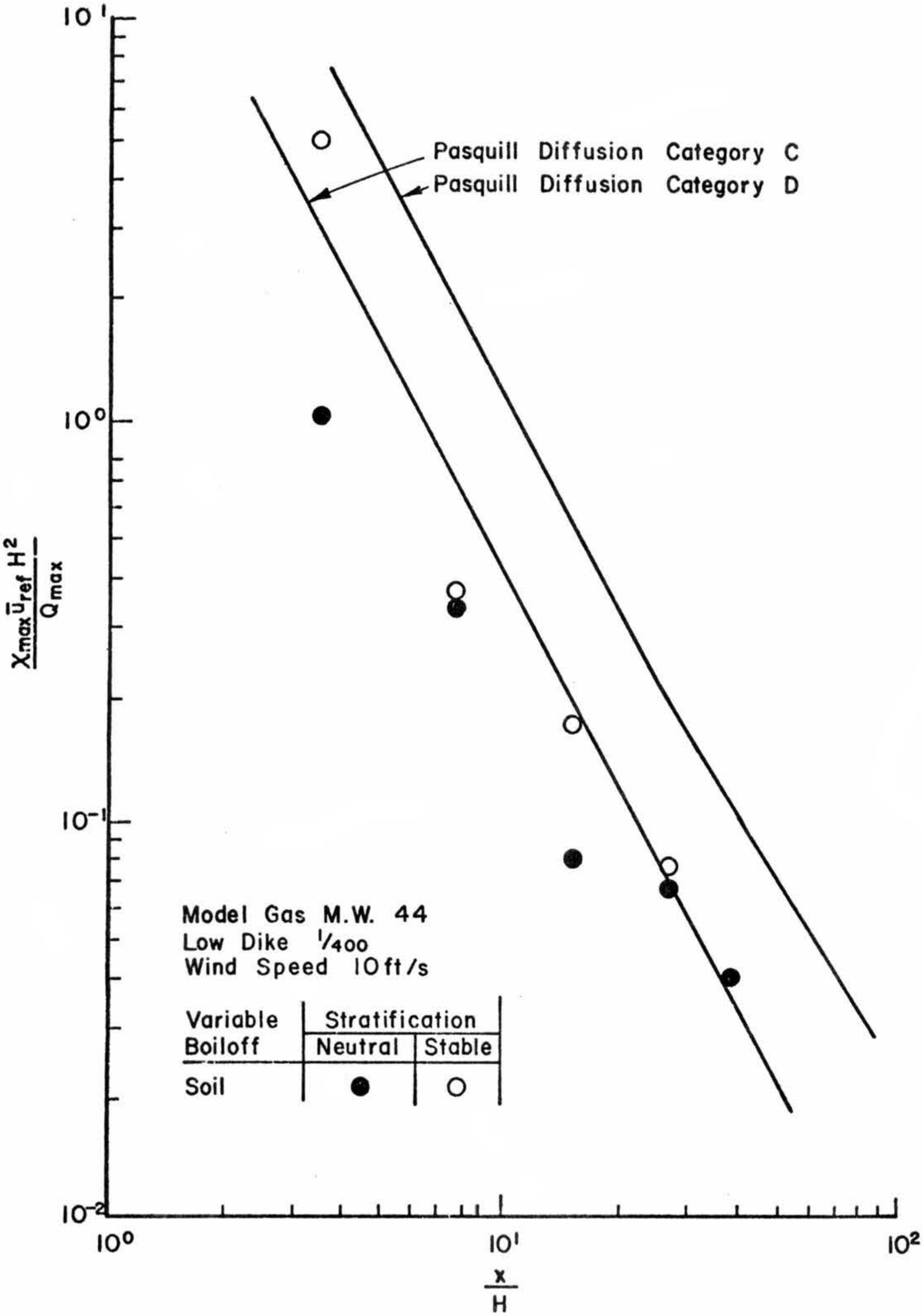

Figure 24-2. Dimensionless Concentration Coefficient Versus Non-Dimensional Downwind Distance Variable Boiloff Results

Please refer to errata on verso of title page.

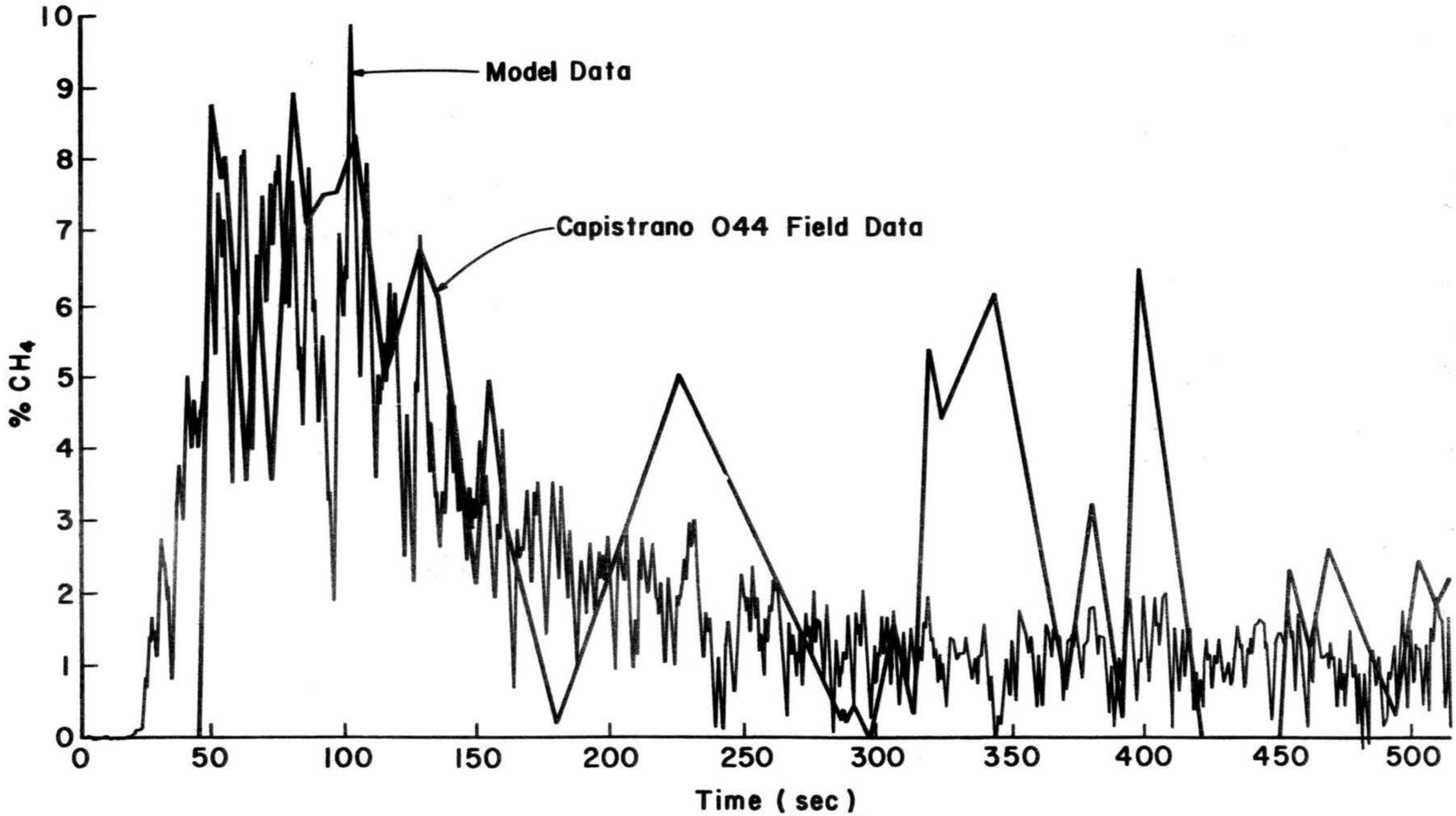

Figure 25. Comparison of Model Data (Case I) with Capistrano 044 Field Data for a Sample Location at (320', 0', 0')

Figure 20 to 36 Please refer to errata on verso of title page.

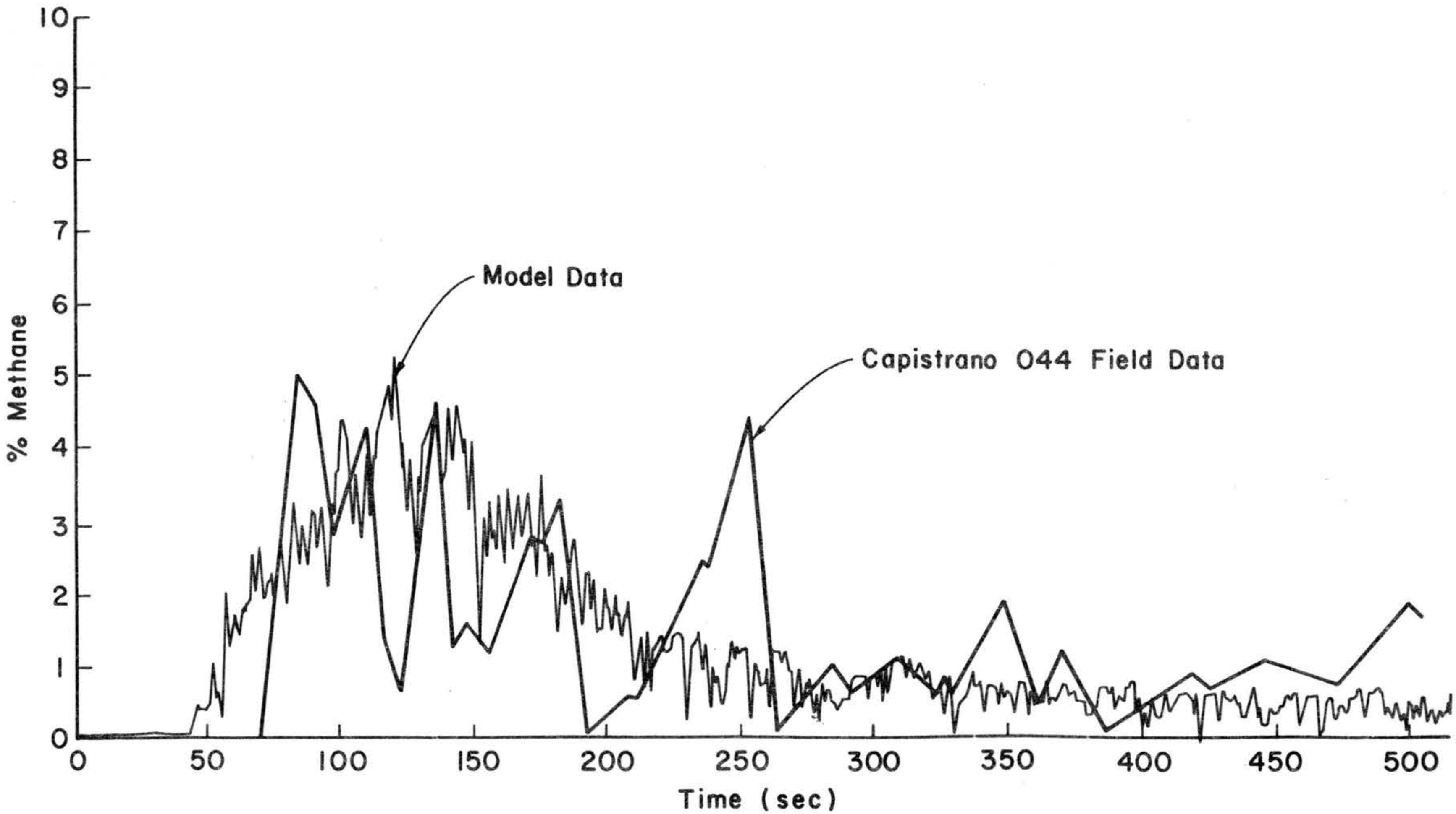

Figure 26. Comparison of Model Data (Case I) with Capistrano 044 Field Data for a Sample Location at (640', 0', 0')

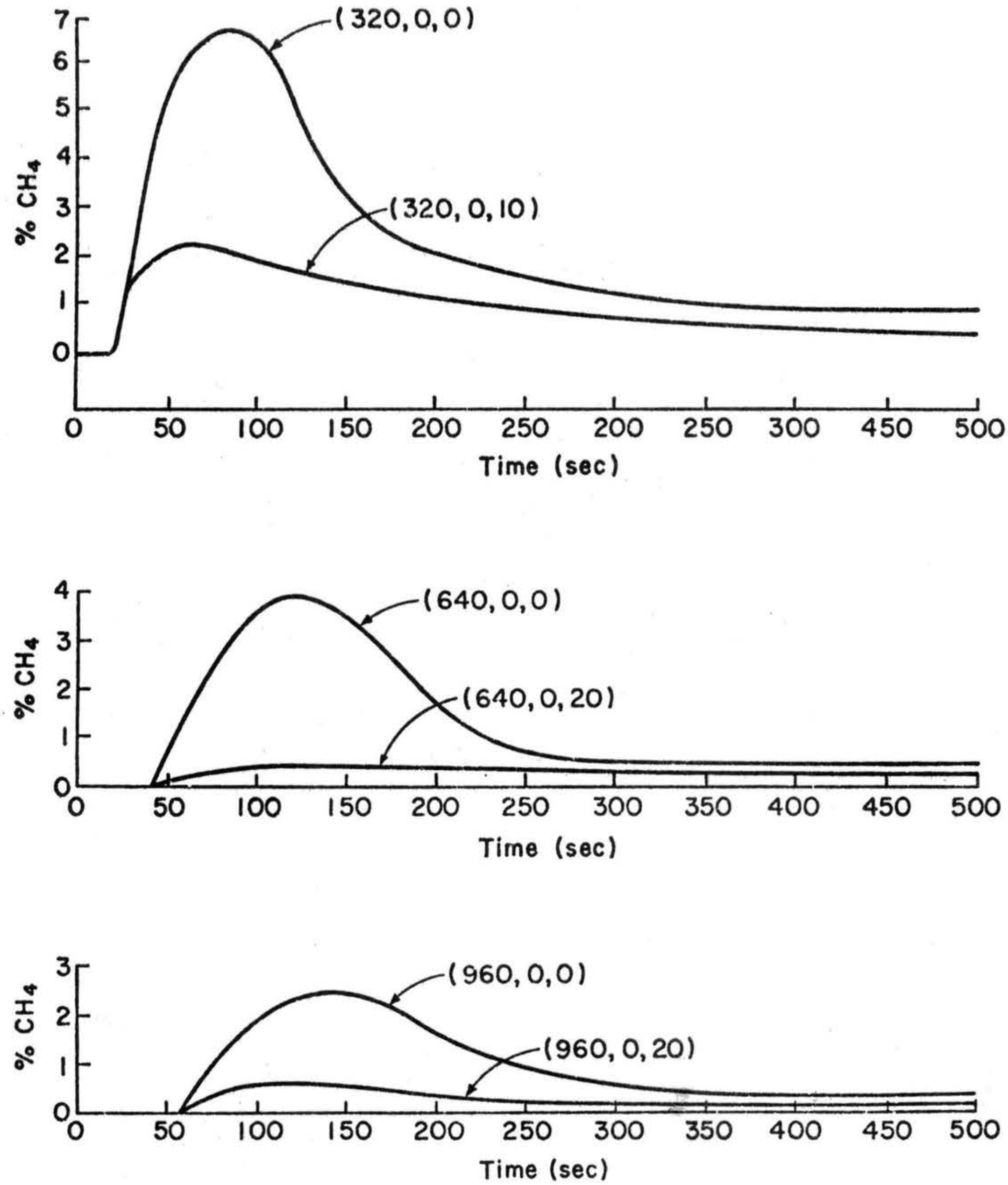

Figure 27a. Mean Concentration Decay with Height at Different Downwind Distances for Capistrano 044 Case I

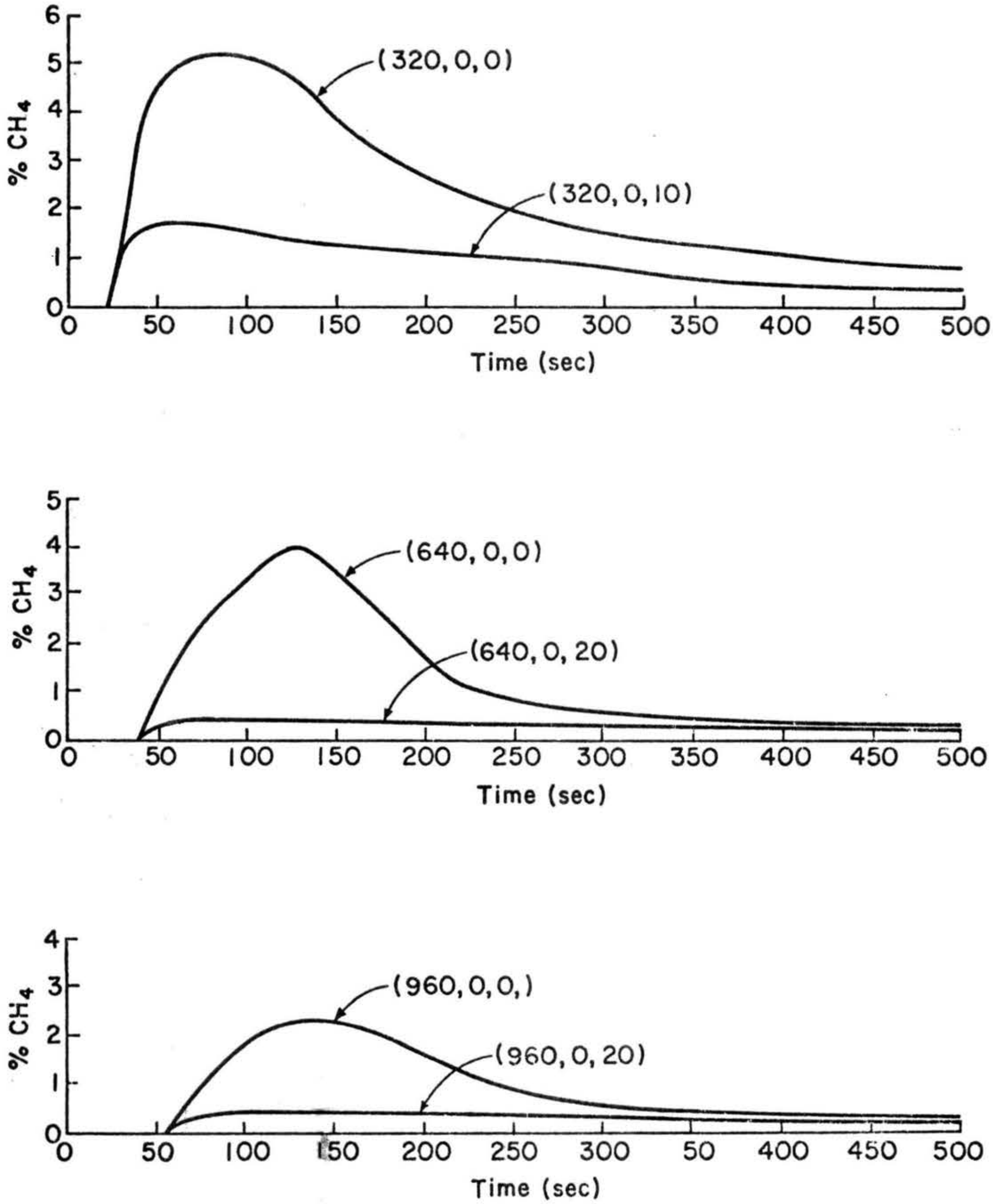

Figure 27b. Mean Concentration Decay with Height at Different Downwind Distances for Capistrano 044 Case II

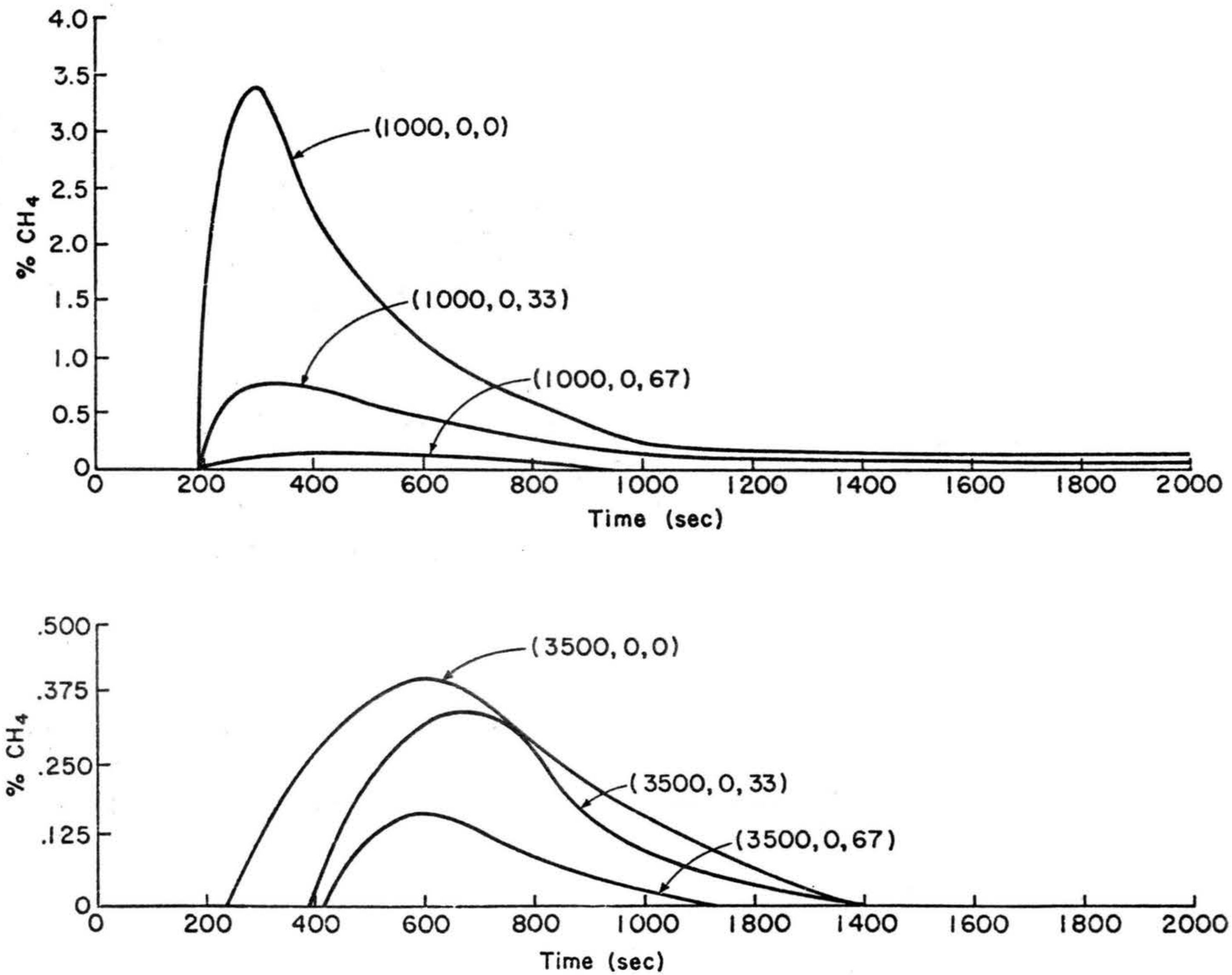

Figure 28. Mean Concentration Decay with Height at Different Downwind Distances for High Dike, Soil, Neutral Flow, 7 mph

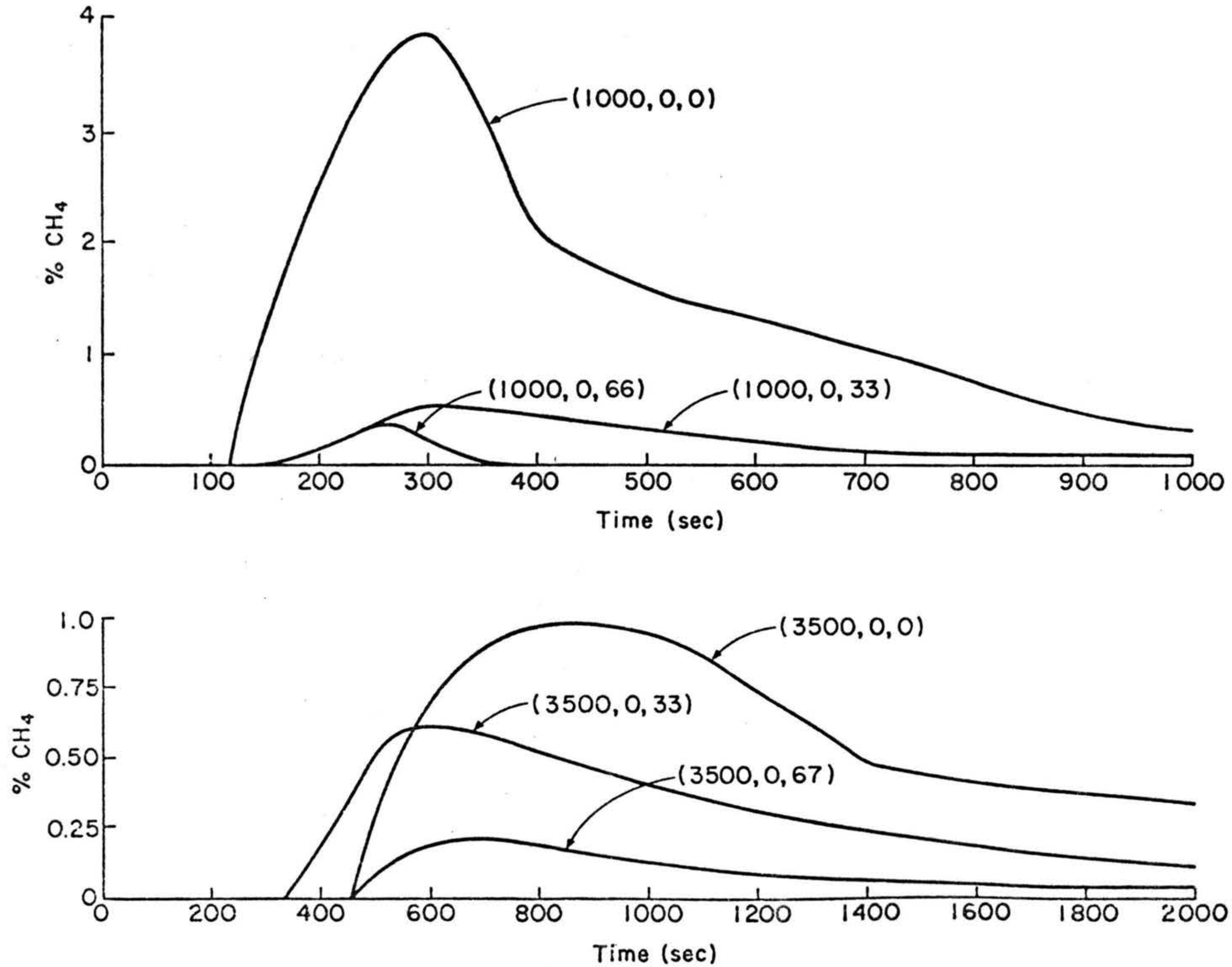

Figure 29. Mean Concentration Decay with Height at Different Downwind Distances for Low Dike, Soil, Neutral Flow, 7 mph

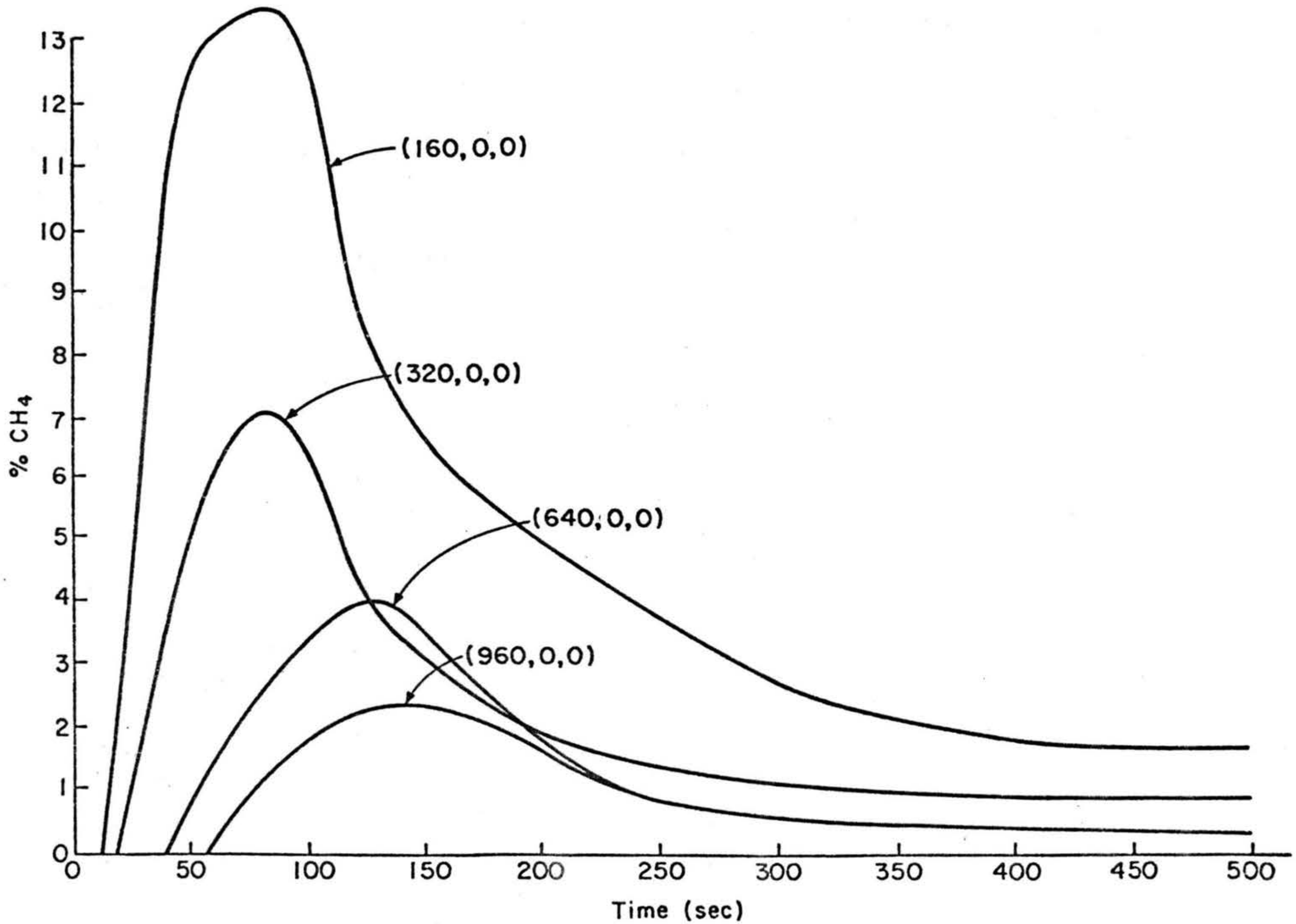

Figure 30a. Mean Concentration Decay with Distance for Capistrano 044 Case I

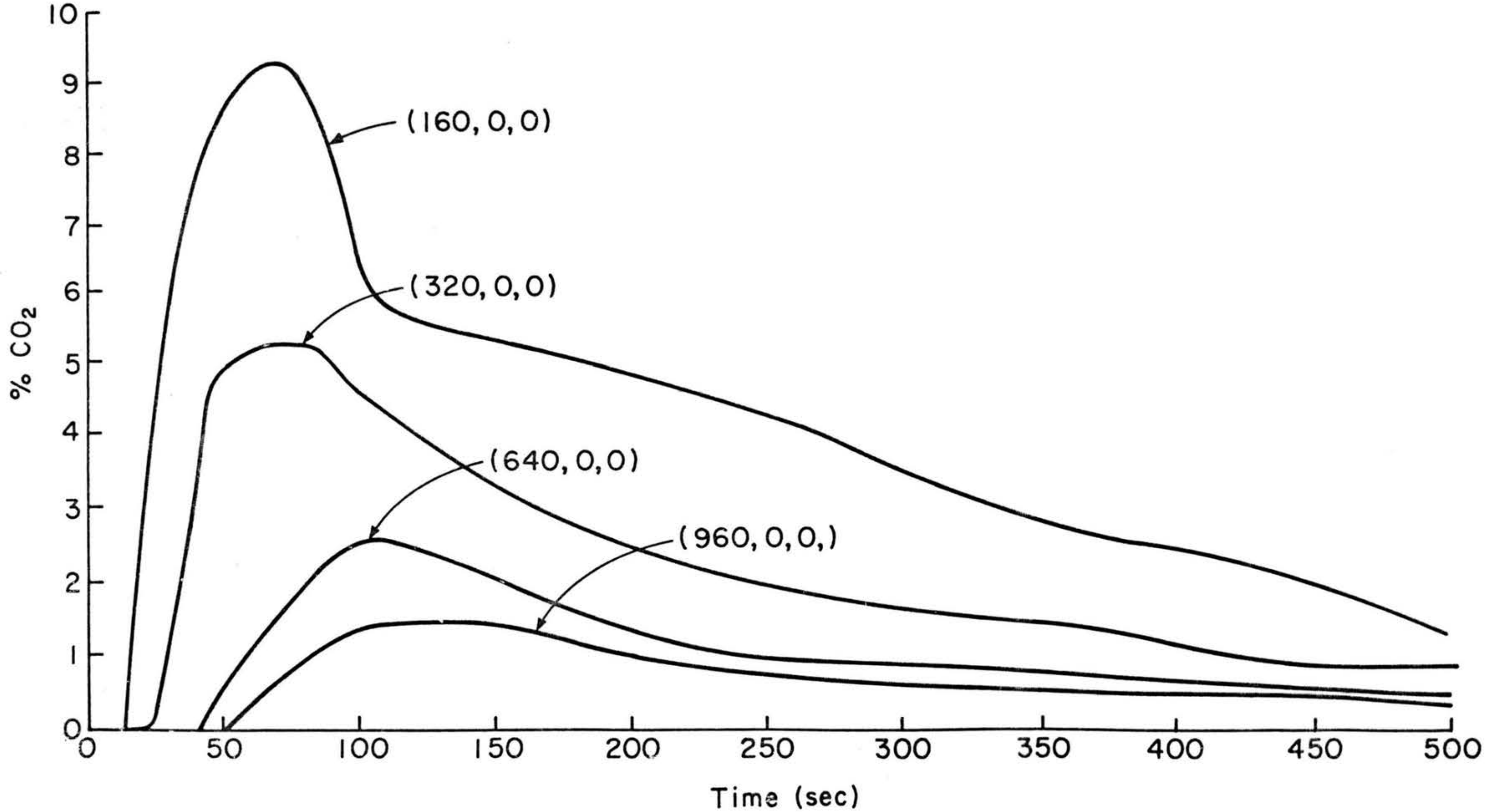

Figure 30b. Mean Concentration Decay with Distance for Capistrano 044 Case II

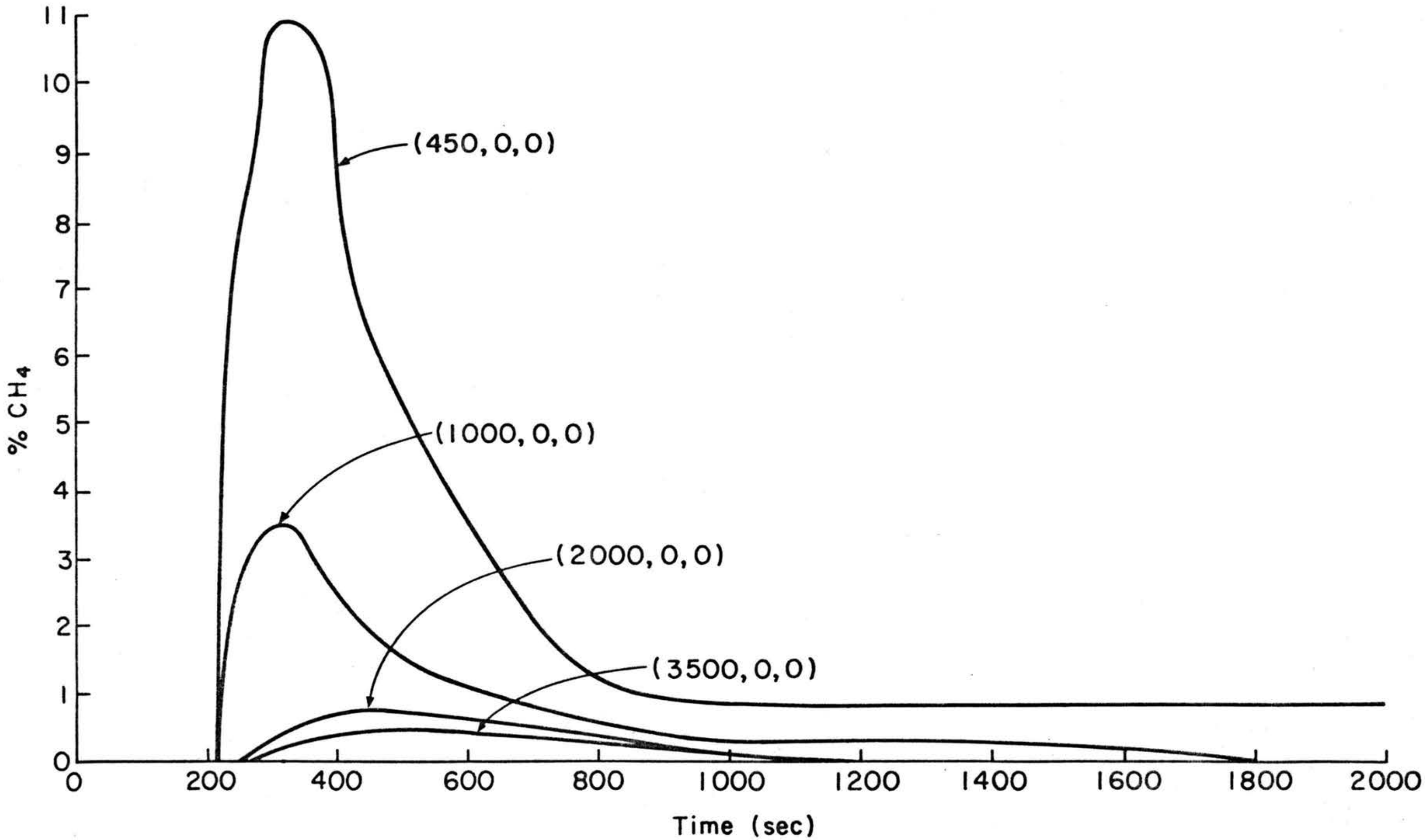

Figure 31. Mean Concentration Decay with Distance for High Dike, Soil, Neutral Flow, 7 mph

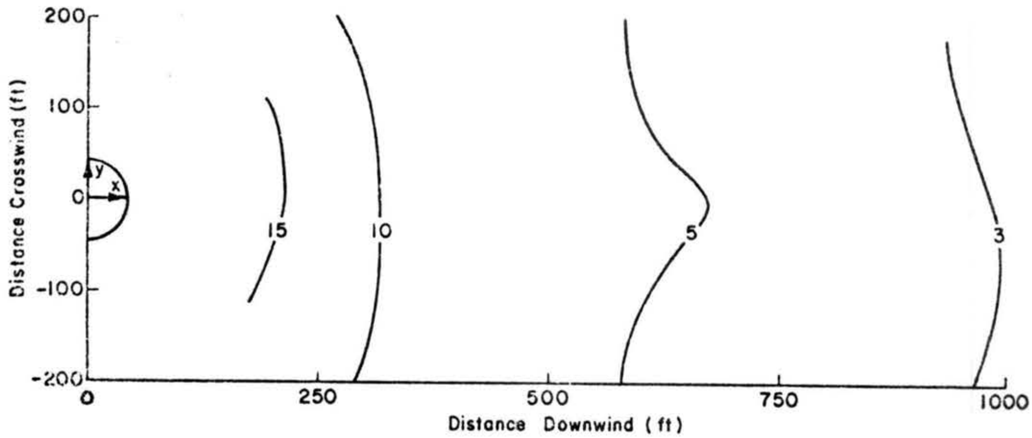

Case I

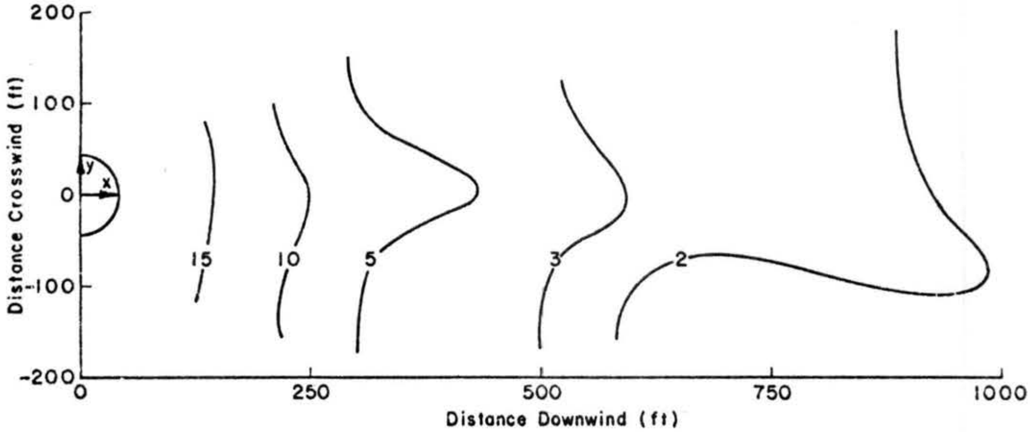

Case II

Figure 32. Ground Contour Plots of Peak Concentration for Capistrano Cases I and II

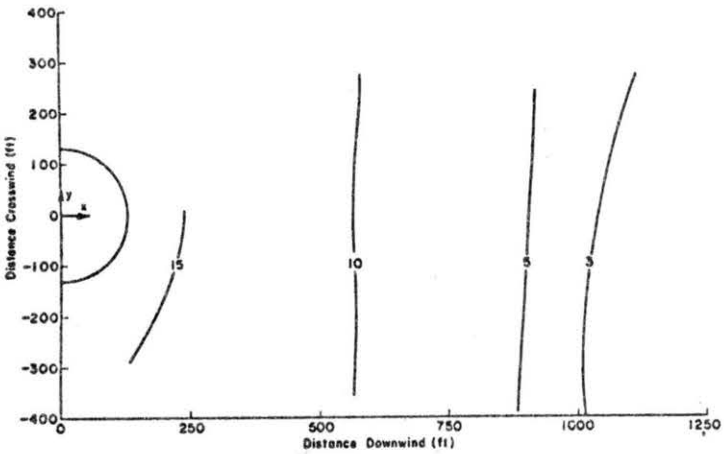

Soil
7 mph
Neutral Atmosphere

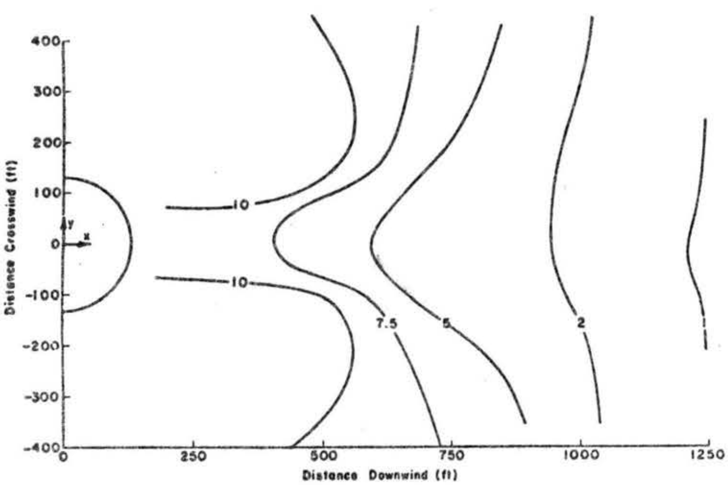

Soil
16 mph
Neutral Atmosphere

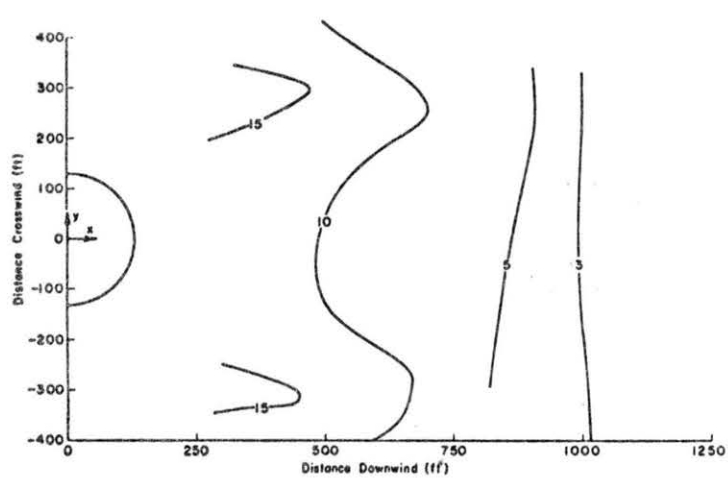

Soil
7 mph
Stable Atmosphere

Figure 33. Ground Contour Plots of Peak Concentration for the High Dike

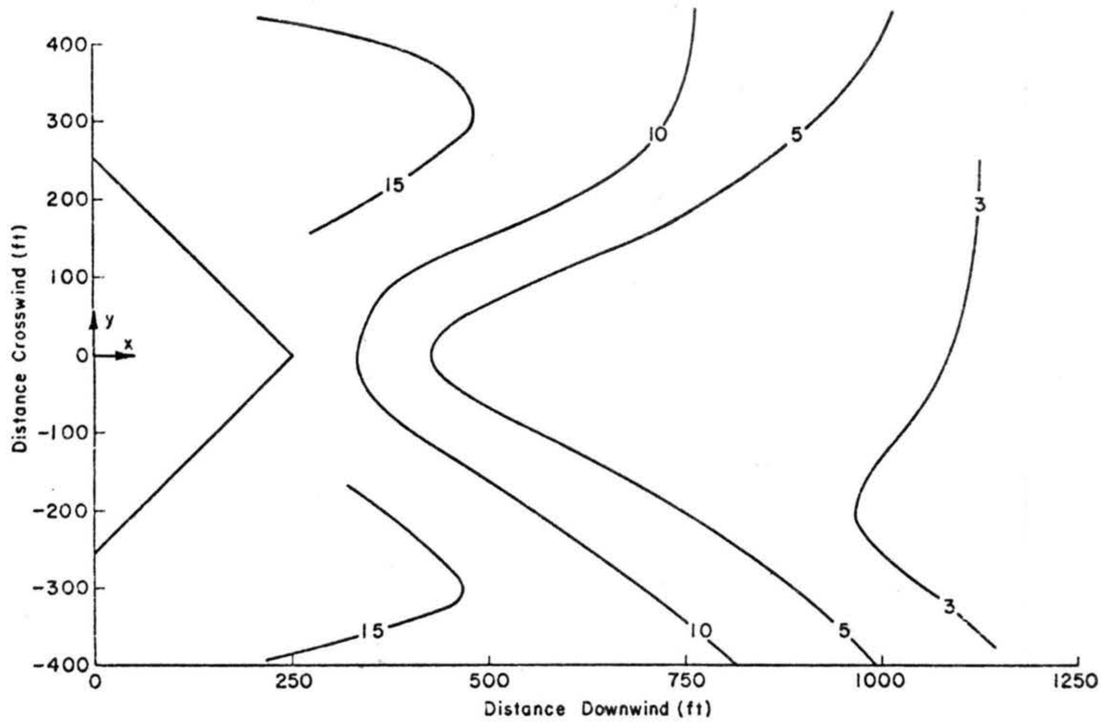

Soil, 7 mph, Neutral Atmosphere

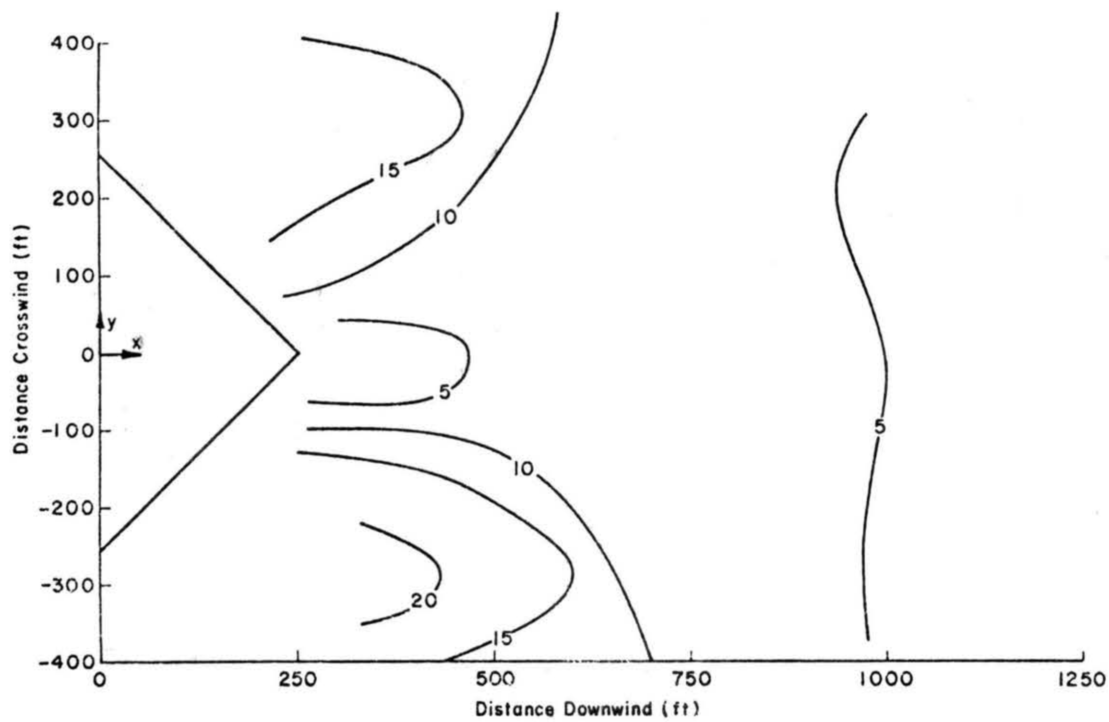

Soil, 7 mph, Stable Atmosphere

Figure 34. Ground Contour Plots of Peak Concentration for the Low Dike

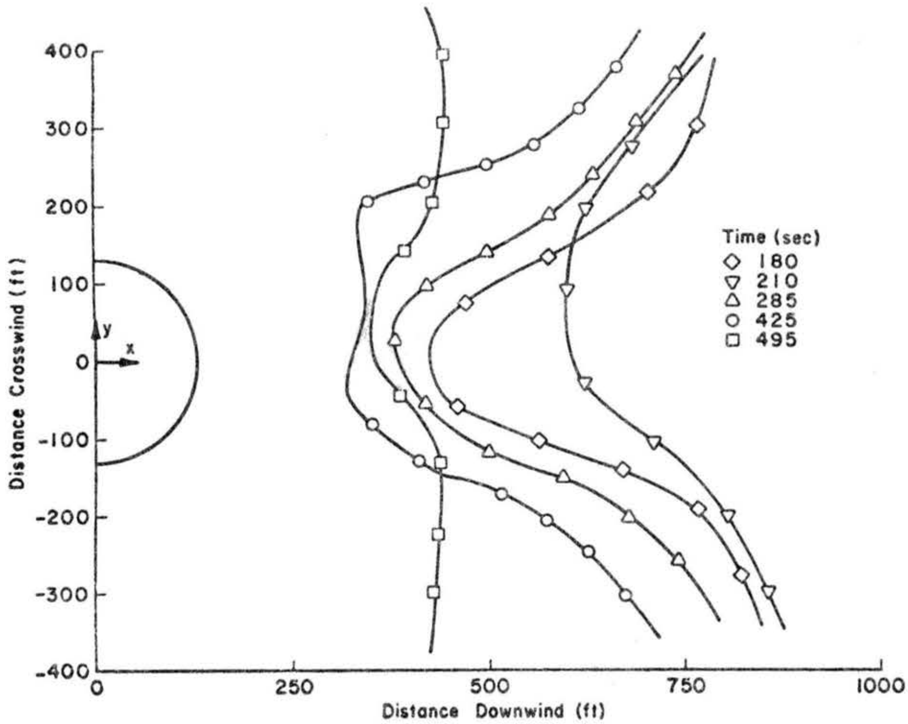

High Dike, Soil, 16 mph, Neutral Atmosphere

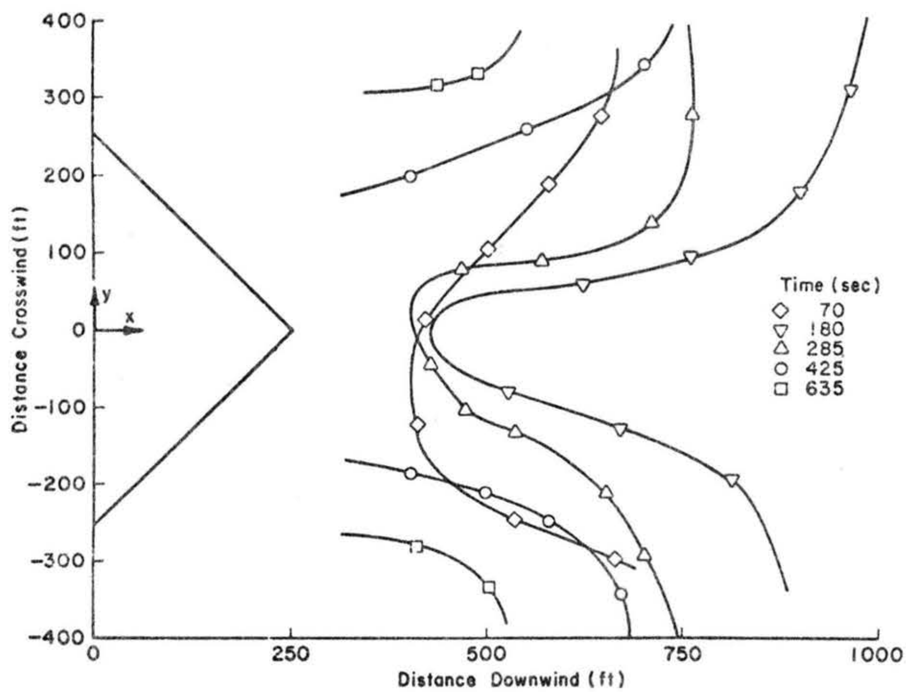

Low Dike, Soil, 7 mph, Neutral Atmosphere

Figure 35. Observed Lower Flammability Limit (LFL = 5%) Contours as a Function of Time from the Spill

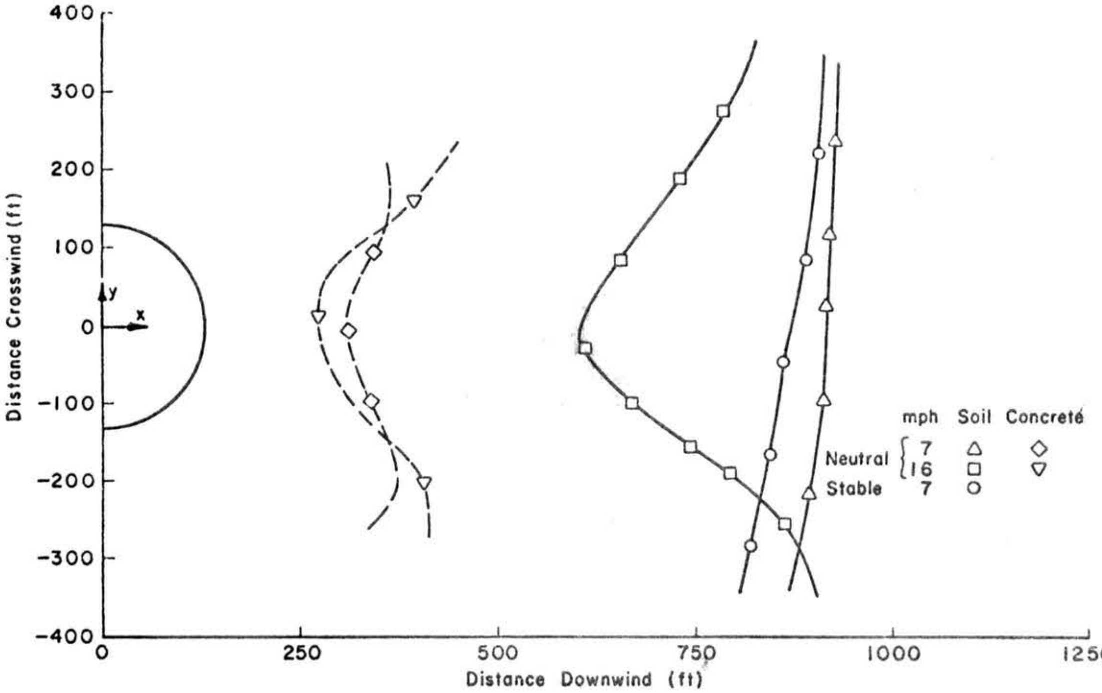

High Dike

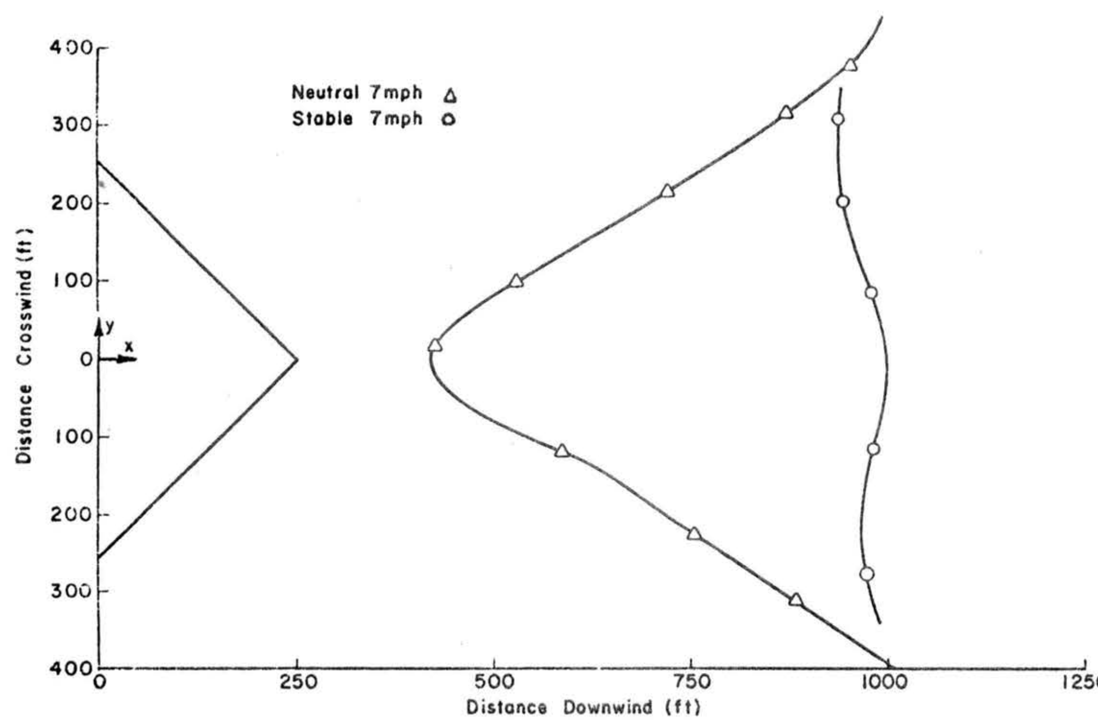

Low Dike

Figure 36. Observed Hazard Zone Contours

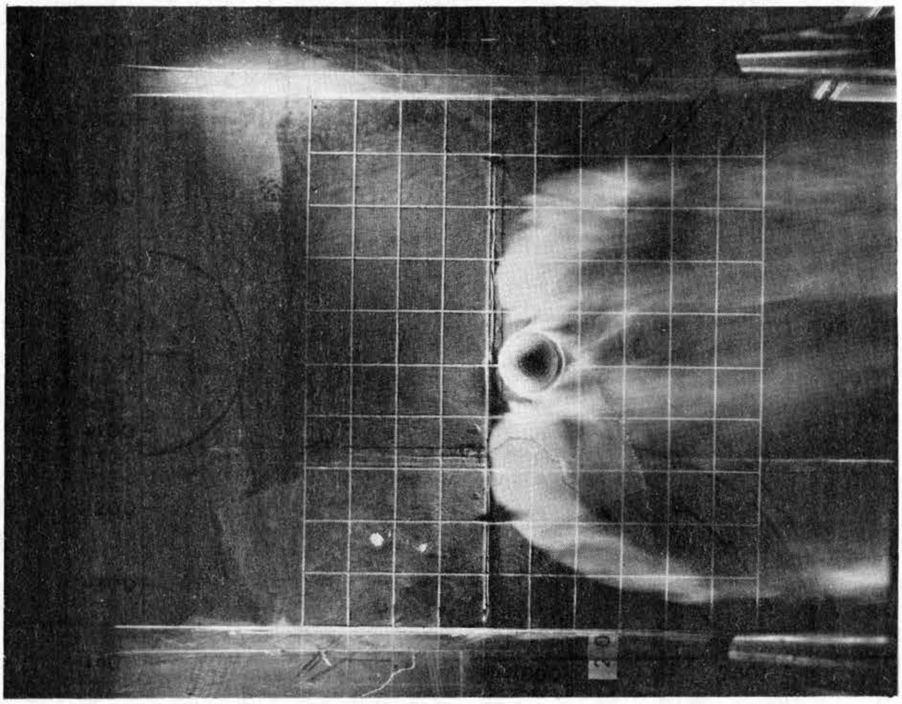

Picture 20; U = 23 ft/sec, $\dot{m}$ = 2400 lbm/sec

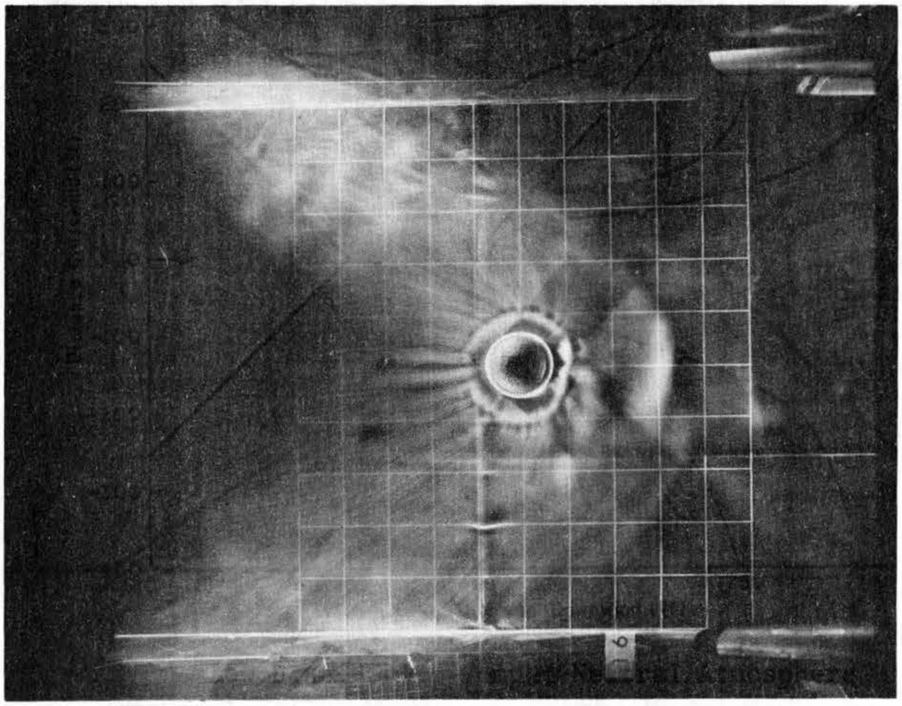

Picture 16; U = 16 ft/sec, $\dot{m}$ = 2400 lbm/sec

Figure 37. High Dike on Sloping Ground Surface

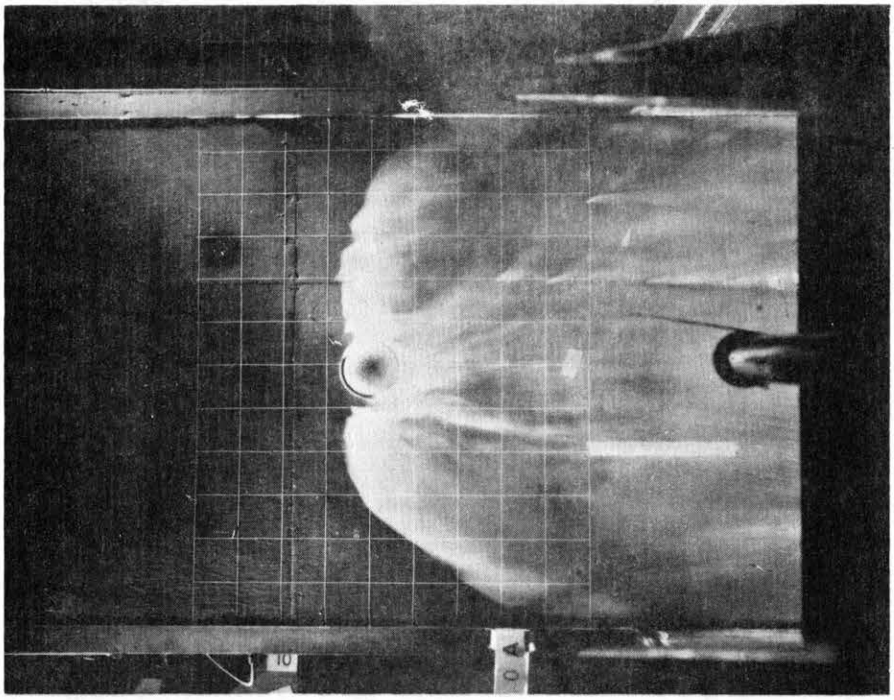

Picture 20A; U = 23 ft/sec, $\dot{m}$ = 2400 lbm/sec

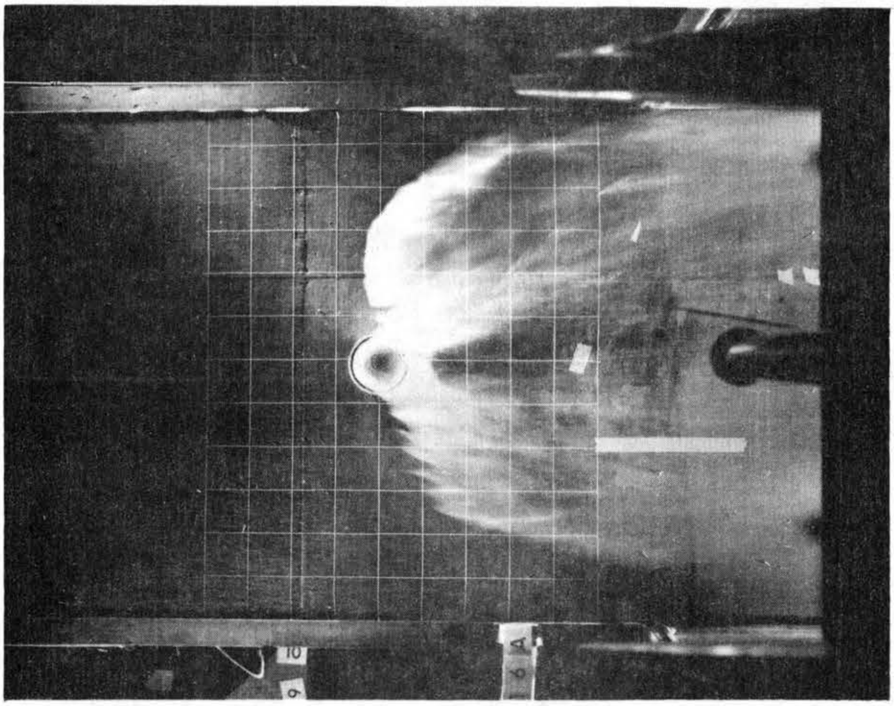

Picture 16A; U = 23 ft/sec, $\dot{m}$ = 2400 lbm/sec

Figure 38. High Dike on Flat (Zero Slope) Ground Surface

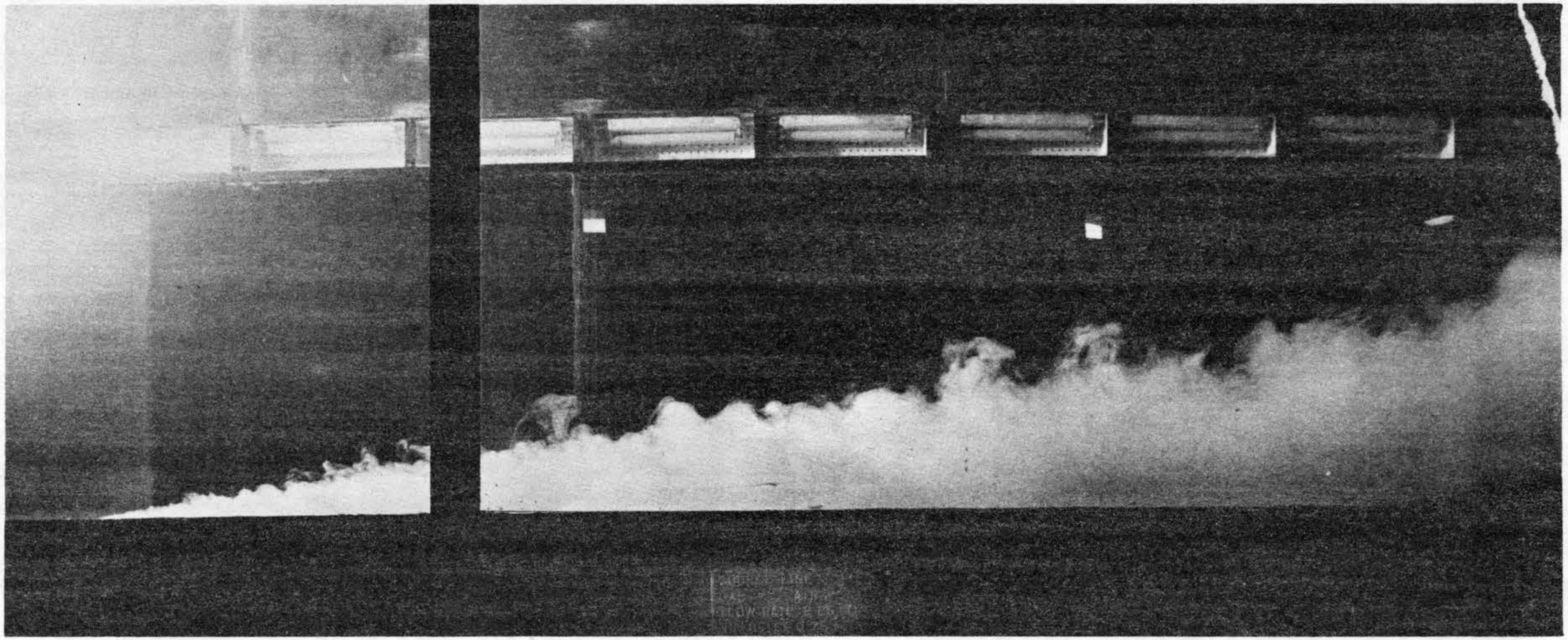

Figure 39a. Line Source in a Shear Layer: Q = 2.25 cfm, U = 0.75 ft/sec

Air

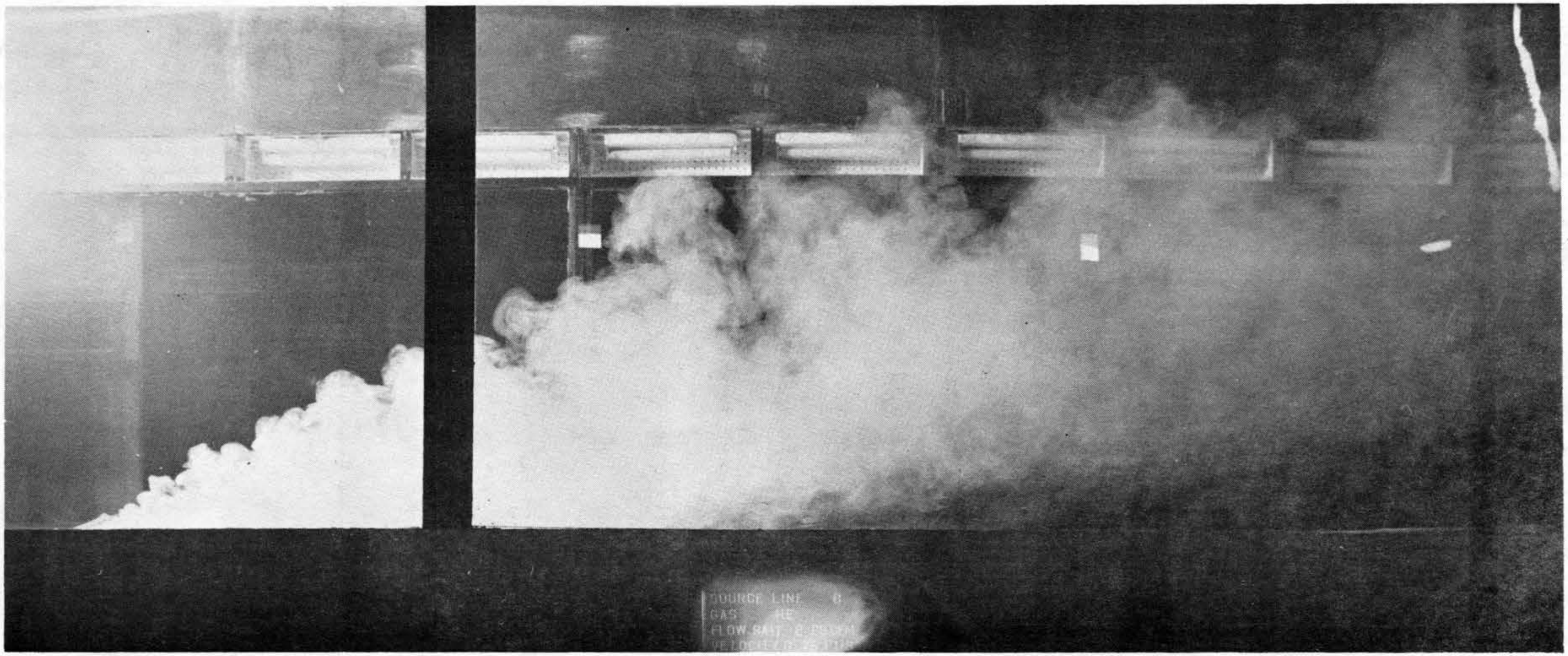

Figure 39b. Line Source in a Shear Layer: Q = 2.25 cfm, U = 0.75 ft/sec

Helium

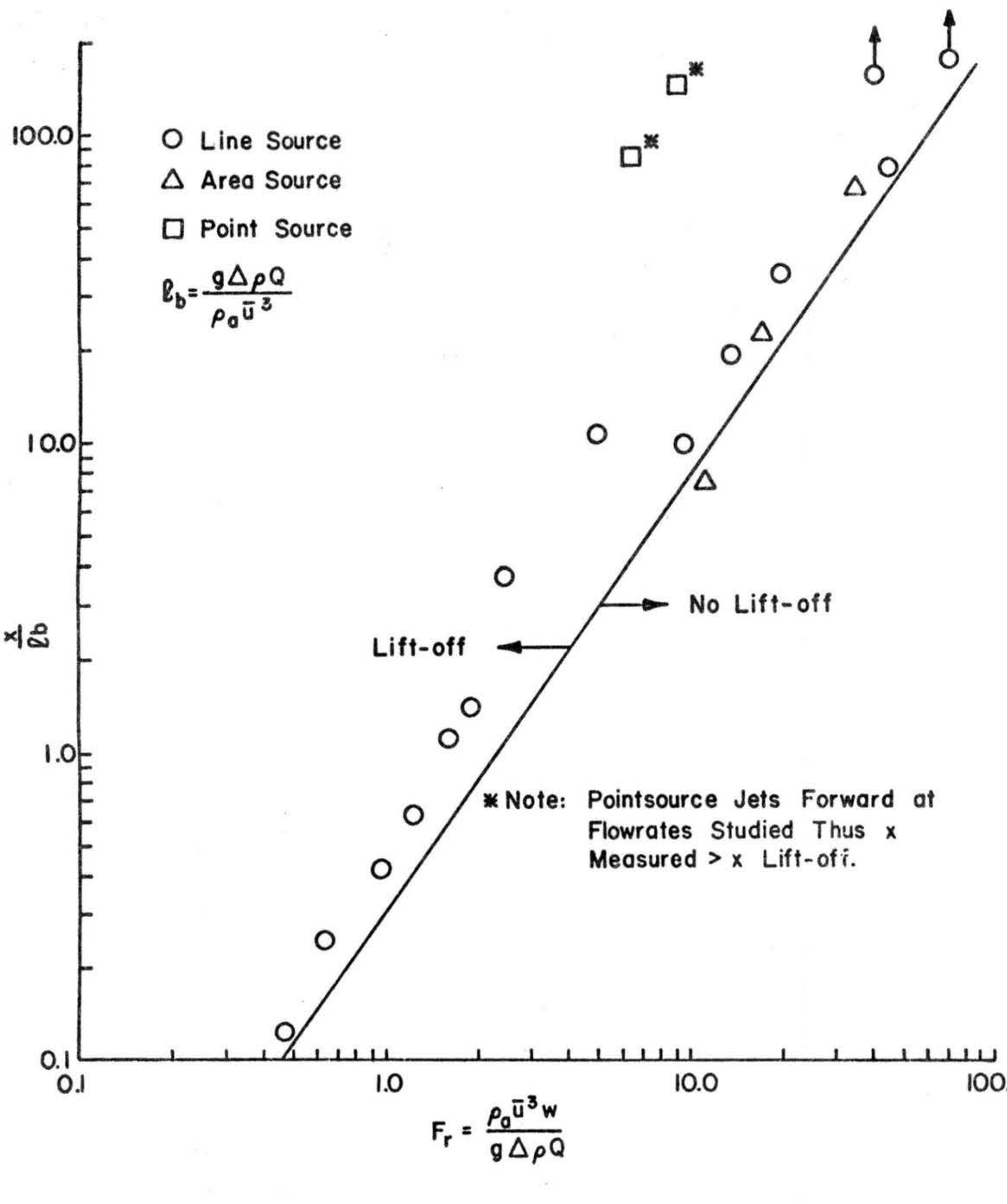

Figure 40. Dimensionless Lift Off Distance vs. Froude Number for Buoyant Surface Released Plumes

T A B L E S

TABLE 1

PROTOTYPE CONDITIONS

Characteristic			Full Scale High Dike	Full Scale Low Dike	Capistrano
Tank Diameter D		(ft)	240	128	-
Height H		(ft)	129	121	-
Dike Diameter d		(ft)	260	330 x 305	80
Height h		(ft)	80	21	-
Boiloff Rates	m_{mx}	$\frac{lbm}{sec}$	2680	2513	202
	Q_{mx}	cfm	1.54×10^6	1.44×10^6	1.6×10^5
	m_{min}	$\frac{lbm}{sec}$	100.0	231.6	20.2
	Q_{min}	cfm	5.59×10^4	1.33×10^5	1.6×10^4
Velocity U_H		mph	7*, 16	7, 16	12^{Δ}
ΔT		$^oF/1000$ ft	25	25	0
$S.G._{CH_4}$ @ boiloff			1.4	1.4	1.4
$\Delta\rho/\rho_a$			0.4	0.4	0.4
$Re_D = U_H d/\nu$			1.55×10^7, 3.56×10^7	2.13×10^7, 4.89×10^7	8.40×10^6
$Fr_d = \frac{U_H^2}{g \frac{\Delta\rho}{\rho_a} d}$			0.030, 0.16	0.022, 0.12	0.302
$Ri_{B_p} = Ri_{B_m}$			0.67	0.67	0
Times		sec	1, 200, 1000	1, 200, 1000	1, 200, 1000

$T_B = 201^oR$, $\rho_L = 26.5$ lbm/ft^3, $\rho_{g_B} = 0.1047$ lbm/ft^3, $\nu = 1.68 \times 10^{-4}$ ft^2/sec

* at 10 meters
Δ at 5 feet

TABLE 2

MODEL CONDITIONS

Characteristic		Full-Scale 1/200 Model High Dike	Full-Scale 1/200 Model Low Dike	Full-Scale 1/400 Model High Dike	Full-Scale 1/400 Model Low Dike	Capistrano 1/106
Tank Diameter D	(in)	14.4	7.68	7.2	3.84	-
Height H	(in)	7.74	7.26	3.87	3.63	-
Dike Diameter d	(in)	15.6	19.8 x 18.3	7.8	9.9 x 9.15	9.1
Height h	(in)	4.8	1.26	2.4	.63	-
$Fr_m = Fr_p$		0.03, 0.16	0.022, 0.12	0.03, 0.16	0.022, 0.12	0.302
$S.G._{CH_4}$ @ boiloff		1.4	1.4	1.4	1.4	1.4
$(\Delta\rho/\rho_a)_m = (\frac{\Delta\rho}{\rho_a})_p$		0.4	0.4	0.4	0.4	0.4
U_H^*	ft/sec	0.7, 1.6	0.7, 1.6	0.5, 1.2	0.5, 1.2	1.7
$Re_{Dm} = U_H d/\nu$		5494, 12535	7563, 17260	1935, 4643	2664, 6233	7637
$Ri_{B_m} = \frac{(T_H - T_{.14H})(H - .14H)g}{\overline{T}(U_H - U_{.14H})^2}$		0	0	0.67	0.67	0
ΔT	^{o}F/ft	0	0	9	9	0
Boiloff= Rates Q_{mx}	cfm	2.72	2.55	0.48	0.45	1.0
Q_{min}	cfm	0.10	0.24	0.018	.042	0.1
Time^o	sec	0.07, 14.1 70.7	0.07, 14.1 70.7	0.05, 10, 50	0.05, 10, 50	0.1, 19.4, 97.1

$$*U_{Hm} = \left(\frac{1}{L.S.}\right)^{1/2} U_{Hp} \qquad {}^{\Delta}\Delta T_m = \Delta T_p \left(\frac{U_m}{U_p}\right)^2 \left(\frac{H_{T_p}}{H_{T_m}}\right) = \Delta T_p \left[\left(\frac{1}{L.S.}\right)^{1/2}\right]^2 L.S. = \Delta T_p$$

$$^o t_m = \left(\frac{U_{\infty p}}{U_{\infty m}}\right)\left(\frac{L_m}{L_p}\right) = (L.S.)^{1/2} \frac{1}{L.S.} t_p = \left(\frac{1}{L.S.}\right)^{1/2} t_p \qquad {}^{=}Q_m = Q_p \frac{U_m}{U_p} \left(\frac{L_m}{L_p}\right)^2 = Q_p \left(\frac{1}{L.S.}\right)^{1/2} \left(\frac{1}{L.S.}\right)^2 = Q_p \left(\frac{1}{L.S.}\right)^{2.5}$$

TABLE 3

FILM LOG FOR FLOW VISUALIZATION

Reel No. 1 - 2% Upwind Grade Tests Filmed in the Industrial Aerodynamics Wind Tunnel. Model Gas of CO_2 @ 22°C.

RUN #	SOURCE DESCRIPTION	SIMULATED WIND SPEED (fps)	SIMULATED BOILOFF RATE (lb_m/sec)
1	Area Source (Capistrano 044 1/106 Scale Model)	23	160
2	"	23	420
3	"	23	1200
4	"	23	2400
5	"	16	160
6	"	16	420
7	"	16	1200
8	"	16	2400
9	"	30	160
10	"	30	420
11	"	30	1200
12	"	30	2400
13	High Dike (1/400 Scale Model)	16	160
14	"	16	420
15	"	16	1200
16	"	16	2400
17	"	23	460
18	"	23	420
19	"	23	1200
20	"	23	2400
21	"	30	160
22	"	30	420
23	"	30	1200
24	"	30	2400

TABLE 3 (continued)

FILM LOG FOR FLOW VISUALIZATION

Reel No. 1 (continued) - 2% Upwind Grade Tests Filmed in the Industrial Aerodynamics Wind Tunnel. Model Gas of CO_2 @ 22°C.

RUN #	SOURCE DESCRIPTION	SIMULATED WIND SPEED (fps)	SIMULATED BOILOFF RATE (lb_m/sec)
25	High Dike (1/400 Scale Model with 2 Upstream Obstacles)	30	160
26	"	30	420
27	"	30	1200
28	"	30	2400
29	"	23	160
30	"	23	420
31	"	23	1200
32	"	23	2400
33	"	16	160
34	"	16	420
35	"	16	1200
36	"	16	2400
37	High Dike (1/400 Scale Model with 1 Upstream Obstacle)	16	160
38	"	16	420
39	"	16	1200
40	"	16	2400
41	"	23	160
42	"	23	420
43	"	23	1200
44	"	23	2400
45	"	30	160
46	"	30	420
47	"	30	1200
48	"	30	1400

TABLE 3 (continued)

FILM LOG FOR FLOW VISUALIZATION

Reel No. 2 - Flat Grade Tests Filmed in the Industrial Aerodynamics Wind Tunnel. Model Gas of CO_2 @ 22° C.

RUN #	SOURCE DESCRIPTION	SIMULATED WIND SPEED (fps)	SIMULATED BOILOFF RATE (lb_m/sec)
1-A	Area Source (Capistrano 044 1/106 Scale Model)	16	160
2-A	"	16	420
3-A	"	16	1200
4-A	"	16	2400
5-A	"	23	160
6-A	"	23	420
7-A	"	23	1200
8-A	"	23	2400
9-A	"	30	160
10-A	"	30	420
11-A	"	30	1200
12-A	"	30	2400
13-A	High Dike (1/400 Scale Model)	30	160
14-A	"	30	420
15-A	"	30	1200
16-A	"	30	2400
17-A	"	23	160
18-A	"	23	420
19-A	"	23	1200
20-A	"	23	2400
21-A	"	16	160
22-A	"	16	420
23-A	"	16	1200
24-A	"	16	2400

TABLE 3 (continued)

FILM LOG FOR FLOW VISUALIZATION

Reel No. 3 - Variable Boiloff Tests Filmed in the Meteorological Wind Tunnel.

RUN #	SOURCE DESCRIPTION	SIMULATION GAS	SIMULATED BOILOFF CHARACTERISTIC OF:	SIMULATED WIND SPEED (fps)
1V	High Dike (1:200)	CO_2 @ 22°C.	Soil	10
1VA	"	"	Concrete	10
2V	"	"	Soil	16
3V	"	"	Soil	23
4V	Low Dike (1:200)	"	Soil	10
4VA	"	"	Concrete	10
5V	"	"	Soil	16
6V	"	"	Soil	23
7V	High Dike (1:400)	"	Soil	10
8V	"	"	Soil	23
9V	Low Dike (1:400)	"	Soil	10
10V	"	"	Soil	23
11V	High Dike (1:400)	50% He - 50% N_2 @ -160°C.	Soil	10
12V	"	"	Soil	23
13V	Low Dike (1:400)	"	Soil	10
14V	"	"	Soil	23

TABLE 4

SUMMARY OF CONCENTRATION TESTS

RUN NO.	MODEL	WIND SPEED (mph)	STRATIFICATION	BOILOFF RATE (lbm/sec)	SURFACES MODEL	FLOOR
1	High 1:400	7*	Neutral	2400	Steel	Aluminum
2	High 1:400	7	Neutral	1400	Steel	Aluminum
3	High 1:400	16*	Neutral	2400	Steel	Aluminum
4	High 1:400	16	Neutral	1400	Steel	Aluminum
5	Low 1:400	7	Neutral	2400	Steel	Aluminum
6R	High 1:400	7	Stable	2400	Steel	Aluminum
7R	High 1:400	7	Stable	1400	Steel	Aluminum
8R	Low 1:400	7	Stable	2400	Steel	Aluminum
9	Capistrano	12Δ	Neutral	202	Steel	Aluminum
10	Capistrano	12	Neutral	141	Steel	Aluminum
11R	High 1:200	7	Neutral	1400	Steel	Aluminum
45	High 1:400	7	Neutral	2400	Cold Steel	Aluminum
46	High 1:400	16	Neutral	2400	Cold Steel	Aluminum
47	Low 1:400	7	Neutral	2400	Cold Steel	Aluminum
48	Low 1:400	16	Neutral	2400	Cold Steel	Aluminum
49	High 1:400	7	Neutral	2400	Cold Steel	Styrofoam
50	High 1:400	16	Neutral	2400	Cold Steel	Styrofoam
51	Low 1:400	7	Neutral	2400	Cold Steel	Styrofoam
52	Low 1:400	16	Neutral	2400	Cold Steel	Styrofoam
53	High 1:400	7	Stable	2400	Cold Steel	Aluminum
54	Low 1:400	7	Stable	2400	Steel	Aluminum
13	High 1:400	7	Neutral	Soil†	Steel	Aluminum
14	High 1:400	7	Neutral	Concrete	Steel	Aluminum
15	High 1:400	7	Neutral	Insulated Concrete	Steel	Aluminum
16	High 1:400	16	Neutral	Soil	Steel	Aluminum
17	High 1:400	16	Neutral	Concrete	Steel	Aluminum
18	High 1:400	16	Neutral	Insulated Concrete	Steel	Aluminum
19	Low 1:400	7	Neutral	Soil	Steel	Aluminum
20	High 1:400	7	Stable	Soil	Steel	Aluminum
22	Low 1:400	7	Stable	Soil	Steel	Aluminum
23	Capistrano	12	Neutral	Case I	Steel	Aluminum
24	Capistrano	12	Neutral	Case II	Steel	Aluminum

* at 10 meters

Δ at 5 feet

† refer to Variable Boiloff Curves, Figures

TABLE 5a

APPROXIMATE DISTANCE (FT) DOWNWIND TO THE LFL
(Obtain by Simulation Gas Pure CO_2 of M.W. 44 @ 70^{o}F)

Model	Wind Direction	Surface Description: Aluminum	Surface Description: Insulated	Continuous Boiloff (lbm/sec)	STRATIFICATION: Neutral 10 ft/sec	Neutral 16 ft/sec	Neutral 23 ft/sec	Stable Cat. G. 10 ft/sec	Stable Cat. G. 16 ft/sec	Stable Cat. G. 23 ft/sec	$\frac{X}{H}$
High Dike	0	X		2400	730						5.6
1/400 Scale Model		X		1400	400						3.00
Steel Construction		X		2400			450				3.50
		X		1400			-				-
		X		2400				1500			11.50
		X		1400				1080			8.50
Low Dike	0	X		2400	1730						14.50
1/400 Scale Model		X		2400				1500			12.50
Steel Construction											
Capistrano 044	0	X		202		420					
		X		141		300					
High Dike	0	X		1400	2370						18.2
1/200 Scale Model		X		1400							
Styrofoam Construction											

* H = Height of tank L.D. = 121 ft.
H.D. = 129 ft.

TABLE 5b

APPROXIMATE DISTANCE (FT) DOWNWIND TO THE LFL
(Obtain by Simulation Gas He-N_2 of M.W. 16 @ -260°F)

Model	Wind Direction	Surface Description: Aluminum	Surface Description: Insulated	Continuous Boiloff (lbm/sec)	STRATIFICATION: Neutral 10 ft/sec	Neutral 16 ft/sec	Neutral 23 ft/sec	Stable Cat. G 10 ft/sec	Stable Cat. G 16 ft/sec	Stable Cat. G 23 ft/sec	$\frac{X}{H}$ *
High Dike	0	X		2400	900						7.00
1/400 Scale Model		X		2400			1200				9.00
Steel Construction			X	2400	587						4.50
			X	2400			1210				9.50
		X		2400				-			-
Low Dike	0	X		2400	1590						13.25
1/400 Scale Model		X		2400			1130				9.50
Steel Construction			X	2400	1710						14.25
			X	2400			1700				14.00
		X		2400				963			8.00

* H = height of tank L.D. = 121 ft.
H.D. = 129 ft.

TABLE 6

APPROXIMATE DISTANCES (FT) DOWNWIND TO THE LFL
FOR A VARIABLE RELEASE OF CO_2

MODEL	NEUTRAL			STABLE
	7 mph	12 mph	16 mph	7 mph
High Soil	~850		~700	~800
High Concrete	~300		<300	
High Insulated Concrete	<300		<300	
Low Soil	1000			1000
Capistrano Case I		700		
Capistrano Case II		400		

TABLE 7-1

PEAK CONCENTRATION DATA FOR VARIABLE BOILOFF

Low Soil - 1:400
Wind Speed - 7 mph
Stratification - Neutral

Position (ft)			Maximum	Maximum Peak Occurs at Time (sec)														
X	Y	Z	Peak	71	106	141	177	212	283	354	424	495	566	636	707	849	1061	1414
450	-300	0	15.5	9.2	15.5	14.5	12.6	10.7	7.8	6.8	6.3	5.8	5.3	5.1	4.8	0	0	0
450	-150	0	11.1	2.9	6.8	11.1	10.4	7.0	5.3	2.1	2.3	1.3	2.4	2.5	2.4	0	0	0
450	0	0	4.4	2.2	2.9	3.4	3.2	4.4	2.5	.4	.2	.9	1.2	1.2	1.0	0	0	0
450	150	0	11.1	10.7	11.1	10.7	8.6	7.6	5.8	4.8	4.6	2.9	2.9	4.4	3.9	2.5	.4	0
450	300	0	15.2	6.8	15.2	14.0	11.1	8.7	6.3	5.8	5.3	4.8	4.6	4.9	3.9	3.6	0	0
1000	-400	0	5.1	0	0	1.2	4.6	5.1	3.9	3.3	2.7	2.2	1.9	1.7	1.7	1.9	.5	0
1000	-200	0	2.6	0	.6	2.1	2.6	1.8	1.3	.8	1.0	.5	.9	1.1	1.2	0	0	0
1000	0	0	4.0	0	1.5	2.9	3.6	4.0	2.5	2.1	1.9	1.3	.9	1.0	1.6	0	0	0
1000	0	33	.8	0	.3	.2	.8	.8	.5	.5	.6	.5	.3	.3	.2	0	0	0
1000	0	66	1.0	0	.2	.2	1.0	.8	.2	.2	.3	.6	.4	.2	.3	0	0	0
1000	200	0	3.8	0	1.3	2.7	2.5	3.8	2.4	1.7	1.6	1.4	1.6	1.2	1.3	0	0	0
1000	400	0	4.9	0	0	4.0	4.7	4.9	4.1	2.9	2.8	2.7	2.3	2.2	2.0	1.8	.7	0
2000	0	0	1.2	0	0	0	0	.2	1.0	1.1	1.2	1.1	1.0	.9	.7	.5	.3	.1
3500	0	0	1.0	0	0	0	0	0	0	.4	.8	1.0	1.0	1.0	1.0	.7	.5	.4
3500	0	33	.8	0	0	0	.1	.1	.3	.6	.8	.7	.7	.6	.6	.4	.4	.2
3500	0	66	.7	0	0	0	0	0	0	.4	.7	.5	.4	.4	.4	.4	.3	.2
5000	0	0	.6	0	0	0	0	0	0	.1	.2	.2	.4	.5	.5	.4	.2	.2

TABLE 7-2

PEAK CONCENTRATION DATA FOR VARIABLE BOILOFF

Low Soil - 1:400
Wind Speed - 7 mph
Stratification - Stable

Position (ft)			Maximum	Maximum Peak Occurs at Time (sec)														
X	Y	Z	Peak	71	106	141	177	212	283	354	424	495	566	636	707	849	1061	1414
450	-300	0	19.6	13.6	19.6	18.6	15.0	12.5	7.9	6.1	5.4	5.7	4.6	4.5	4.6	1.3	0	0
450	-150	0	13.9	10.7	12.9	13.9	13.2	11.8	8.9	9.3	8.9	8.6	8.4	8.6	8.6	5.4	1.8	.7
450	0	0	3.6	1.1	1.8	3.0	3.6	2.7	2.3	3.2	2.3	2.3	2.7	2.5	2.9	3.2	3.0	2.7
450	150	0	8.9	5.0	8.2	8.9	7.9	6.4	5.7	5.0	5.4	5.7	5.0	5.0	5.0	2.9	.4	0
450	300	0	16.9	3.6	16.8	16.9	15.4	10.7	7.1	5.7	5.0	4.3	3.9	3.6	3.6	1.1	0	0
450	450	0	13.2	0	7.1	13.2	10	7.9	5.0	3.9	2.9	1.8	1.6	1.4	1.1	0	0	0
1000	-200	0	4.2	0	.4	2.3	3.6	4.2	3.4	2.7	1.4	1.1	.6	.7	.5	.7	0	0
1000	0	0	5.0	0	0	1.2	3.9	4.8	5.0	3.2	2.9	3.2	2.2	2.1	2.1	1.8	0	0
1000	0	33	2.5	.5	.3	1.6	2.5	2.3	1.2	1.6	1.7	1.1	.7	1.1	1.4	.5	.5	.7
1000	0	66	1.9	.5	.5	.7	.9	.9	1.0	1.1	1.2	1.3	1.3	1.4	1.5	1.6	1.9	0
1000	200	0	3.6	0	0	1.8	3.6	2.9	2.5	1.3	.7	.9	.9	.9	.6	.7	.5	0
2000	0	0	2.3	.1	.1	.1	.2	.3	1.1	2.1	2.1	2.0	2.0	1.8	1.6	1.2	.9	.4
3500	0	0	1.0	0	0	0	0	0	0	.2	.4	.9	.9	.9	.9	.7	.3	.1

TABLE 7-3

PEAK CONCENTRATION DATA FOR VARIABLE BOILOFF

High Soil - 1:400
Wind Speed - 7 mph
Stratification - Neutral

Position (ft)			Maximum	Maximum Peak Occurs at Time (sec)															
X	Y	Z	Peak	71	106	141	177	212	283	354	424	495	566	636	707	849	1061	1414
450	-450	0	8.3	0	8.0	8.3	7.2	6.3	5.2	4.4	3.6	3.1	3.5	3.5	2.5	0	0	0
450	-300	0	11.5	6.8	11.5	10.8	7.8	7.5	6.2	5.3	4.8	4.4	3.8	3.4	2.8	0	0	0
450	0	0	11.5	.1	11.5	11.0	6.1	4.7	1.0	1.1	1.5	1.7	2.2	1.5	.7	0	0	0
1000	-200	0	3.1	0	0	2.9	3.0	3.1	2.5	1.9	1.5	1.5	1.2	1.1	.8	.6	.7	0
1000	0	0	3.7	0	0	.5	3.0	3.7	2.5	1.7	1.4	1.0	.8	.6	.8	.6	.8	0
1000	0	33	2.4	0	.3	2.4	1.2	1.3	1.8	1.0	.7	.8	.5	.3	.6	.4	.3	0
1000	0	66	.6	.2	.5	.4	.6	.2	.6	.1	.4	.4	.1	.1	.2	.3	.2	0
1000	200	0	4.1	0	0	2.8	4.1	3.7	2.8	1.8	.7	.7	.3	.5	.3	.2	.2	0
2000	0	0	.8	.1	0	.1	.1	.4	.7	.8	.6	.6	.5	.3	.2	.2	.1	.1
3500	0	0	.4	0	0	0	.1	.1	.3	.4	.4	.3	.3	.2	.2	.1	0	0
3500	0	33	.5	.1	.1	.1	0	0	.2	.4	.5	.5	.4	.3	.5	.2	.1	.1
3500	0	66	.5	0	0	.1	0	.1	.1	.4	.5	.2	.3	.2	.2	.1	.1	0
5000	0	0	.2	0	0	0	0	0	0	0	.1	.2	.2	.2	.2	.1	.1	0

TABLE 7-4

PEAK CONCENTRATION DATA FOR VARIABLE BOILOFF

High Soil - 1:400
Wind Speed - 7 mph
Stratification - Stable

Position (ft)			Maximum	Maximum Peak Occurs at Time (sec)														
X	Y	Z	Peak	71	106	141	177	212	283	354	424	495	566	636	707	849	1061	1414
450	0	0	10.3	7.8	10.3	4.3	3.9	5.4	4.3	5.0	5.2	5.4	7.3	6.4	7.1	7.8	7.5	0
450	150	0	11.8	8.2	11.8	11.0	10.0	9.3	8.2	8.2	8.2	8.6	9.5	9.6	10.3	11.1	8.9	7.1
450	300	0	15.4	1.1	14.3	15.4	12.1	10.7	7.9	5.4	3.9	3.9	3.2	2.1	2.1	.7	0	0
450	450	0	10.0	0	7.5	8.9	10.0	7.9	3.6	1.8	.5	.4	.4	0	0	0	0	0
1000	-200	0	3.0	.2	.4	1.1	2.5	3.0	2.1	1.2	0	0	0	0	0	0	0	0
1000	0	0	2.7	.9	.5	.6	2.7	2.1	1.2	.2	4.5	.9	.9	1.1	0	0	0	0
1000	0	33	1.1	.2	.5	.7	.6	.4	.5	.5	.5	.5	.7	.8	.9	1.1	0	0
1000	200	0	2.9	.4	.9	2.1	2.5	2.7	2.7	2.0	2.0	1.8	1.2	1.4	1.8	1.8	0	0
2000	0	0	1.4	0	0	0	.1	0	.4	1.1	1.4	1.4	1.0	.8	.8	.4	.1	0

TABLE 7-5

PEAK CONCENTRATION DATA FOR VARIABLE BOILOFF

High Soil - 1:400
Wind Speed - 16 mph @ 10 meters
Stratification - Neutral

Position (ft)			Maximum	Maximum Peak Occurs at Time (sec)														
X	Y	Z	Peak	71	106	141	177	212	283	354	424	495	566	636	707	849	1061	1414
450	-300	0	11.1	0	0	2.9	7.7	11.1	9.3	7.8	6.8	4.8	3.3	2.9	2.7	2.5	.8	.6
450	-150	0	11.1	0	1.0	4.8	11.1	9.7	8.1	6.8	5.2	4.7	4.5	2.9	2.5	2.3	2.7	1.4
450	0	0	6.4	3.9	3.9	3.9	3.5	6.4	1.4	1.4	1.4	1.0	3.5	1.4	1.0	.8	.1	0
450	150	0	12.4	0	0	3.9	12.4	11.0	6.8	5.2	4.3	3.9	3.3	2.3	1.9	1.4	1.4	.8
450	300	0	12.4	0	0	4.8	9.1	12.4	7.8	5.8	5.4	4.8	3.5	2.7	2.1	.97	.5	.4
450	450	0	10.9	0	0	0	6.8	10.9	10.9	9.7	6.8	4.8	3.7	1.4	0	0	0	0
450	600	0	2.1	0	0	0	0	0	.5	2.1	.5	0	0	0	0	0	0	0
1000	-200	0	2.1	0	1.6	2.0	2.1	1.6	1.2	.8	.6	.6	.5	.3	.3	0	0	0
1000	0	0	1.4	0	1.2	1.2	1.3	1.4	.8	.5	.3	.3	.2	.1	.1	.2	.4	0
1000	0	33	1.5	.1	1.4	1.5	.6	.6	.6	.5	.4	.4	.3	.3	.4	0	0	0
1000	0	66	1.7	.2	1.7	.8	.6	.9	.8	.4	.4	.3	.3	.3	.2	0	0	0
1000	200	0	2.2	0	.1	.2	.8	1.8	1.8	2.2	1.3	1.1	1.1	.8	.5	.3	.4	.2
2000	0	0	.5	.1	.8	.4	.5	.4	.3	.2	.2	.1	.1	.1	.1	.1	.1	0
3500	0	0	.3	0	0	0	.1	.2	.3	.3	.1	.1	.2	.1	.1	.1	.1	0
3500	0	33	.3	.1	.1	.1	.2	.3	.3	.2	.2	.2	.2	.2	.2	.2	0	0
3500	0	66	.4	.1	.1	.1	.1	.3	.3	.2	.2	.1	.1	.1	.1	.2	0	0
5000	0	0	.3	0	.1	.1	.1	.1	.3	.3	.3	.1	.2	.1	.1	0	0	0

TABLE 7-6

PEAK CONCENTRATION DATA FOR VARIABLE BOILOFF

High Concrete - 1:400
Wind Speed - 7 mph
Stratification - Neutral

Position (ft)			Maximum	Maximum Peak Occurs at Time (sec)															
X	Y	Z	Peak	71	106	141	177	212	283	354	424	495	566	636	707	849	1061	1414	
450	-150	0	3.3	0	.4	2.6	3.0	3.3	2.2	2.0	1.8	1.9	2.1	1.1	.9	1.2	.7	0	
450	0	0	1.9	0	.7	1.5	1.5	1.6	1.8	1.5	1.4	.9	.8	1.2	1.3	.6	.4	.2	
450	150	0	2.6	.1	.7	2.4	2.6	2.6	1.5	1.5	1.5	1.7	1.2	1.4	1.4	1.2	.6	0	
1000	-200	0	.9	0	.1	.3	.4	.6	.8	.9	.7	.6	.4	.5	.3	.3	.1	.1	
1000	0	0	.5	.1	.1	.1	.1	.2	.5	.5	.4	.3	.3	.3	.2	.2	.2	.1	
1000	0	33	.5	.1	.1	.2	.3	.3	.4	.4	.4	.4	.3	.3	.3	.3	.2	.2	
1000	0	66	.4	.1	.1	.2	.3	.4	.3	.4	.4	.3	.3	.3	.3	.2	.2	.2	
1000	200	0	.8	0	.1	.2	.4	.6	.6	.3	.3	.5	.4	.4	.4	.3	.2	.1	
2000	0	0	.2	.1	.1	.1	.1	.1	.1	.1	.2	.2	.2	.2	.1	.2	.2	.1	
3500	0	0	.1	.1	.1	.1	.1	.1	.1	.1	.1	.1	.1	.1	.1	.1	.1	0	

TABLE 7-7

PEAK CONCENTRATION DATA FOR VARIABLE BOILOFF

High Concrete
Wind Speed - 16 mph
Stratification - Neutral

Position (ft)			Maximum	Maximum Peak Occurs at Time (sec)														
X	Y	Z	Peak	71	106	141	177	212	283	354	424	495	566	636	707	849	1061	1414
450	0	0	1.1	0	.5	1.1	1.0	1.1	1.0	.9	.7	.5	.6	.5	.5	.5	.2	.1
1000	-200	0	.6	0	0	.3	.4	.5	.5	.6	.3	.4	.4	.3	.2	.2	.2	0
1000	0	0	.6	0	.1	.2	.5	.6	.5	.5	.5	.4	.3	.3	.2	.2	.1	0
1000	0	33	.4	.1	.1	.2	.3	.4	.3	.4	.4	.3	.3	.3	.3	.2	.1	0
1000	0	66	.4	0	.1	.3	.2	.2	.3	.3	.2	.3	.3	.4	.2	.2	.2	0
1000	200	0	.5	0	0	.2	.4	.5	.4	.4	.4	.4	.4	.4	.3	.2	.2	0
2000	0	0	.2	0	0	0	.1	.1	.2	.1	.1	.1	.1	.1	.1	.1	.1	0

TABLE 7-8

PEAK CONCENTRATION DATA FOR VARIABLE BOILOFF

High Insulated Concrete - 1:400
Wind Speed - 7 mph
Stratification - Neutral

Position (ft)			Maximum	Maximum Peak Occurs at Time (sec)														
X	Y	Z	Peak	71	106	141	177	212	283	354	424	495	566	636	707	849	1061	1414
450	0	0	.5	0	0	0	.1	.1	.3	.3	.2	.3	.4	.4	.4	.3	.4	0
1000	-200	0	.2	0	0	.1	.1	0	.1	.1	.1	.2	.1	.1	.1	.1	.1	0
1000	0	0	.3	0	0	.2	.1	.2	.2	.2	.3	.2	.3	.1	.2	.2	.1	0
1000	0	33	.3	0	.1	.1	.1	.1	.2	.2	.1	.1	.3	.2	.2	.3	.1	0
1000	200	0	.2	0	0	0	.1	0	.1	.2	.2	.1	.2	.2	.2	.1	.1	0

TABLE 7-9

PEAK CONCENTRATION DATA FOR VARIABLE BOILOFF

High Insulated Concrete - 1:400
Wind Speed - 16 mph
Stratification - Neutral

Position (ft)			Maximum	Maximum Peak Occurs at Time (sec)														
X	Y	Z	Peak	71	106	141	177	212	283	354	424	495	566	636	707	849	1061	1414
450	0	0	.5	0	0	0	.2	.3	.3	.3	.5	.4	.5	.3	.3	0	0	0
1000	-200	0	.2	0	.1	.1	.1	.1	.1	.1	.1	.1	.2	.1	0	0	0	0
1000	0	0	.3	.1	.1	.1	.1	.1	.1	.1	.2	.3	.2	.2	.2	0	0	0
1000	200	0	.1	0	0	0	0	0	0	.1	.1	0	0	0	0	0	0	0

TABLE 7-10

PEAK CONCENTRATION DATA FOR VARIABLE BOILOFF

Capistrano Case I
Wind Speed - 12 mph @ 5 ft.
Stratification - Neutral

Position (ft)			Maximum	Maximum Peak that occurs at time (sec)												
x	y	z	Peak	51	77	103	129	154	206	257	309	360	412	463	515
160	0	0	16.9	14.1	16.9	16.5	11.8	9.3	7.1	4.9	3.8	3.0	3.0	3.4	3.0
320	-80	0	9.9	6.2	9.0	9.0	10.0	5.4	1.8	0.8	0.5	0.2	0.6	0.1	0.4
320	0	0	9.9	7.5	8.8	9.9	6.9	4.3	3.2	2.3	2.1	1.7	1.9	1.7	1.5
320	0	10	4.7	3.9	4.7	2.4	3.8	3.0	2.4	2.3	1.5	1.1	1.2	1.6	1.4
320	80	0	9.2	5.4	9.2	8.3	6.7	3.4	1.0	0.4	0	0	0	0	0
640	-100	0	4.7	0.6	3.8	4.7	3.9	3.6	0.3	0.2	0.2	0.2	0.1	0.2	0
640	0	0	5.3	1.3	4.1	4.7	5.2	4.1	2.8	1.3	1.1	0.8	0.6	0.6	0.6
640	0	20	2.0	0.8	1.1	2.0	1.0	0.9	1.1	0.5	0.5	0.6	0.5	0.7	0.3
640	100	0	4.1	1.2	3.6	4.1	3.9	2.9	0.7	0.3	0	0	0	0	0
960	-80	0	3.1	0.2	1.4	2.3	3.1	2.6	1.6	0.8	0.6	0.4	0.3	0.5	0.4
960	0	0	3.0	0.2	1.5	2.8	2.8	2.6	1.5	1.3	0.8	0.6	0.6	0.5	0.5
960	0	20	1.9	0.1	0.8	1.6	1.9	1.5	0.8	0.6	0.4	0.4	0.5	0.5	0.3
960	80	0	2.4	0.2	1.4	1.7	2.1	2.4	1.2	0.9	0.5	0.6	0.4	0.3	0.2

TABLE 7-11

PEAK CONCENTRATION DATA FOR VARIABLE BOILOFF

Capistrano Case II
Wind Speed - 12 mph @ 5 ft.
Stratification - Neutral

Position (ft)			Maximum	Maximum Peak that occurs at time (sec)											
x	y	z	Peak	51	77	103	129	154	206	257	309	360	412	463	515
160	0	0	13.7	13.7	10.3	7.8	8.0	6.6	6.0	5.8	3.4	4.0	3.6	3.4	2.3
320	-80	0	4.8	2.3	4.8	4.0	1.7	0.8	2.1	0.3	0.9	1.3	0.7	0.1	0.2
320	0	0	6.6	6.6	6.1	4.7	6.0	4.0	3.8	2.5	2.2	2.2	1.6	1.5	1.0
320	0	10	3.4	3.2	2.4	3.0	3.4	2.2	2.8	3.0	2.2	1.2	2.3	1.9	1.1
320	80	0	4.9	3.2	4.9	3.0	2.4	2.8	0.1	0.1	0.1	0.1	0.1	0.1	0
640	-100	0	1.4	0.4	1.4	1.2	1.2	1.0	0.5	0.8	0.4	0.3	0.6	0.1	0.3
640	0	0	2.7	1.1	2.7	2.7	2.7	1.9	1.6	1.3	1.4	1.0	1.0	0.9	0.7
640	0	20	1.1	0.7	0.7	0.9	0.8	0.6	1.1	0.6	0.5	0.7	0.7	0.6	0.8
640	100	0	2.2	0.2	0.6	2.2	1.7	1.1	1.0	1.0	0.2	0	0.3	0.3	0
960	-80	0	2.1	0	1.1	1.7	2.1	1.5	0.5	1.0	0.6	0.6	0.4	0.4	0.8
960	0	0	1.7	0	1.1	1.6	1.7	1.7	1.5	1.0	0.9	0.6	0.5	0.6	0.5
960	0	20	1.0	0	0.9	0.9	0.9	0.9	0.9	1.0	0.7	0.5	0.5	0.4	0.4
960	80	0	1.8	0	0.4	1.8	1.6	1.7	1.0	0.7	0.7	0.2	0.1	0.3	0.3

TABLE 8

LOCATOR TABLE MEAN CONCENTRATION RESULTS

Model	Boiloff Rate (lbm/sec)	CO_2 Release MW44 Wind Speed 7 mph (10 ft/sec)	12 mph (18 ft/sec)	16 mph (23 ft/sec)	H_e-N_2 Release MW16 Wind Speed 7 mph (10 ft/sec)	16 mph (23 ft/sec)
High Dike	2400	1,6,9		3	17,21,25	18,22
1/400	1400	2,7,10		4		
High Dike	1400	14				
1/200	250	15		16		
Low Dike	2400	5,8,11			19,23,26	20,24
1/400						
Capistrano 044	202		12			
1/106	141		13			

Table 8-1

8-1 to 8-26 Please refer to errata on verso of title page.

RUN NUMBER ONE
DIKE TYPE HIGH
SCALE 1 TO 400
STRATIFICATION NEUTRAL
WIND SPEED 7 MPH
BOIL OFF RATE 2400 LB/S

X(FT)	Y(FT)	Z(FT)	DILLUTION	K COEF X 10-2
450.00000	-600.00000	-0.00000	4.21353	2.06417
450.00000	-300.00000	-0.00000	3.37087	1.65136
450.00000	-0.00000	-0.00000	2.17170	1.06390
450.00000	300.00000	-0.00000	6.44982	3.15971
450.00000	600.00000	-0.00000	4.31076	2.11180
1000.00000	-800.00000	-0.00000	2.91713	1.42908
1000.00000	-400.00000	-0.00000	3.63015	1.77838
1000.00000	-0.00000	-0.00000	3.27364	1.60373
1000.00000	-0.00000	33.00000	.68084	.33354
1000.00000	-0.00000	66.00000	.16228	.07950
1000.00000	400.00000	-0.00000	.19469	.09538
1000.00000	800.00000	-0.00000	.22710	.11125
2000.00000	-0.00000	-0.00000	.06505	.03187
3500.00000	-800.00000	-0.00000	.16228	.07950
3500.00000	-400.00000	-0.00000	.03264	.01599
3500.00000	-0.00000	-0.00000	.22710	.11125
3500.00000	-0.00000	33.00000	0.00000	0.00000
3500.00000	-0.00000	100.00000	.45397	.22240
3500.00000	-0.00000	200.00000	.14607	.07156
3500.00000	400.00000	-0.00000	0.00000	0.00000
3500.00000	800.00000	-0.00000	.61602	.30178
5000.00000	-0.00000	-0.00000	.74566	.36529
6500.00000	-0.00000	-0.00000	.58361	.28591
-0.00000	-0.00000	-0.00000	0.00000	0.00000
-0.00000	-0.00000	-0.00000	0.00000	0.00000

Table 8-2

RUN NUMBER TWO
DIKE TYPE HIGH
SCALE 1/400
STRATIFICATION NEUTRAL
WIND SPEED 7 MPH
BOIL OFF RATE 1400 LB/S

X(FT)	Y(FT)	Z(FT)	DILLUTION	K COEF X 10-2
450.00000	-600.00000	-0.00000	2.69026	2.21413
450.00000	-300.00000	-0.00000	2.53145	2.08343
450.00000	-0.00000	-0.00000	2.27865	1.87537
450.00000	300.00000	-0.00000	4.57004	3.76122
450.00000	600.00000	-0.00000	2.97871	2.45153
1000.00000	-800.00000	-0.00000	2.06151	1.69666
1000.00000	-400.00000	-0.00000	2.80694	2.31016
1000.00000	-0.00000	-0.00000	2.39533	1.97140
1000.00000	-0.00000	33.00000	.63871	.52567
1000.00000	-0.00000	66.00000	.17524	.14423
1000.00000	400.00000	-0.00000	0.00000	0.00000
1000.00000	800.00000	-0.00000	.14932	.12289
2000.00000	-0.00000	-0.00000	.13959	.11489
3500.00000	-800.00000	-0.00000	.66139	.54434
3500.00000	-400.00000	-0.00000	.12663	.10422
3500.00000	-0.00000	-0.00000	.19145	.15757
3500.00000	-0.00000	33.00000	.23682	.19491
3500.00000	-0.00000	100.00000	.40860	.33628
3500.00000	-0.00000	200.00000	.23358	.19224
3500.00000	400.00000	-0.00000	.71001	.58435
3500.00000	800.00000	-0.00000	.58037	.47765
5000.00000	-0.00000	-0.00000	.42156	.34695
6500.00000	-0.00000	-0.00000	.34702	.28560
-0.00000	-0.00000	-0.00000	0.00000	0.00000
-0.00000	-0.00000	-0.00000	0.00000	0.00000

Table 8-3

RUN NUMBER THREE
DIKE TYPE HIGH
SCALE 1/400
STRATIFICATION NEUTRAL
WIND SPEED 16 MPH
BOIL OFF RATE 2400 LB/S

X(FT)	Y(FT)	Z(FT)	DILLUTION	K COEF X 10-2
450.00000	-600.00000	-0.00000	.57713	.40469
450.00000	-300.00000	-0.00000	3.97370	2.78642
450.00000	-0.00000	-0.00000	1.70176	1.19330
450.00000	300.00000	-0.00000	4.98489	3.49549
450.00000	600.00000	-0.00000	.35998	.25242
1000.00000	-800.00000	-0.00000	.43452	.30470
1000.00000	-400.00000	-0.00000	3.24771	2.27735
1000.00000	-0.00000	-0.00000	1.00494	.70468
1000.00000	-0.00000	33.00000	.61278	.42969
1000.00000	-0.00000	66.00000	.33405	.23424
1000.00000	400.00000	-0.00000	.30164	.21152
1000.00000	800.00000	-0.00000	.34702	.24333
2000.00000	-0.00000	-0.00000	0.00000	0.00000
3500.00000	-800.00000	-0.00000	.71001	.49787
3500.00000	-400.00000	-0.00000	.11367	.07970
3500.00000	-0.00000	-0.00000	.17848	.12516
3500.00000	-0.00000	33.00000	.12339	.08652
3500.00000	-0.00000	100.00000	.39887	.27970
3500.00000	-0.00000	200.00000	.21089	.14788
3500.00000	400.00000	-0.00000	.57389	.40242
3500.00000	800.00000	-0.00000	.70029	.49105
5000.00000	-0.00000	-0.00000	.45073	.31606
6500.00000	-0.00000	-0.00000	.40536	.28424
-0.00000	-0.00000	-0.00000	0.00000	0.00000
-0.00000	-0.00000	-0.00000	0.00000	0.00000

Table 8-4

RUN NUMBER FOUR
DIKE TYPE HIGH
SCALE 1/400
STRATIFICATION NEUTRAL
WIND SPEED 16 MPH
BOIL OFF RATE 1400 LB/S

X(FT)	Y(FT)	Z(FT)	DILLUTION	K COEF X 10-2
450.00000	-600.00000	-0.00000	.14283	.16826
450.00000	-300.00000	-0.00000	2.15225	2.53545
450.00000	-0.00000	-0.00000	1.41006	1.66112
450.00000	300.00000	-0.00000	2.16198	2.54691
450.00000	600.00000	-0.00000	.34053	.40117
1000.00000	-800.00000	-0.00000	.36646	.43171
1000.00000	-400.00000	-0.00000	2.15549	2.53927
1000.00000	-0.00000	-0.00000	.52527	.61879
1000.00000	-0.00000	33.00000	.39239	.46225
1000.00000	-0.00000	66.00000	.27896	.32862
1000.00000	400.00000	-0.00000	.23358	.27517
1000.00000	800.00000	-0.00000	1.47489	1.73748
2000.00000	-0.00000	-0.00000	0.00000	0.00000
3500.00000	-800.00000	-0.00000	.60630	.71425
3500.00000	-400.00000	-0.00000	.17200	.20263
3500.00000	-0.00000	-0.00000	.20441	.24081
3500.00000	-0.00000	33.00000	.26275	.30953
3500.00000	-0.00000	100.00000	.20765	.24463
3500.00000	-0.00000	200.00000	.05209	.06136
3500.00000	400.00000	-0.00000	.25303	.29808
3500.00000	800.00000	-0.00000	.20117	.23699
5000.00000	-0.00000	-0.00000	.26275	.30953
6500.00000	-0.00000	-0.00000	.25303	.29808
-0.00000	-0.00000	-0.00000	0.00000	0.00000
-0.00000	-0.00000	-0.00000	0.00000	0.00000

Table 8-5

RUN NUMBER FIVE
DIKE TYPE LOW
SCALE 1/400
STRATIFICATION NEUTRAL
WIND SPEED 7 MPH
BOIL OFF RATE 2400 LB/S

X(FT)	Y(FT)	Z(FT)	DILLUTION	K COEF X 10-2
450.00000	-600.00000	-0.00000	6.28777	3.08032
450.00000	-300.00000	-0.00000	4.73209	2.31821
450.00000	-0.00000	-0.00000	2.00965	.98451
450.00000	300.00000	-0.00000	13.32074	6.52572
450.00000	600.00000	-0.00000	10.72794	5.25553
1000.00000	-800.00000	-0.00000	5.31547	2.60400
1000.00000	-400.00000	-0.00000	6.44982	3.15971
1000.00000	-0.00000	-0.00000	4.34317	2.12768
1000.00000	-0.00000	33.00000	2.00965	.98451
1000.00000	-0.00000	66.00000	.42156	.20652
1000.00000	400.00000	-0.00000	1.84760	.90512
1000.00000	800.00000	-0.00000	2.98195	1.46083
2000.00000	-0.00000	-0.00000	.09746	.04774
3500.00000	-800.00000	-0.00000	1.62073	.79398
3500.00000	-400.00000	-0.00000	.00347	.00170
3500.00000	-0.00000	-0.00000	1.55591	.76223
3500.00000	-0.00000	33.00000	1.16699	.57170
3500.00000	-0.00000	100.00000	.77807	.38117
3500.00000	-0.00000	200.00000	.22710	.11125
3500.00000	400.00000	-0.00000	1.58832	.77810
3500.00000	800.00000	-0.00000	1.32904	.65109
5000.00000	-0.00000	-0.00000	1.23181	.60345
6500.00000	-0.00000	-0.00000	1.03735	.50819
-0.00000	-0.00000	-0.00000	0.00000	0.00000
-0.00000	-0.00000	-0.00000	0.00000	0.00000

Table 8-6

RUN NUMBER SIXR
DIKE TYPE HIGH
SCALE 1/400
STRATIFICATION G STRAT
WIND SPEED 7 MPH
BOIL OFF RATE 2400 LBM/S

X(FT)	Y(FT)	Z(FT)	DILLUTION	K COEF X 10-2
450.00000	-600.00000	-0.00000	16.41760	8.04284
450.00000	-300.00000	-0.00000	21.12960	10.35121
450.00000	-0.00000	-0.00000	4.26560	2.08968
450.00000	300.00000	-0.00000	12.07760	5.91671
450.00000	600.00000	-0.00000	9.92000	4.85972
1000.00000	-800.00000	-0.00000	7.56400	3.70554
1000.00000	-400.00000	-0.00000	8.75440	4.28871
1000.00000	-0.00000	-0.00000	6.29920	3.08592
1000.00000	-0.00000	33.00000	4.31520	2.11398
1000.00000	-0.00000	66.00000	3.91840	1.91959
1000.00000	400.00000	-0.00000	.91760	.44952
1000.00000	800.00000	-0.00000	0.00000	0.00000
2000.00000	-0.00000	-0.00000	2.82720	1.38502
3500.00000	-800.00000	-0.00000	.66960	.32803
3500.00000	-400.00000	-0.00000	.84320	.41308
3500.00000	-0.00000	-0.00000	1.41360	.69251
3500.00000	-0.00000	33.00000	1.66160	.81400
3500.00000	-0.00000	100.00000	1.24000	.60747
3500.00000	-0.00000	200.00000	1.71120	.83830
3500.00000	400.00000	-0.00000	.37200	.18224
3500.00000	800.00000	-0.00000	0.00000	0.00000
5000.00000	-0.00000	-0.00000	1.11600	.54672
6500.00000	-0.00000	-0.00000	.79360	.38878
-0.00000	-0.00000	-0.00000	0.00000	0.00000
-0.00000	-0.00000	-0.00000	0.00000	0.00000

Table 8-7

RUN NUMBER SEVENR
DIKE TYPE HIGH
SCALE 1/400
STRATIFICATION G STRAT
WIND SPEED M MPH
BOIL OFF RATE 1400 LBM/S

X(FT)	Y(FT)	Z(FT)	DILLUTION	K COEF X 10-2
450.00000	-600.00000	-0.00000	9.30000	7.65406
450.00000	-300.00000	-0.00000	13.14400	10.81774
450.00000	-0.00000	-0.00000	1.63680	1.34712
450.00000	300.00000	-0.00000	7.14240	5.87832
450.00000	600.00000	-0.00000	6.12560	5.04148
1000.00000	-800.00000	-0.00000	4.71200	3.87806
1000.00000	-400.00000	-0.00000	5.38160	4.42915
1000.00000	-0.00000	-0.00000	2.60400	2.14314
1000.00000	-0.00000	33.00000	1.68640	1.38794
1000.00000	-0.00000	66.00000	1.90960	1.57163
1000.00000	400.00000	-0.00000	.29760	.24493
1000.00000	800.00000	-0.00000	0.00000	0.00000
2000.00000	-0.00000	-0.00000	.76880	.63274
3500.00000	-800.00000	-0.00000	.54560	.44904
3500.00000	-400.00000	-0.00000	.37200	.30616
3500.00000	-0.00000	-0.00000	.32240	.26534
3500.00000	-0.00000	33.00000	.12400	.10205
3500.00000	-0.00000	100.00000	.07440	.06123
3500.00000	-0.00000	200.00000	.19840	.16329
3500.00000	400.00000	-0.00000	0.00000	0.00000
3500.00000	800.00000	-0.00000	0.00000	0.00000
5000.00000	-0.00000	-0.00000	.37200	.30616
6500.00000	-0.00000	-0.00000	.32240	.26534
-0.00000	-0.00000	-0.00000	0.00000	0.00000
-0.00000	-0.00000	-0.00000	0.00000	0.00000

Table 8-8

RUN NUMBER EIGHTR
DIKE TYPE LOW
SCALE 1/400
STRATIFICATION G STRAT
WIND SPEED 7 MPH
BOIL OFF RATE 2400 LBM/S

X(FT)	Y(FT)	Z(FT)	DILLUTION	K COEF X 10-2
450.00000	-600.00000	-0.00000	15.12800	7.41108
450.00000	-300.00000	-0.00000	21.05520	10.31476
450.00000	-0.00000	-0.00000	2.30640	1.12989
450.00000	300.00000	-0.00000	12.97040	6.35409
450.00000	600.00000	-0.00000	11.53200	5.64943
1000.00000	-800.00000	-0.00000	5.70400	2.79434
1000.00000	-400.00000	-0.00000	8.55600	4.19151
1000.00000	-0.00000	-0.00000	5.55520	2.72144
1000.00000	-0.00000	33.00000	5.55520	2.72144
1000.00000	-0.00000	66.00000	2.80240	1.37287
1000.00000	400.00000	-0.00000	1.06640	.52242
1000.00000	800.00000	-0.00000	0.00000	0.00000
2000.00000	-0.00000	-0.00000	1.48800	.72896
3500.00000	-800.00000	-0.00000	.66960	.32803
3500.00000	-400.00000	-0.00000	.34720	.17009
3500.00000	-0.00000	-0.00000	.91760	.44952
3500.00000	-0.00000	33.00000	1.48800	.72896
3500.00000	-0.00000	100.00000	1.31440	.64391
3500.00000	-0.00000	200.00000	1.36400	.66821
3500.00000	400.00000	-0.00000	.09920	.04860
3500.00000	800.00000	-0.00000	0.00000	0.00000
5000.00000	-0.00000	-0.00000	.94240	.46167
6500.00000	-0.00000	-0.00000	.57040	.27943
-0.00000	-0.00000	-0.00000	0.00000	0.00000
-0.00000	-0.00000	-0.00000	0.00000	0.00000

Table 8-9

Please refer to errata on verso of title page.

RUN NUMBER SIX
DIKE TYPE HIGH
SCALE 1/400
STRATIFICATION G STABLE
WIND SPEED 7 MPH
BOIL OFF RATE 2400 LB/S

X(FT)	Y(FT)	Z(FT)	DILLUTION	K COEF X 10-2
450.00000	-600.00000	-0.00000	.00023	.00011
450.00000	-300.00000	-0.00000	3.33846	1.63548
450.00000	-0.00000	-0.00000	1.03735	.50819
450.00000	300.00000	-0.00000	3.33846	1.63548
450.00000	600.00000	-0.00000	.03264	.01599
1000.00000	-800.00000	-0.00000	1.39386	.68284
1000.00000	-400.00000	-0.00000	1.88001	.92100
1000.00000	-0.00000	-0.00000	.42156	.20652
1000.00000	-0.00000	33.00000	.19469	.09538
1000.00000	-0.00000	66.00000	.16228	.07950
1000.00000	400.00000	-0.00000	.61602	.30178
1000.00000	800.00000	-0.00000	.06505	.03187
2000.00000	-0.00000	-0.00000	.00023	.00011
3500.00000	-800.00000	-0.00000	.55120	.27003
3500.00000	-400.00000	-0.00000	.37294	.18270
3500.00000	-0.00000	-0.00000	.35674	.17476
3500.00000	-0.00000	33.00000	.32433	.15889
3500.00000	-0.00000	100.00000	.16228	.07950
3500.00000	-0.00000	200.00000	.03264	.01599
3500.00000	400.00000	-0.00000	.25951	.12713
3500.00000	800.00000	-0.00000	.29192	.14301
5000.00000	-0.00000	-0.00000	.35674	.17476
6500.00000	-0.00000	-0.00000	.35674	.17476
-0.00000	-0.00000	-0.00000	0.00000	0.00000
-0.00000	-0.00000	-0.00000	0.00000	0.00000

Table 8-10

Please refer to errata on verso of title page.

RUN NUMBER SEVEN
DIKE TYPE HIGH
SCALE 1/400
STRATIFICATION G STABLE
WIND SPEED 7 MPH
BOIL OFF RATE 1400 LB/

X(FT)	Y(FT)	Z(FT)	DILLUTION	K COEF X 10-2
450.00000	-600.00000	-0.00000	.00023	.00019
450.00000	-300.00000	-0.00000	1.49109	1.22719
450.00000	-0.00000	-0.00000	.87530	.72039
450.00000	300.00000	-0.00000	1.23181	1.01380
450.00000	600.00000	-0.00000	.00023	.00019
1000.00000	-800.00000	-0.00000	.22710	.18691
1000.00000	-400.00000	-0.00000	1.39386	1.14717
1000.00000	-0.00000	-0.00000	.35674	.29360
1000.00000	-0.00000	33.00000	.22710	.18691
1000.00000	-0.00000	66.00000	.09746	.08021
1000.00000	400.00000	-0.00000	.48638	.40030
1000.00000	800.00000	-0.00000	.16228	.13356
2000.00000	-0.00000	-0.00000	.00023	.00019
3500.00000	-800.00000	-0.00000	.00023	.00019
3500.00000	-400.00000	-0.00000	0.00000	0.00000
3500.00000	-0.00000	-0.00000	.32433	.26693
3500.00000	-0.00000	33.00000	.22710	.18691
3500.00000	-0.00000	100.00000	.22710	.18691
3500.00000	-0.00000	200.00000	.12987	.10689
3500.00000	400.00000	-0.00000	.19469	.16023
3500.00000	800.00000	-0.00000	.22710	.18691
5000.00000	-0.00000	-0.00000	.22710	.18691
6500.00000	-0.00000	-0.00000	.25951	.21358
-0.00000	-0.00000	-0.00000	0.00000	0.00000
-0.00000	-0.00000	-0.00000	0.00000	0.00000

Table 8-11

please refer to errata on verso of title page.

RUN NUMBER EIGHT
DIKE TYPE LOW
SCALE 1/400
STRATIFICATION G STABLE
WIND SPEED 7 MPH
BOIL OFF RATE 2400 LB/S

X(FT)	Y(FT)	Z(FT)	DILLUTION	K COEF X 10-2
450.00000	-600.00000	-0.00000	1.84760	.90512
450.00000	-300.00000	-0.00000	6.32018	3.09620
450.00000	-0.00000	-0.00000	.35674	.17476
450.00000	300.00000	-0.00000	5.96367	2.92155
450.00000	600.00000	-0.00000	2.69026	1.31794
1000.00000	-800.00000	-0.00000	.61602	.30178
1000.00000	-400.00000	-0.00000	2.49580	1.22267
1000.00000	-0.00000	-0.00000	.29192	.14301
1000.00000	-0.00000	33.00000	.16228	.07950
1000.00000	-0.00000	66.00000	.06505	.03187
1000.00000	400.00000	-0.00000	1.16699	.57170
1000.00000	800.00000	-0.00000	1.71796	.84161
2000.00000	-0.00000	-0.00000	.00023	.00011
3500.00000	-800.00000	-0.00000	.64843	.31766
3500.00000	-400.00000	-0.00000	.45397	.22240
3500.00000	-0.00000	-0.00000	.45397	.22240
3500.00000	-0.00000	33.00000	.25951	.12713
3500.00000	-0.00000	100.00000	.09746	.04774
3500.00000	-0.00000	200.00000	0.00000	0.00000
3500.00000	400.00000	-0.00000	.16228	.07950
3500.00000	800.00000	-0.00000	.35674	.17476
5000.00000	-0.00000	-0.00000	.35674	.17476
6500.00000	-0.00000	-0.00000	.38915	.19064
-0.00000	-0.00000	-0.00000	0.00000	0.00000
-0.00000	-0.00000	-0.00000	0.00000	0.00000

Table 8-12

RUN NUMBER NINE
DIKE TYPE CAPISTRANO
SCALE 1/106
STRATIFICATION NEUTRAL
WIND SPEED 12 MPH
BOIL OFF RATE 202 LB/S

X(FT)	Y(FT)	Z(FT)	DILLUTION	K COEF X 10-2
160.00000	-0.00000	-0.00000	1.90448	.48850
320.00000	-78.00000	-0.00000	.86966	.22307
320.00000	-0.00000	-0.00000	5.77420	1.48108
320.00000	-0.00000	11.00000	2.97409	.76285
320.00000	78.00000	-0.00000	3.85239	.98814
640.00000	-102.00000	-0.00000	1.95666	.50188
640.00000	-0.00000	-0.00000	3.15671	.80970
640.00000	-0.00000	20.00000	2.43494	.62456
640.00000	102.00000	-0.00000	1.93927	.49742
960.00000	-78.00000	-0.00000	.05224	.01340
960.00000	-0.00000	-0.00000	.03484	.00894
960.00000	20.00000	-0.00000	.00006	.00002
960.00000	78.00000	-0.00000	.86966	.22307
-0.00000	-0.00000	-0.00000	.16528	.04240
-0.00000	-0.00000	-0.00000	0.00000	0.00000
-0.00000	-0.00000	-0.00000	0.00000	0.00000
-0.00000	-0.00000	-0.00000	0.00000	0.00000
-0.00000	-0.00000	-0.00000	0.00000	0.00000
-0.00000	-0.00000	-0.00000	0.00000	0.00000
-0.00000	-0.00000	-0.00000	0.00000	0.00000
-0.00000	-0.00000	-0.00000	0.00000	0.00000
-0.00000	-0.00000	-0.00000	0.00000	0.00000
-0.00000	-0.00000	-0.00000	0.00000	0.00000
-0.00000	-0.00000	-0.00000	0.00000	0.00000
-0.00000	-0.00000	-0.00000	0.00000	0.00000

Table 8-13

RUN NUMBER TEN
DIKE TYPE CAPISTRANO
SCALE 1/106
STRATIFICATION NEUTRAL
WIND SPEED 12 MPH
BOIL OFF RATE 141 LB/S

X(FT)	Y(FT)	Z(FT)	DILLUTION	K COEF X 10-2
160.00000	-0.00000	-0.00000	3.00018	1.09935
320.00000	-78.00000	-0.00000	.49573	.18165
320.00000	-0.00000	-0.00000	4.68720	1.71753
320.00000	-0.00000	11.00000	1.62621	.59589
320.00000	78.00000	-0.00000	1.15663	.42382
640.00000	-102.00000	-0.00000	.72183	.26450
640.00000	-0.00000	-0.00000	2.40016	.87949
640.00000	-0.00000	20.00000	.76531	.28043
640.00000	102.00000	-0.00000	.76531	.28043
960.00000	-78.00000	-0.00000	.60878	.22307
960.00000	-0.00000	-0.00000	.54791	.20077
960.00000	20.00000	-0.00000	0.00000	0.00000
960.00000	78.00000	-0.00000	.43486	.15935
-0.00000	-0.00000	-0.00000	.16528	.06056
-0.00000	-0.00000	-0.00000	0.00000	0.00000
-0.00000	-0.00000	-0.00000	0.00000	0.00000
-0.00000	-0.00000	-0.00000	0.00000	0.00000
-0.00000	-0.00000	-0.00000	0.00000	0.00000
-0.00000	-0.00000	-0.00000	0.00000	0.00000
-0.00000	-0.00000	-0.00000	0.00000	0.00000
-0.00000	-0.00000	-0.00000	0.00000	0.00000
-0.00000	-0.00000	-0.00000	0.00000	0.00000
-0.00000	-0.00000	-0.00000	0.00000	0.00000
-0.00000	-0.00000	-0.00000	0.00000	0.00000
-0.00000	-0.00000	-0.00000	0.00000	0.00000

Table 8-14

RUN NUMBER ELEVENR
DIKE TYPE HIGH
SCALE 1/200
STRATIFICATION NEUTRAL
WIND SPEED 16 MPH
BOIL OFF RATE 1400 LBM/S

X(FT)	Y(FT)	Z(FT)	DILLUTION	K COEF X 10-2
450.00000	-434.00000	-0.00000	19.14560	20.74936
450.00000	-217.00000	-0.00000	19.14560	20.74936
450.00000	-0.00000	-0.00000	21.84880	23.67900
450.00000	217.00000	-0.00000	17.03760	18.46478
450.00000	434.00000	-0.00000	18.79840	20.37308
1000.00000	-434.00000	-0.00000	8.48160	9.19208
1000.00000	-217.00000	-0.00000	11.13520	12.06796
1000.00000	-0.00000	-0.00000	10.21760	11.07349
1000.00000	-0.00000	16.00000	10.01920	10.85848
1000.00000	-0.00000	33.00000	8.70480	9.43397
1000.00000	217.00000	-0.00000	7.76240	8.41263
1000.00000	434.00000	-0.00000	5.15840	5.59050
2000.00000	-0.00000	-0.00000	5.30720	5.75177
3500.00000	-533.00000	-0.00000	2.57920	2.79525
3500.00000	-267.00000	-0.00000	2.72800	2.95652
3500.00000	-0.00000	-0.00000	3.02560	3.27904
3500.00000	-0.00000	16.00000	3.96800	4.30039
3500.00000	-0.00000	50.00000	3.91840	4.24663
3500.00000	-0.00000	100.00000	4.04240	4.38102
3500.00000	267.00000	-0.00000	2.15760	2.33834
3500.00000	533.00000	-0.00000	.34720	.37628
5000.00000	-0.00000	-0.00000	2.50480	2.71462
6500.00000	-0.00000	-0.00000	1.66160	1.80079
-0.00000	-0.00000	-0.00000	0.00000	0.00000
-0.00000	-0.00000	-0.00000	0.00000	0.00000

Table 8-15 *Please refer to errata on verso of title page.*

RUN NUMBER ELEVEN
DIKE TYPE HIGH
SCALE 1/200
STRATIFICATION NEUTRAL
WIND SPEED 7 MPH
BOIL OFF RATE 250 LB/S

X(FT)	Y(FT)	Z(FT)	DILLUTION	K COEF X 10-2
450.00000	-434.00000	-0.00000	0.00000	0.00000
450.00000	-217.00000	-0.00000	0.00000	0.00000
450.00000	-0.00000	-0.00000	0.00000	0.00000
450.00000	217.00000	-0.00000	0.00000	0.00000
450.00000	434.00000	-0.00000	0.00000	0.00000
1000.00000	-434.00000	-0.00000	0.00000	0.00000
1000.00000	-217.00000	-0.00000	0.00000	0.00000
1000.00000	-0.00000	-0.00000	0.00000	0.00000
1000.00000	-0.00000	16.00000	0.00000	0.00000
1000.00000	-0.00000	33.00000	0.00000	0.00000
1000.00000	217.00000	-0.00000	0.00000	0.00000
1000.00000	434.00000	-0.00000	0.00000	0.00000
2000.00000	-0.00000	-0.00000	0.00000	0.00000
3500.00000	-533.00000	-0.00000	0.00000	0.00000
3500.00000	-267.00000	-0.00000	0.00000	0.00000
3500.00000	-0.00000	-0.00000	0.00000	0.00000
3500.00000	-0.00000	16.00000	0.00000	0.00000
3500.00000	-0.00000	50.00000	0.00000	0.00000
3500.00000	-0.00000	100.00000	0.00000	0.00000
3500.00000	267.00000	-0.00000	0.00000	0.00000
3500.00000	533.00000	-0.00000	0.00000	0.00000
5000.00000	-0.00000	-0.00000	0.00000	0.00000
6500.00000	-0.00000	-0.00000	0.00000	0.00000
-0.00000	-0.00000	-0.00000	0.00000	0.00000
-0.00000	-0.00000	-0.00000	0.00000	0.00000

Table 8-16

Please refer to errata on verso of title page.

RUN NUMBER TWELVE
DIKE TYPE HIGH 1
SCALE /200
STRATIFICATION NEUTRAL
WIND SPEED 16 MPH
BOIL OFF RATE 250 LB/S

X(FT)	Y(FT)	Z(FT)	DILLUTION	K COEF X 10-2
450.00000	-434.00000	-0.00000	0.00000	0.00000
450.00000	-217.00000	-0.00000	0.00000	0.00000
450.00000	-0.00000	-0.00000	0.00000	0.00000
450.00000	217.00000	-0.00000	0.00000	0.00000
450.00000	434.00000	-0.00000	0.00000	0.00000
1000.00000	-434.00000	-0.00000	0.00000	0.00000
1000.00000	-217.00000	-0.00000	0.00000	0.00000
1000.00000	-0.00000	-0.00000	0.00000	0.00000
1000.00000	-0.00000	16.00000	0.00000	0.00000
1000.00000	-0.00000	33.00000	0.00000	0.00000
1000.00000	217.00000	-0.00000	0.00000	0.00000
1000.00000	434.00000	-0.00000	0.00000	0.00000
2000.00000	-0.00000	-0.00000	0.00000	0.00000
3500.00000	-533.00000	-0.00000	0.00000	0.00000
3500.00000	-267.00000	-0.00000	0.00000	0.00000
3500.00000	-0.00000	-0.00000	0.00000	0.00000
3500.00000	-0.00000	16.00000	0.00000	0.00000
3500.00000	-0.00000	50.00000	0.00000	0.00000
3500.00000	-0.00000	100.00000	0.00000	0.00000
3500.00000	267.00000	-0.00000	0.00000	0.00000
3500.00000	533.00000	-0.00000	0.00000	0.00000
5000.00000	-0.00000	-0.00000	0.00000	0.00000
6500.00000	-0.00000	-0.00000	0.00000	0.00000
-0.00000	-0.00000	-0.00000	0.00000	0.00000
-0.00000	-0.00000	-0.00000	0.00000	0.00000

Table 8-17

RUN NUMBER FORTYFIVE
DIKE TYPE HIGH
SCALE 1/400
STRATIFICATION NEUTRAL
WIND SPEED 7 MPH
BOIL OFF RATE 2400 LBM/S

X(FT)	Y(FT)	Z(FT)	DILLUTION	K COEF X 10-2
450.00000	-600.00000	-0.00000	0.00000	0.00000
450.00000	-300.00000	-0.00000	0.00000	0.00000
450.00000	-0.00000	-0.00000	13.06340	6.39965
450.00000	300.00000	-0.00000	.30380	.14883
450.00000	600.00000	-0.00000	0.00000	0.00000
1000.00000	-800.00000	-0.00000	0.00000	0.00000
1000.00000	-400.00000	-0.00000	0.00000	0.00000
1000.00000	-0.00000	-0.00000	.15190	.07441
1000.00000	-0.00000	33.00000	3.34180	1.63712
1000.00000	-0.00000	66.00000	.07595	.03721
1000.00000	400.00000	-0.00000	.15190	.07441
1000.00000	800.00000	-0.00000	2.20255	1.07901
2000.00000	-0.00000	-0.00000	3.03800	1.48829
3500.00000	-800.00000	-0.00000	.51646	.25301
3500.00000	-400.00000	-0.00000	0.00000	0.00000
3500.00000	-0.00000	-0.00000	0.00000	0.00000
3500.00000	-0.00000	33.00000	0.00000	0.00000
3500.00000	-0.00000	100.00000	0.00000	0.00000
3500.00000	-0.00000	200.00000	0.00000	0.00000
3500.00000	400.00000	-0.00000	0.00000	0.00000
3500.00000	800.00000	-0.00000	0.00000	0.00000
5000.00000	-0.00000	-0.00000	0.00000	0.00000
6500.00000	-0.00000	-0.00000	0.00000	0.00000
-0.00000	-0.00000	-0.00000	0.00000	0.00000
-0.00000	-0.00000	-0.00000	0.00000	0.00000

Table 8-18

RUN NUMBER FORTYXIX
DIKE TYPE HIGH
SCALE 1/400
STRATIFICATION NEUTRAL
WIND SPEED 16 MPH
BOIL OFF RATE 2400 LBM/S

X(FT)	Y(FT)	Z(FT)	DILLUTION	K COEF X 10-2
450.00000	-600.00000	-0.00000	0.00000	0.00000
450.00000	-300.00000	-0.00000	.92659	1.04137
450.00000	-0.00000	-0.00000	10.63300	11.95009
450.00000	300.00000	-0.00000	1.97470	2.21930
450.00000	600.00000	-0.00000	0.00000	0.00000
1000.00000	-800.00000	-0.00000	.15190	.17072
1000.00000	-400.00000	-0.00000	.65317	.73408
1000.00000	-0.00000	-0.00000	5.69625	6.40184
1000.00000	-0.00000	33.00000	1.59495	1.79251
1000.00000	-0.00000	66.00000	0.00000	0.00000
1000.00000	400.00000	-0.00000	5.69625	6.40184
1000.00000	800.00000	-0.00000	4.70890	5.29218
2000.00000	-0.00000	-0.00000	2.23293	2.50952
3500.00000	-800.00000	-0.00000	0.00000	0.00000
3500.00000	-400.00000	-0.00000	.44051	.49508
3500.00000	-0.00000	-0.00000	1.16963	1.31451
3500.00000	-0.00000	33.00000	.92659	1.04137
3500.00000	-0.00000	100.00000	.27342	.30729
3500.00000	-0.00000	200.00000	1.41267	1.58766
3500.00000	400.00000	-0.00000	1.21520	1.36573
3500.00000	800.00000	-0.00000	.69874	.78529
5000.00000	-0.00000	-0.00000	.97216	1.09258
6500.00000	-0.00000	-0.00000	.57722	.64872
-0.00000	-0.00000	-0.00000	0.00000	0.00000
-0.00000	-0.00000	-0.00000	0.00000	0.00000

Table 8-19

RUN NUMBER FORTYSEVEN
DIKE TYPE LOW
SCALE 1/400
STRATIFICATION NEUTRAL
WIND SPEED 7MPH
BOIL OFF RATE 2400 LBM/S

X(FT)	Y(FT)	Z(FT)	DILLUTION	K COEF X 10-2
450.00000	-600.00000	-0.00000	11.69630	5.72992
450.00000	-300.00000	-0.00000	10.13173	4.96345
450.00000	-0.00000	-0.00000	4.02535	1.97198
450.00000	300.00000	-0.00000	21.03815	10.30641
450.00000	600.00000	-0.00000	9.11400	4.46487
1000.00000	-800.00000	-0.00000	2.70382	1.32458
1000.00000	-400.00000	-0.00000	6.00005	2.93937
1000.00000	-0.00000	-0.00000	2.43040	1.19063
1000.00000	-0.00000	33.00000	10.63300	5.20902
1000.00000	-0.00000	66.00000	2.09622	1.02692
1000.00000	400.00000	-0.00000	.83545	.40928
1000.00000	800.00000	-0.00000	.53165	.26045
2000.00000	-0.00000	-0.00000	1.13925	.55811
3500.00000	-800.00000	-0.00000	.50127	.24557
3500.00000	-400.00000	-0.00000	.91140	.44649
3500.00000	-0.00000	-0.00000	.68355	.33487
3500.00000	-0.00000	33.00000	.51646	.25301
3500.00000	-0.00000	100.00000	.44051	.21580
3500.00000	-0.00000	200.00000	.39494	.19348
3500.00000	400.00000	-0.00000	4891.18000	2396.14716
3500.00000	800.00000	-0.00000	.30380	.14883
5000.00000	-0.00000	-0.00000	.42532	.20836
6500.00000	-0.00000	-0.00000	.19747	.09674
-0.00000	-0.00000	-0.00000	0.00000	0.00000
-0.00000	-0.00000	-0.00000	0.00000	0.00000

Table 8-20

RUN NUMBER FORTYEIGHT
DIKE TYPE LOW
SCALE 1/400
STRATIFICATION NEUTRAL
WIND SPEED 16 MPH
BOIL OFF RATE 2400 LBM/S

X(FT)	Y(FT)	Z(FT)	DILLUTION	K COEF X 10-2
450.00000	-600.00000	-0.00000	4.86080	5.46290
450.00000	-300.00000	-0.00000	5.77220	6.48719
450.00000	-0.00000	-0.00000	.86583	.97308
450.00000	300.00000	-0.00000	16.32925	18.35193
450.00000	600.00000	-0.00000	12.54694	14.10111
1000.00000	-800.00000	-0.00000	2.70382	3.03874
1000.00000	-400.00000	-0.00000	4.01016	4.50689
1000.00000	-0.00000	-0.00000	.98735	1.10965
1000.00000	-0.00000	33.00000	5.19498	5.83847
1000.00000	-0.00000	66.00000	3.29623	3.70453
1000.00000	400.00000	-0.00000	.48608	.54629
1000.00000	800.00000	-0.00000	.37975	.42679
2000.00000	-0.00000	-0.00000	.45570	.51215
3500.00000	-800.00000	-0.00000	.45570	.51215
3500.00000	-400.00000	-0.00000	.48608	.54629
3500.00000	-0.00000	-0.00000	.34937	.39265
3500.00000	-0.00000	33.00000	1.62533	1.82666
3500.00000	-0.00000	100.00000	.53165	.59750
3500.00000	-0.00000	200.00000	.80507	.90479
3500.00000	400.00000	-0.00000	501.27000	563.36160
3500.00000	800.00000	-0.00000	.30380	.34143
5000.00000	-0.00000	-0.00000	.63798	.71701
6500.00000	-0.00000	-0.00000	.56203	.63165
-0.00000	-0.00000	-0.00000	0.00000	0.00000
-0.00000	-0.00000	-0.00000	0.00000	0.00000

Table 8-21

RUN NUMBER FORTYNINE
DIKE TYPE HIGH INSFL
SCALE 1/400
STRATIFICATION NEUTRAL
WIND SPEED 7 MPH
BOIL OFF RATE 2400 LBM/S

X(FT)	Y(FT)	Z(FT)	DILLUTION	K COEF X 10-2
450.00000	-600.00000	-0.00000	.37975	.18604
450.00000	-300.00000	-0.00000	.36456	.17859
450.00000	-0.00000	-0.00000	11.72668	5.74480
450.00000	300.00000	-0.00000	.42532	.20836
450.00000	600.00000	-0.00000	.31899	.15627
1000.00000	-800.00000	-0.00000	.41013	.20092
1000.00000	-400.00000	-0.00000	.36456	.17859
1000.00000	-0.00000	-0.00000	3.44813	1.68921
1000.00000	-0.00000	33.00000	.07595	.03721
1000.00000	-0.00000	66.00000	.03038	.01488
1000.00000	400.00000	-0.00000	.34937	.17115
1000.00000	800.00000	-0.00000	2.62787	1.28737
2000.00000	-0.00000	-0.00000	.31899	.15627
3500.00000	-800.00000	-0.00000	.34937	.17115
3500.00000	-400.00000	-0.00000	.33418	.16371
3500.00000	-0.00000	-0.00000	.25823	.12650
3500.00000	-0.00000	33.00000	.25823	.12650
3500.00000	-0.00000	100.00000	0.00000	0.00000
3500.00000	-0.00000	200.00000	.21266	.10418
3500.00000	400.00000	-0.00000	.19747	.09674
3500.00000	800.00000	-0.00000	.36456	.17859
5000.00000	-0.00000	-0.00000	.42532	.20836
6500.00000	-0.00000	-0.00000	0.00000	0.00000
-0.00000	-0.00000	-0.00000	0.00000	0.00000
-0.00000	-0.00000	-0.00000	0.00000	0.00000

Table 8-22

RUN NUMBER FIFTY
DIKE TYPE HIGH INSFL
SCALE 1/400
STRATIFICATION NEUTRAL
WIND SPEED 16 MPH
BOIL OFF RATE 2400 LBM/S

X(FT)	Y(FT)	Z(FT)	DILLUTION	K COEF X 10-2
450.00000	-600.00000	-0.00000	.37975	.42679
450.00000	-300.00000	-0.00000	3.91902	4.40446
450.00000	-0.00000	-0.00000	15.03810	16.90085
450.00000	300.00000	-0.00000	19.13940	21.51017
450.00000	600.00000	-0.00000	.36456	.40972
1000.00000	-800.00000	-0.00000	.48608	.54629
1000.00000	-400.00000	-0.00000	1.57976	1.77544
1000.00000	-0.00000	-0.00000	5.80258	6.52134
1000.00000	-0.00000	33.00000	5.28612	5.94090
1000.00000	-0.00000	66.00000	.09114	.10243
1000.00000	400.00000	-0.00000	4.01016	4.50689
1000.00000	800.00000	-0.00000	3.37218	3.78989
2000.00000	-0.00000	-0.00000	2.06584	2.32173
3500.00000	-800.00000	-0.00000	.12152	.13657
3500.00000	-400.00000	-0.00000	.60760	.68286
3500.00000	-0.00000	-0.00000	1.09368	1.22915
3500.00000	-0.00000	33.00000	1.42786	1.60473
3500.00000	-0.00000	100.00000	0.00000	0.00000
3500.00000	-0.00000	200.00000	1.88356	2.11687
3500.00000	400.00000	-0.00000	.83545	.93894
3500.00000	800.00000	-0.00000	.74431	.83651
5000.00000	-0.00000	-0.00000	.85064	.95601
6500.00000	-0.00000	-0.00000	.53165	.59750
-0.00000	-0.00000	-0.00000	0.00000	0.00000
-0.00000	-0.00000	-0.00000	0.00000	0.00000

Table 8-23

RUN NUMBER FIFTYONE
DIKE TYPE LOW INSFLR
SCALE 1/400
STRATIFICATION NEUTRAL
WIND SPEED 7 MPH
BOIL OFF RATE 2400 LBM/S

X(FT)	Y(FT)	Z(FT)	DILLUTION	K COEF X 10-2
450.00000	-600.00000	-0.00000	7.74690	3.79514
450.00000	-300.00000	-0.00000	4.07092	1.99431
450.00000	-0.00000	-0.00000	6.77474	3.31889
450.00000	300.00000	-0.00000	15.44823	7.56796
450.00000	600.00000	-0.00000	.54684	.26789
1000.00000	-800.00000	-0.00000	2.08103	1.01948
1000.00000	-400.00000	-0.00000	2.70382	1.32458
1000.00000	-0.00000	-0.00000	3.08357	1.51061
1000.00000	-0.00000	33.00000	6.71398	3.28912
1000.00000	-0.00000	66.00000	0.00000	0.00000
1000.00000	400.00000	-0.00000	.72912	.35719
1000.00000	800.00000	-0.00000	.83545	.40928
2000.00000	-0.00000	-0.00000	.24304	.11906
3500.00000	-800.00000	-0.00000	.30380	.14883
3500.00000	-400.00000	-0.00000	.30380	.14883
3500.00000	-0.00000	-0.00000	.25823	.12650
3500.00000	-0.00000	33.00000	.65317	.31998
3500.00000	-0.00000	100.00000	.15190	.07441
3500.00000	-0.00000	200.00000	.44051	.21580
3500.00000	400.00000	-0.00000	.22785	.11162
3500.00000	800.00000	-0.00000	.31899	.15627
5000.00000	-0.00000	-0.00000	.34937	.17115
6500.00000	-0.00000	-0.00000	.33418	.16371
-0.00000	-0.00000	-0.00000	0.00000	0.00000
-0.00000	-0.00000	-0.00000	0.00000	0.00000

Table 8-24

RUN NUMBER FIFTYTWO
DIKE TYPE LOW INFLR
SCALE 1/400
STRATIFICATION NEUTRAL
WIND SPEED 16 MPH
BOIL OFF RATE 2400 LBM/S

X(FT)	Y(FT)	Z(FT)	DILLUTION	K COEF X 10-2
450.00000	-600.00000	-0.00000	1.15444	1.29744
450.00000	-300.00000	-0.00000	8.90134	10.00394
450.00000	-0.00000	-0.00000	1.97470	2.21930
450.00000	300.00000	-0.00000	18.16724	20.41759
450.00000	600.00000	-0.00000	1.79242	2.01444
1000.00000	-800.00000	-0.00000	1.21520	1.36573
1000.00000	-400.00000	-0.00000	6.50132	7.30663
1000.00000	-0.00000	-0.00000	1.06330	1.19501
1000.00000	-0.00000	33.00000	5.10384	5.73605
1000.00000	-0.00000	66.00000	1.09368	1.22915
1000.00000	400.00000	-0.00000	.97216	1.09258
1000.00000	800.00000	-0.00000	.66836	.75115
2000.00000	-0.00000	-0.00000	1.03292	1.16087
3500.00000	-800.00000	-0.00000	.27342	.30729
3500.00000	-400.00000	-0.00000	.88102	.99015
3500.00000	-0.00000	-0.00000	.82026	.92186
3500.00000	-0.00000	33.00000	.88102	.99015
3500.00000	-0.00000	100.00000	1.15444	1.29744
3500.00000	-0.00000	200.00000	.72912	.81944
3500.00000	400.00000	-0.00000	.54684	.61458
3500.00000	800.00000	-0.00000	0.00000	0.00000
5000.00000	-0.00000	-0.00000	.60760	.68286
6500.00000	-0.00000	-0.00000	.66836	.75115
-0.00000	-0.00000	-0.00000	0.00000	0.00000
-0.00000	-0.00000	-0.00000	0.00000	0.00000

Table 8-25

RUN NUMBER FIFTYTHREE
DIKE TYPE HIGH
SCALE G STRAT
STRATIFICATION 7 MPH
WIND SPEED 2400 LBM/
BOIL OFF RATE S

X(FT)	Y(FT)	Z(FT)	DILLUTION	K COEF X 10-2
450.00000	-600.00000	-0.00000	0.00000	0.00000
450.00000	-300.00000	-0.00000	0.00000	0.00000
450.00000	-0.00000	-0.00000	2.68863	1.31714
450.00000	300.00000	-0.00000	.39494	.19348
450.00000	600.00000	-0.00000	.24304	.11906
1000.00000	-800.00000	-0.00000	.36456	.17859
1000.00000	-400.00000	-0.00000	.36456	.17859
1000.00000	-0.00000	-0.00000	2.61268	1.27993
1000.00000	-0.00000	33.00000	.82026	.40184
1000.00000	-0.00000	66.00000	.16709	.08186
1000.00000	400.00000	-0.00000	2.49116	1.22040
1000.00000	800.00000	-0.00000	2.96205	1.45108
2000.00000	-0.00000	-0.00000	1.04811	.51346
3500.00000	-800.00000	-0.00000	0.00000	0.00000
3500.00000	-400.00000	-0.00000	0.00000	0.00000
3500.00000	-0.00000	-0.00000	.56203	.27533
3500.00000	-0.00000	33.00000	.42532	.20836
3500.00000	-0.00000	100.00000	0.00000	0.00000
3500.00000	-0.00000	200.00000	.60760	.29766
3500.00000	400.00000	-0.00000	.57722	.28278
3500.00000	800.00000	-0.00000	.50127	.24557
5000.00000	-0.00000	-0.00000	.31899	.15627
6500.00000	-0.00000	-0.00000	0.00000	0.00000
-0.00000	-0.00000	-0.00000	0.00000	0.00000
-0.00000	-0.00000	-0.00000	0.00000	0.00000

Table 8-26

RUN NUMBER FIFTYFOUR
DIKE TYPE LOW
SCALE 1/400
STRATIFICATION G STRAT
WIND SPEED 7 MPH
BOIL OFF RATE 2400 LBM/S

X(FT)	Y(FT)	Z(FT)	DILLUTION	K COEF X 10-2
450.00000	-600.00000	-0.00000	.48608	.23813
450.00000	-300.00000	-0.00000	7.82285	3.83235
450.00000	-0.00000	-0.00000	1.16963	.57299
450.00000	300.00000	-0.00000	10.58743	5.18669
450.00000	600.00000	-0.00000	2.43040	1.19063
1000.00000	-800.00000	-0.00000	1.67090	.81856
1000.00000	-400.00000	-0.00000	4.81523	2.35894
1000.00000	-0.00000	-0.00000	1.12406	.55067
1000.00000	-0.00000	33.00000	3.55446	1.74130
1000.00000	-0.00000	66.00000	.16709	.08186
1000.00000	400.00000	-0.00000	.30380	.14883
1000.00000	800.00000	-0.00000	.24304	.11906
2000.00000	-0.00000	-0.00000	.39494	.19348
3500.00000	-800.00000	-0.00000	.15190	.07441
3500.00000	-400.00000	-0.00000	.45570	.22324
3500.00000	-0.00000	-0.00000	.44051	.21580
3500.00000	-0.00000	33.00000	.60760	.29766
3500.00000	-0.00000	100.00000	1.09368	.53578
3500.00000	-0.00000	200.00000	.89621	.43905
3500.00000	400.00000	-0.00000	.66836	.32742
3500.00000	800.00000	-0.00000	.27342	.13395
5000.00000	-0.00000	-0.00000	1.12406	.55067
6500.00000	-0.00000	-0.00000	1.01773	.49858
-0.00000	-0.00000	-0.00000	0.00000	0.00000
-0.00000	-0.00000	-0.00000	0.00000	0.00000

TABLE 9-1
TAPED DATA RECORD OF ASPIRATING PROBE RESPONSE
FOR VARIABLE BOILOFF SIMULATION WITH CO_2 GAS

MODELING INFORMATION	POSITION NO.	TAPE CHANNELS CONC.	TIME CODE	TIME CODE DAY	START	STOP
Low-Soil 1:400 Wind Speed -.67 ft/s neutral	1	1	14	1	10"	2'5"
"	1	1	14	2	10"	1'51"
"	1	1	14	3	15"	2'25"
"	1	1	14	4	15"	1'45"
"	1	1	14	5	10"	1'20"
"	1	1	14	6	15"	1'25"
"	3	1	14	7	10"	1'22"
"	3	1	14	8	10"	1'20"
"	3	1	14	9	10"	1'20"
"	3	1	14	10	10"	1'20"
"	3	1	14	11	10"	1'20"
"	3	1	14	12	10"	1'20"
"	5	1	14	13	10"	1'20"
"	5	1	14	14	10"	1'20"
"	5	1	14	15	10"	1'20"
"	5	1	14	16	10"	1'20"
"	5	1	14	17	10"	1'20"
"	6	1	14	18	10"	1'20"
"	6	1	14	19	10"	1'20"
"	6	1	14	20	10"	1'20"
" (no good)	4	1	14	21	10"	1'20"
"	4	1	14	22	10"	1'20"

TABLE 9-2

TAPED DATA RECORD OF ASPIRATING PROBE RESPONSE FOR VARIABLE BOILOFF SIMULATION WITH CO_2 GAS

MODELING INFORMATION	POSITION NO.	TAPE CHANNELS CONC.	TAPE CHANNELS TIME CODE	TIME CODE DAY	TIME CODE START	TIME CODE STOP
Low-Soil 1:400 Wind Speed -.67 ft/s neutral	4	1	14	23	10"	1'20"
"	4	1	14	24	10"	1'20"
"	2	1	14	25	10"	1'20"
"	2	1	14	26	10"	1'20"
"	2	1	14	27	10"	1'20"
"	7	1	14	28	10"	2'10"
"	7	1	14	29	10"	2'10"
"	7	1	14	30	10"	2'10"
"	8	1	14	31	10"	2'10"
"	8	1	14	32	10"	2'57"
"	8	2	13	33	10"	2'10"
"	8	2	13	34	10"	2'10"
"	9	2	13	35	10"	2'10"
"	9	2	13	36	10"	2'10"
"	10	2	13	37	10"	2'10"
"	10	2	13	38	10"	2'10"
"	10	2	13	39	10"	2'10"
"	10	2	13	40	10"	2'10"
"	10	2	13	41	10"	2'10"
"	11	2	13	42	10"	1'41"
"	11	2	13	43	10"	2'10"
"	11	2	13	44	10"	2'10"

TABLE 9-3
TAPED DATA RECORD OF ASPIRATING PROBE RESPONSE
FOR VARIABLE BOILOFF SIMULATION WITH CO_2 GAS

MODELING INFORMATION	POSITION NO.	TAPE CHANNELS CONC.	TIME CODE	TIME CODE DAY	START	STOP
Low-Soil 1:400 Wind Speed -.67 ft/s neutral	B	2	13	45	10"	1'20"
"	B	2	13	46	10"	1'20"
"	B	2	13	47	10"	1'20"
"	B	2	13	48	10"	1'20"
"	A	2	13	49	10"	1'20"
"	A	2	13	50	10"	1'20"
"	A	2	13	51	10"	1'20"
"	A	2	13	52	10"	1'20"
"	C	2	13	53	10"	1'20"
"	C	2	13	55	10"	1'50"
"	C	2	13	56	10"	2'00"
"	D	2	13	57	10"	1'50"
"	D	2	13	58	10"	1'50"
"	D	2	13	59	10"	1'30"
"	E	2	13	60	15"	1'40"
" (out of tape)	E	2	13	61	9"	1'22"
"	E	3	12	62	10"	1'41"
"	E	3	12	63	10"	1'40"
"	F	3	12	64	10"	2'00"
"	F	3	12	65	10"	1'50"
"	F	3	12	66	10"	1'50"

TABLE 9-4
TAPED DATA RECORD OF ASPIRATING PROBE RESPONSE
FOR VARIABLE BOILOFF SIMULATION WITH CO_2 GAS

MODELING INFORMATION	POSITION NO.	TAPE CHANNELS CONC.	TIME CODE	TIME CODE DAY	START	STOP
High-Soil 1:400 Wind Speed -.67 ft/s neutral	1	3	12	67	10"	1'15"
"	1	3	12	68	10"	1'10"
"	1	3	12	69	10'	1'20"
"	3	3	12	70	10"	1'10"
"	3	3	12	71	10"	1'40"
"	3	3	12	72	10"	1'40"
"	3	3	12	73	10"	1'40"
"	5	3	12	74	10"	1'20"
"	5	3	12	75	10"	1'35"
"	5	3	12	76	11"	1'45"
"	6	3	12	77	10"	1'30"
"	6	3	12	78	10"	1'35"
"	6	3	12	79	10"	(1'30")
"	6	3	12	80	10"	1'50"
"	2	3	12	81	10"	1'35"
"	2	3	12	82	10"	1'30"
"	2	3	12	83	10"	1'45"
"	4	3	12	84	10"	1'42"
"	4	3	12	85	10"	1'40"
"	4	3	12	86	10"	1'00"
" (signal jumped)	7	3	12	87	10"	2'05"
"	7	3	12	88	10"	1'30"

TABLE 9-5

TAPED DATA RECORD OF ASPIRATING PROBE RESPONSE
FOR VARIABLE BOILOFF SIMULATION WITH CO_2 GAS

MODELING INFORMATION	POSITION NO.	TAPE CHANNELS CONC.	TAPE CHANNELS TIME CODE	TIME CODE DAY	TIME CODE START	TIME CODE STOP
High-Soil 1:400 Wind Speed -.67 ft/s neutral	7	3	12	89	10"	1'12"
"	7	3	12	90	10"	1'52"
"	8	3	12	91	10"	1'51"
"	8	3	12	92	10"	1'45"
" (no good)	9	3	12	93	10"	1'20"
"	9	4	11	94	10"	2'10"
"	9	4	11	95	10"	2'00"
"	10	4	11	96	10"	1'52"
"	10	4	11	97	10"	1'54"
"	10	4	11	98	10"	1'50"
"	11	4	11	99	10"	1'50"
"	11	4	11	100	10"	1'50"
"	11	4	11	101	10"	1'50"
"	11	4	11	102	10"	2'15"
"	A	4	11	103	10"	1'22"
"	A	4	11	104	10"	1'20"
"	α	4	11	105	15"	1'25"
High-Concrete 1:400 Wind speed .67 ft/s neutral	1	4	11	106	10"	1'40"
"	1	4	11	107	10"	1'54"
"	1	4	11	108	13"	1'58"
"	1	4	11	109	10"	1'40"

TABLE 9-6
TAPED DATA RECORD OF ASPIRATING PROBE RESPONSE
FOR VARIABLE BOILOFF SIMULATION WITH CO_2 GAS

MODELING INFORMATION	POSITION NO.	TAPE CHANNELS CONC.	TIME CODE	TIME CODE DAY	START	STOP
High-Concrete 1:400 Wind speed .67 ft/s neutral (background)	3	4	11	110	10"	2'04"
"	3	4	11	120	10"	1'45"
"	3	4	11	112	11"	2'00"
"	3	4	11	113	10"	1'50"
"	3	4	11	114	10"	1'50"
"	5	4	11	115	10"	1'40"
"	5	4	11	116	10"	1'41"
"	5	4	11	117	10"	2'00"
"	5	4	11	118	10"	1'40"
"	6	4	11	119	10"	1'40"
" (end of tape)	6	4	11	120	10"	1'58"
"	6	5	10	121	10"	1'41"
" (no x-y plot)	2	5	10	122	10"	1'35"
"	2	5	10	123	10"	((1'35"))
"	2	5	10	124	10"	1'50"
"	2	5	10	125	10"	1'45"
"	4	5	10	126	10"	1'50"
"	4	5	10	127	10"	1'30"
"	4	5	10	128	10"	1'30"
"	7	5	10	129	10"	1'40"
"	7	5	10	130	10"	1'50"

TABLE 9-7
TAPED DATA RECORD OF ASPIRATING PROBE RESPONSE
FOR VARIABLE BOILOFF SIMULATION WITH CO_2 GAS

MODELING INFORMATION	POSITION NO.	TAPE CHANNELS CONC.	TAPE CHANNELS TIME CODE	TIME CODE DAY	TIME CODE START	TIME CODE STOP
"	8	5	10	131	10"	2'00"
"	B	5	10	132	10"	1'45"
"	B	5	10	133	10"	(1'30")
" (time code off by 40 sec)	B	5	10	134	10"	1'45"
"	B	5	10	135	10"	1'30"
"	C	5	10	136	10"	2'20"
"	C	5	10	137	10"	2'00"
High - R&D Concrete* 1:400 Wind speed .67 ft/sec neutral	1	5	10	138	10"	1'40"
"	1	5	10	139	10"	1'30"
"	1	5	10	140	10"	1'40"
"	3	5	10	141	10"	1'20"
"	3	5	10	142	10"	1'20"
"	3	5	10	143	10"	1'40"
"	5	5	10	144	5"	1'30"
"	5	5	10	145	5"	1'20"
"	5	5	10	146	5"	1'20"
"	2	5	10	147	7"	1'20"
" (background)	2	5	10	148	5"	1'10"
"	4	5	10	149	5"	1'32"
"	4	5	10	150	5"	1'20"
" (tape end)	4	5	10	151	5"	1'10"

TABLE 9-8
TAPED DATA RECORD OF ASPIRATING PROBE RESPONSE
FOR VARIABLE BOILOFF SIMULATION WITH CO_2 GAS

MODELING INFORMATION	POSITION NO.	TAPE CHANNELS CONC.	TAPE CHANNELS TIME CODE	TIME CODE DAY	TIME CODE START	TIME CODE STOP
High - R&D Concrete* 1:400 Wind speed .67 ft/sec neutral (not recorded)	2	5	10	152		
High - R&D Concrete* 1:400 Wind speed 1.16 ft/sec neutral	3	6 (maybe 4)	9	153	5"	60"
"	2	6	9	155	5"	50"
"	4	6	9	156	5"	50"
"	1	6	9	157	6"	1'16"
"	1	6	9	158	5"	1'38"
High - Concrete 1:400 Wind speed 1.16 ft/sec neutral	1	6	9	159	5"	1'26"
"	1	6	9	160	5"	1'16"
"	1	6	9	161	5"	1'11"
"	3	6	9	162	6"	1'22"
"	3	6	9	163	5"	1'31"
"	3	6	9	164	5"	1'20"
"	5	6	9	165	5"	1'20"
"	5	6	9	166	6"	1'20"
"	6	6	9	167	5"	1'20"
" (motor off valve open)	6	6	9	168	5"	1'25"
"	6	6	9	169	5"	1'10"
"	6	6	9	170	5"	1'10"

TABLE 9-9
TAPED DATA RECORD OF ASPIRATING PROBE RESPONSE
FOR VARIABLE BOILOFF SIMULATION WITH CO_2 GAS

MODELING INFORMATION	POSITION NO.	TAPE CHANNELS CONC.	TIME CODE	TIME CODE DAY	START	STOP
High - Concrete 1:400 Wind speed 1.16 ft/sec neutral	4	6	9	171	10"	1'20"
"	4	6	9	172	5"	1'20"
"	2	6	9	173	15"	1'25"
"	2	6	9	174	10"	1'25"
"	7	6	9	175	15"	1'15"
High - Soil 1:400 Wind speed 1.16 ft/sec neutral	7	6	9	176	10"	1'25"
"	7	6	9	177	10"	1'10"
"	7	6	9	178	10"	1' ?"
"	7	6	9	179	10"	1'10"
"	8	6	9	180	10"	1'20"
"	9	6	9	181	10"	1'30"
"	9	6	9	182	10"	1'20"
"	10	6	9	183	10"	1'20"
"	11	6	9	184	10"	1'00"
"	11	6	9	185	10"	1'10"
"	11	6	9	186	10"	1'10"
"	3	6	9	187	10"	1'20"
"	3	6	9	188	10"	1'20"
"	5	6	9	189	10"	1'10"
"	5	6	9	190	10"	1'00"
"	5	6	9	191	10"	1'10"

TABLE 9-10

TAPED DATA RECORD OF ASPIRATING PROBE RESPONSE FOR VARIABLE BOILOFF SIMULATION WITH CO_2 GAS

MODELING INFORMATION	POSITION NO.	TAPE CHANNELS CONC.	TAPE CHANNELS TIME CODE	TIME CODE DAY	TIME CODE START	TIME CODE STOP
High - Soil 1:400 Wind speed 1.16 ft/sec neutral (ran out of tape)	5	6	9	192	10"	1'10"
"	5	7	8	193	10"	1'20"
"	5	7	8	194	10"	1'05"
"	6	7	8	195	10"	1'10"
"	6	7	8	196	10"	1'00"
"	6	7	8	197	10"	1'00"
"	4	7	8	198	10"	1'00"
"	4	7	8	199	10"	1'00"
"	2	7	8	200	10"	1'00"
"	2	7	8	201	10"	1'00"
"	1	7	8	202	10"	1'10"
"	1	7	8	203	10"	1'25"
"	1	7	8	204	10"	1'20"
"	B	7	8	205	20"	1'30"
"	B	7	8	206	20"	1'20"
"	A	7	8	207	20"	1'10"
"	A	7	8	208	20"	1'10"
"	C	7	8	209	20"	1'20"
"	C	7	8	210	20"	1'20"
"	D	7	8	211	20"	1'10"
"	Δ	7	8	212	20"	1'10"
"	τ	7	8	213	20"	1'10"

TABLE 9-11

TAPED DATA RECORD OF ASPIRATING PROBE RESPONSE FOR VARIABLE BOILOFF SIMULATION WITH CO_2 GAS

MODELING INFORMATION	POSITION NO.	TAPE CONC.	CHANNELS TIME CODE	TIME CODE DAY	START	STOP
Capistrano - Case I Wind speed 2.45 ft/sec neutral	1	7	8	214	30"	1'41"
"	1	7	8	215	20"	2'10"
" (motor off, value open continuous)	2	7	8	216	20"	1'11"
" (no 217)	2	7	8	218	20"	1'27"
"	2	7	8	219	20"	1'26"
"	2	7	8	220	20"	1'30"
"	3	7	8	221	20"	1'26"
"	3	7	8	222	22"	1'29"
"	4	7	8	223	20"	(1'30")
"	4	7	8	224	20"	1'22"
"	4	7	8	225	20"	1'30"
"	5	7	8	226	20"	1'25"
"	5	7	8	227	20"	1'05"
"	5	7	8	228	16"	1'15"
"	6	7	8	229	20"	1'05"
"	6	7	8	230	23"	55"
"	6	7	8	231	20"	50"
Low - Soil 1:400 Wind speed - .67 ft/sec stable	B	1	2	1B	35"	2'10"
"	1	1	2	2	20"	2'30"
"	1	1	2	3	25"	2'25"

TABLE 9-12

TAPED DATA RECORD OF ASPIRATING PROBE RESPONSE
FOR VARIABLE BOILOFF SIMULATION WITH CO_2 GAS

MODELING INFORMATION	POSITION NO.	TAPE CHANNELS CONC.	TAPE CHANNELS TIME CODE	TIME CODE DAY	TIME CODE START	TIME CODE STOP
Low - Soil 1:400 Wind speed - .67 ft/sec stable	(3)	1	2	4	32"	2'10"
"	3	1	2	5	20"	1'30"
"	5	1	2	6	30"	?
" (16^o C)	6	1	2	7	20"	1'50"
" (17^o C)	4	1	2	8	20"	1'30"
" (12^o C)	2	1	2	9	20"	1'40"
"	7	1	2	10	40"	2'15"
" (10^o C)	7	1	2	11	20"	2'00"
" (10^o C)	8	1	2	12	20"	2'15"
" (13^o C)	9	1	2	13	20"	2'10"
"	A	1	2	14	40"	1'55"
" (13^o C)	C	1	2	15	20"	1'25"
" (11^o C)	Δ	1	2	16	20"	1'20"
" (11^o C)	Δ	1	2	17	20"	1'10"
High - Soil 1:400 Wind speed .67 ft/sec stable						
" (11^o C)	Δ	1	2	18	20"	1'00"
" (11^o C)	Δ	1	2	19	20"	1'10"
" (12^o C)	C	1	2	20	20"	2'05"
" (14^o C)	1	1	2	21	20"	1'30"
" (13^o C)	3	1	2	22	20"	1'25"
" (13^o C)	3	1	2	23	20"	1'10"
" (16^o C)	5	1	2	24	30"	2'20"

TABLE 9-13

TAPED DATA RECORD OF ASPIRATING PROBE RESPONSE
FOR VARIABLE BOILOFF SIMULATION WITH CO_2 GAS

MODELING INFORMATION	POSITION NO.	TAPE CHANNELS		TIME CODE		
		CONC.	TIME CODE	DAY	START	STOP
High - Soil 1:400 Wind speed .67 ft/sec stable						
" (17° C)	5	1	2	25	25"	1'15"
" (17° C)	4	1	2	26	25"	1'10"
" (13° C)	2	1	2	27	20"	1'15"
" (11° C)	7	1	2	28	25"	1'55"
" (11° C)	8	1	2	29	20"	1'25"

TABLE 10

APPROXIMATE DISTANCES TO LIFTOFF FOR GROUND RELEASED BUOYANT PLUMES IN A CROSSFLOW BOUNDARY LAYER

Line Source: y = 4 feet, x_o = 40 feet from tunnel entrance

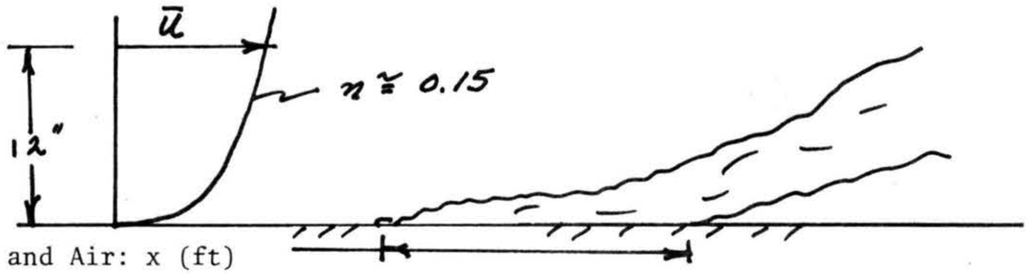

Helium and Air: x (ft)

Velocity (ft/sec)	Flow Rate (cfm) 0.75 cfm (10)	1.5 cfm (20)	2.25 cfm (30)	3.00 cfm (40)
0.55	3	1.5-2	1.5	1
0.75	9	6	2-3	2
1.5	x > 15	7	6	4
2.5	x > 15	x > 11	x > 11	7

Area Source: 9 inch diameter, x (ft)

Velocity (ft/sec)	Flow Rate (cfm) 0.75 cfm	1.5 cfm	2.25 cfm	3.00 cfm
0.52	0	0	0	0
0.75	0	0	0	0
1.50	0	0	0	0
2.50	1.5	1	0.5	0
4.00	x > 15	x > 15	8	5

Point Source: x (ft)

Velocity (ft/sec)	Flow Rate (cfm) 0.75 cfm	1.5 cfm	2.25 cfm	3.00 cfm
2.50	0	0	0	0
4.00	?	1.5	1.5	0
6.50	?	2.5-3.0	2.0	2.0

TABLE 11-1

IDENTIFICATION CHART FOR
CONTINUOUS FLOW VISUALIZATION EXPERIMENTS

PURE CO_2 TRACER

SOURCE DESCRIPTION	TERRAIN DESCRIPTION	PICTURE* NUMBER	SIMULATED WIND SPEED (fps)	SIMULATED BOILOFF RATE (lb_m/sec)
Area Source (Capistrano 044 1/106 Scale Model)	2% Grade Upwind	1	23	160
"	"	2	23	420
"	"	3	23	1200
"	"	4	23	2400
"	"	5	16	160
"	"	6	16	420
"	"	7	16	1200
"	"	8	16	2400
"	"	9	30	160
"	"	10	30	420
"	"	11	30	1200
"	"	12	30	2400
High Dike (1/400 Scale Model)	"	13	16	160
"	"	14	16	420
"	"	15	16	1200
"	"	16	16	2400
"	"	17	23	460
"	"	18	23	420
"	"	19	23	1200
"	"	20	23	2400
"	"	21	30	160
"	"	22	30	420
"	"	23	30	1200
"	"	24	30	2400

*Photographs provided separately to R&D Associates

TABLE 11-2 (continued)

IDENTIFICATION CHART FOR
CONTINUOUS FLOW VISUALIZATION EXPERIMENTS

PURE CO_2 TRACER

SOURCE DESCRIPTION	TERRAIN DESCRIPTION	PICTURE* NUMBER	SIMULATED WIND SPEED (fps)	SIMULATED BOILOFF RATE (lb_m/sec)
Area Source (Capistrano 044 1/106 Scale Model)	Flat Surface	1-A	16	160
"	"	2-A	16	420
"	"	3-A	16	1200
"	"	4-A	16	2400
"	"	5-A	23	160
"	"	6-A	23	420
"	"	7-A	23	1200
"	"	8-A	23	2400
"	"	9-A	30	160
"	"	10-A	30	420
"	"	11-A	30	1200
"	"	12-A	30	2400
High Dike (1/400 Scale Model)	"	13-A	30	160
"	"	14-A	30	420
"	"	15-A	30	1200
"	"	16-A	30	2400
"	"	17-A	23	160
"	"	18-A	23	420
"	"	19-A	23	1200
"	"	20-A	23	2400
"	"	21-A	16	160
"	"	22-A	16	420
"	"	23-A	16	1200
"	"	24-A	16	2400

*Photographs provided separately to R&D Associates

TABLE 11-3 (continued)

IDENTIFICATION CHART FOR
CONTINUOUS FLOW VISUALIZATION EXPERIMENTS

PURE CO_2 TRACER

SOURCE DESCRIPTION	TERRAIN DESCRIPTION	PICTURE* NUMBER	SIMULATED WIND SPEED (fps)	SIMULATED BOILOFF RATE (lb_m/sec)
High Dike (1/400 Scale Model with 2 Upstream Obstacles)	2% Grade Upwind	25	30	160
"	"	26	30	420
"	"	27	30	1200
"	"	28	30	2400
"	"	29	23	160
"	"	30	23	420
"	"	31	23	1200
"	"	32	23	2400
"	"	33	16	160
"	"	34	16	420
"	"	35	16	1200
"	"	36	16	2400
High Dike (1/400 Scale Model with 1 Upstream Obstacle)	"	37	16	160
"	"	38	16	420
"	"	39	16	1200
"	"	40	16	2400
"	"	41	23	160
"	"	42	23	420
"	"	43	23	1200
"	"	44	23	2400
"	"	45	30	160
"	"	46	30	420
"	"	47	30	1200
"	"	48	30	1400

*Photographs provided separately to R&D Associates